An in vitro evaluation of *Hypoxis hemerocallidea* (African potato) corm, *Helichrysum caespititium* and *Dicoma anomala* effects on the proliferation of DU145 prostate cancer cell line

LERATO MILLICENT TOONA

Dissertation submitted in fulfilment of the requirements of the degree
Master of Health Sciences in Biomedical Technology

Department of Health Science Biomedical Technology
Faculty of Health and Environmental Sciences

Supervisor: Prof. P.H. Mfengwana (DHSc)
Co-supervisor: Ms J. Mthombeni (MPH)

NOVEMBER 2024

DECLARATION

I, LERATO MILLICENT TOONA, with student number ######## and identity number ##############, hereby certify that the dissertation submitted by me for the degree MASTER OF HEALTH SCIENCES IN BIOMEDICAL TECHNOLOGY (M HBIO), is my own independent work and complies with the Code of Academic Integrity, as well as other relevant policies, procedures, rules, and regulations of the Central University of Technology, Free State. I hereby declare that this research project has not previously been submitted to any university or faculty for the attainment of any qualification.

ANTI-PLAGIARISM DECLARATION

1. Plagiarism is to present someone else's ideas as my own.
2. Where material written by other people has been used (either from a printed source or from the Internet), this has been carefully acknowledged and referenced. I have used the Harvard form citation and referencing. Every contribution to and quotation from the work of other people in this essay has been acknowledged through citation and reference.
3. I know that plagiarism is wrong.

3.1 I understand what plagiarism is and am aware of the University's policy in this regard.

3.2 I know that I would plagiarise if I do not give credit to my sources, or if I copy sentences or paragraphs from a book, article or Internet source without proper citation.

3.3 I know that even if I only change the wording slightly, I still plagiarise when using someone else's words without proper citation.

3.4 I declare that I have written my own sentences and paragraphs throughout my dissertation, and I have credited all ideas I have gained from other people's work.

4. I declare that this dissertation is my own original work.
5. I have not allowed and will not allow anyone to copy my work with the intention of passing it off as his or her own work.

SIGNATURE _____ DATE: Nov 2024

ACKNOWLEDGMENT

This is to extend words of thanks to everyone who supported me during my study:

I give thanks to the Almighty Jehovah God through Christ Jesus, Sovereign Lord, whom I worship, as well as the local church family, maBaptist, for your prayers (Mrs Van der Walt, *baie dankie*).

To my supervisor, Prof. Mfengwana, your patience, gentleness, and guidance during these times are appreciated; you extended yourself in more areas and I will forever be grateful. To my co-supervisor and my HoD, Mrs Mthombeni, thank you for always picking up your cell phone.

To my family, my matriarchal system (my grandmother, Florah Motshwane, and mother, Margaret Toona) for your immeasurable support. Many thanks to Mr Tshepiso Mpipi for walking with me and for the oral knowledge shared regarding traditional plants. I am grateful, sir.

To the colleagues who supported this study. My appreciation goes to Prof. Van de Venter and Dr Venables at Nelson Mandela University (NMU), Department of Biochemistry and Microbiology, Summerstrand South, for the cell culture work. My time with you will forever be cherished.

To my colleagues at the University of Johannesburg (UJ). Let me acknowledge Prof. Adebo and his team at the Department of Biotechnology and Food Technology, Dr Welcome for assisting me with mounting my specimens in the Department of Botany and Plant Biotechnology, Faculty of Science, Auckland Park Kingsway Campus, and lastly, to Dr Smit at the Department of Chemical Science (UJ) and Dr Wooding for Chromatography and Mass Spectrometry at the Department of Chemistry in the University of Pretoria (UP) for your patience and support with mass spectrometry.

To all my friends; I am so grateful for your love and support.

TABLE OF CONTENTS

DECLARATION i
ACKNOWLEDGEMENTS ii
LIST OF FIGURES vii
LIST OF TABLES x
LIST OF ABBREVIATIONS xi
LIST OF UNITS xii
LIST OF CHEMICAL SYMBOLS xiii
RESEARCH OUTPUTS xiv
ABSTRACT xv

CHAPTER 1: BACKGROUND

1.1 Introduction 1
1.2 Normal prostate 1
1.3 Prostate cancer 2
1.4 DU145 prostate cancer cell line 3
1.5 Traditional medicine 4
1.5.1 Traditional medicinal plants in South Africa 4
1.6 Research rationale 4
1.7 Aim 5
1.8 Objectives 5
1.9 Methodology 6
1.9.1 Plant collection 6
1.9.2 Plant extraction 7
1.9.2.1 Direction maceration method 8
1.10 Thesis outline 8
REFERENCES 9

CHAPTER 2: LITERATURE REVIEW

2.1 Cancer statistics 11
2.2 Prostate cancer statistics 12
2.3 Current prostate cancer treatments 12
2.4 Medicinal plants 13
2.4.1 *H. hemerocallidea* (African potato) 14
2.4.2 *H. caespititium* 16
2.4.3 *D. anomala* 17
REFERENCES 20

CHAPTER 3: PHYTOCHEMICAL SCREENING OF THE PLANTS' CORMS

3.1 Phytochemical screening: High-resolution mass spectrometry (HRMS) 23
3.2 Sample preparation for HRMS 23
3.3 Materials and method for HRMS 24
3.3.1 Waters Acquity Ultra-Performance Liquid Chromatography (UPLC) Synapt G2 High Definition Mass Spectrometer (HDMS) 24
3.4 HRMS analysis 25
3.5 HRMS results 27
3.5.1 Chromatogram profile obtained from methanolic extracts (negative mode) 27
3.5.2 Chromatogram profile obtained from aqueous extracts (negative mode) 33
3.5.3 Chromatogram profile obtained from aqueous extracts (positive mode) 36
3.6 Discussion 39
REFERENCES 42

CHAPTER 4: ANTI-OXIDATION ACTIVITY OF THE CORM OF *H. HEMEROCALLIDEA* (AFRICAN POTATO), *H. CAESPITITIUM*, AND *D. ANOMALA*

4.1 Introduction 44
4.2 Sample preparation for anti-oxidation: Extraction by sonication method 44
4.3 Materials and methods 44
4.3.1 2,2-diphenyl-1-picrylhydrazyl (DPPH) anti-oxidant capacity assay 44

4.3.2 2, 2'-azino-bis (3-ethylbenzothiazoline-6-sulfonic acid) (ABTS) anti-oxidant capacity assay 45
4.3.3 Ferric reducing ability of plasma (FRAP) anti-oxidant capacity assay 46
4.4 Anti-oxidant results: DPPH, ABTS, and FRAP 46
REFERENCES 50

CHAPTER 5: PROSTATE CANCER CELL PROLIFERATION

5.1 Introduction 53
5.2 Prostate gland proliferation: The role of androgen 54
5.3 Prostate gland regulators: Positive regulator in prostate cancer cell proliferation 54
5.4 Downstream targets: Androgen-responsive proliferative pathway 55
5.5 Extracellular matrix microenvironment 56
5.6 Materials 57
5.7 Method 57
5.8 Antiproliferation results 58
5.8.1 Half-maximal inhibitory concentration (IC_{50}) determination 61
5.9 Discussion 62
REFERENCES 66

CHAPTER 6: ANTICANCER MECHANISM ACTIVITY

6.1 Introduction 69
6.2 Apoptosis: Apoptotic programmed cell death (PCD) 69
6.3 Apoptosis signalling system 70
6.3.1 Intrinsic pathway (internal stimuli) 71
6.3.2 Extrinsic pathway (external stimuli) 71
6.3.3 Effector pathway (execution phase) 73
6.4 Modalities of cell death 73
6.5 Autophagy: Non-apoptotic PCD 74
6.6 Necrosis: Non-PCD 75
6.7 Secondary necrosis 76

6.8 Cell cycle cell division 76
6.9 Materials 78
6.10 Method 78
6.10.1 Cell cycle analysis: Phosphatidylserine (PS) translocation 78
6.11 Results for the anticancer mechanism of action 79
6.11.1 Hoechst 33342, Annexin V-FITC, and propidium iodide (HAPI) 79
6.11.2 Cell cycle analysis 82
6.11.3 Mitochondrial membrane potential (MMP) analysis 85
6.11.3.1 MMP results 86
6.11.4 Caspase activation 87
6.11.4.1 Caspase activation results 87
6.12 Data quantification 90
6.13 Discussion 90
REFERENCES 94

CHAPTER 7: CONCLUSIONS AND RECOMMENDATIONS

7.1 Conclusion 97
7.2 Limitations of the study 98
7.3 Recommendations 99
REFERENCES 101

APPENDICES

Appendix A: Additional Results for Chapter 3 111
Appendix B: Additional Results for Chapter 4 125
Appendix C: Additional Results for Chapter 5 128
Appendix D: Project Output: Conference Output (Oral Presentation) 130
Appendix E: Project Output: International Academy of Pathology Conference Output (Poster Presentation) 131
Appendix F: Turnitin Report 132

LIST OF FIGURES

Figure 1.1: Histological cross-section of a prostate gland; (A) prostate cancer, and (B) normal prostate gland 3

Figure 1.2: High- and low-density morphology of the ATCC DU145 prostate cancer cell line 3

Figure 1.3: Google Maps view of Mamoretse, Mogajane village, Bojanala district 6

Figure 2.1: Global prevalence of cancer 11

Figure 2.2: (A) Photographic view of macroscopic plant *H. hemerocallidea*; (B) corm of *H. hemerocallidea* 15

Figure 2.3: (A) Photographic view of macroscopic plant *H. caespititium*; (B) blue circle: corm of *H. caespititium* 17

Figure 2.4: (A) Photographic view of macroscopic plant *D. anomala*; (B) corm of *D. anomala* 18

Figure 3.1: UPLC Synapt G2 HDMS 24

Figure 3.2: Chromatogram profile obtained from Methanolic A: *H. hemerocallidea* in negative mode 27

Figure 3.3: Chromatogram profile obtained from Methanolic B: *H. caespititium* in negative mode 28

Figure 3.4: Chromatogram profile obtained from Methanolic C: *D. anomala* in negative mode 29

Figure 3.5: Chromatogram profile obtained from Methanolic A: *H. hemerocallidea* in positive mode 30

Figure 3.6: Chromatogram profile obtained from Methanolic B: *H. caespititium* in positive mode 31

Figure 3.7: Chromatogram profile obtained from Methanolic C: *D. anomala* in positive mode 32

Figure 3.8: Chromatogram profile obtained from Aqueous A: *H. hemerocallidea* in negative mode 33

Figure 3.9: Chromatogram profile obtained from Aqueous B: *H. caespititium* in negative mode 34

Figure 3.10: Chromatogram profile obtained from Aqueous C: *D. anomala* in negative mode 35

Figure 3.11: Chromatogram profile obtained from Aqueous A: *H. hemerocallidea* in positive mode 36
Figure 3.12: Chromatogram profile obtained from Aqueous B: *H. caespititium* in positive mode 37
Figure 3.13: Chromatogram profile obtained from Aqueous C: *D. anomala* in positive mode 38
Figure 5.1: Two forms of cell division: Mitosis and meiosis 53
Figure 5.2: Control: untreated cell line; solvent: aqueous (ddH_2O); melphalan: cell line treated with melphalan 58
Figure 5.3: Control: untreated cell line; solvent: aqueous (ddH_2O); melphalan: cell line treated with melphalan 59
Figure 5.4: Control: untreated cell line; solvent: MeOH; melphalan: cell line treated with melphalan 60
Figure 5.5: Control: untreated cell line; solvent: MeOH; melphalan: cell line treated with melphalan 61
Figure 5.6: Dose-response curves for the MeOH *D. anomala* extract 62
Figure 6.1: Characteristics of apoptosis 70
Figure 6.2: Apoptosis signalling systems 72
Figure 6.3: Cell death morphological alteration 75
Figure 6.4: Phases of the cell cycle 77
Figure 6.5: HAPI after 24 hours 79
Figure 6.6: HAPI after 48 hours 81
Figure 6.7: DNA structure after 24 hours 82
Figure 6.8: DNA structure after 48 hours 83
Figure 6.9: Morphological changes: (A) control untreated cells; (B) treated with *D. anomala* at 15 µg/mL for 24 hours, with different colours depicting different cell cycle phases 84
Figure 6.10: Morphological changes: (A) control melphalan; (B) treated cells with 15 µg/mL concentration of *D. anomala* after 24 hours 84
Figure 6.11: DNA scatterplot 85
Figure 6.12: Tetramethylrhodamine ethyl ester (TMRE) after 48 hours 86
Figure 6.13: Caspase-3 after 48 hours 88

Figure 6.14: (A) Morphological changes control: melphalan; (B) treated 15 µg/mL concentration of *D. anomala* 89
Figure 6.15: Treated 30 µg/mL concentration of *D. anomala* 89
Figure B1: Standard curve DPPH percentage scavenging activity 125
Figure B2: DPPH assay photograph: Determining anti-oxidant activities 125
Figure B3: Standard curve ABTS percentage scavenging activity 126
Figure B4: ABTS assay photograph: Determining anti-oxidant activity 126
Figure B5: Standard curve FRAP percentage scavenging activity 127
Figure B6: FRAP assay photograph: Determining anti-oxidant activity 127

LIST OF TABLES

Table 2.1: Summary of incidence across cancers: 2019 to 2030 12

Table 4.1: Percentage of scavenging activity by *H. hemerocallidea*, *H. caespititium*, and *D. anomala* methanolic and aqueous extracts 47

Table A1: Characteristics of major peaks from Methanolic A: *H. hemerocallidea* in negative mode 111

Table A2: Characteristics of major peaks from Methanolic B: *H. caespititium* in negative mode 114

Table A3: Characteristics of major peaks from Methanolic C: *D. anomala* in negative mode 116

Table A4: Characteristics of major peaks from Methanolic A: *H. hemerocallidea* in positive mode 119

Table A5: Characteristics of major peaks from Methanolic B: *H. caespititium* in positive mode 121

Table A6: Characteristics of major peaks from Methanolic C: *D. anomala* in positive mode 122

Table C1: Control: untreated cell line, A.W.: *H. hemerocallidea* B.W.: *H. caespititium* C.W.: *D. anomala* with solvent aqueous (ddH_2O), melphalan: cell line treated with melphalan 128

Table C2: Control: untreated cell line, A.M.: *H. hemerocallidea* B.M.: *H. caespititium* C.M.: *D. anomala* with solvent MeOH, Melphalan: cell line treated with melphalan 128

Table C3: Control: untreated cell line, *D. anomala* with MeOH solvent, melphalan: cell line treated with melphalan 129

LIST OF ABBREVIATIONS

ABTS	2,2'-azino-bis (3-ethylbenzothiazoline-6-sulfonic acid)
AgNPs	Silver nanoparticles
APCI	Atmospheric pressure chemical ionisation
AR	Androgen receptor
BCE	Before Common Era
BSA	Bovine serum albumin
CCCP	Carbonyl cyanide m-chlorophenyl hydrazone
CD95L	CD95 ligand
CDK	Cyclin-dependent kinase
COVID-19	Coronavirus disease of 2019
DBE	Double bond equivalent
ddH_2O	Deionised water
dH_2O	Distilled water
DNA	Deoxyribonucleic acid
DPBS	Dulbecco's phosphate buffered saline
DPPH	2,2-diphenyl-1-picrylhydrazyl
EDTA	Ethylenediamine tetraacetic acid
ER	Estrogen receptor
ERα	Estrogen receptor alpha
ERβ	Estrogen receptor beta
ESCI	Electrospray combined ion source
ESI	Electrospray ionisation
FBS	Foetal bovine serum
Fe (II)-TPTZ	Ferrous-tripyridyltriazine
Fe (III)-TPTZ	Ferric-tripyridyltriazine
FITC	Fluorescein isothiocyanate
FRAP	Ferric reducing ability of plasma
G1	Gap 1
G2	Gap 2
HAPI	Hoechst 33342, Annexin V-FITC, and propidium iodide
HDMS	High Definition Mass Spectrometer
HILIC	Hydrophilic interaction liquid chromatography
HIV/AIDS	Human immunodeficiency virus / acquired immunodeficiency syndrome
HRMS	High-resolution mass spectrometry

IC	Inhibition concentration
IC_{50}	Half-maximal inhibitory concentration
KIBRA	Kidney and brain associated protein
M	Mitosis
m/z	Mass-to-charge ratio
MMP	Mitochondrial membrane potential
MOMP	Mitochondrial outer membrane permeabilisation
PCD	Programmed cell death
pH	Potential of hydrogen
PI	Propidium iodide
PS	Phosphatidylserine
PSA	Prostatic-specific antigen
PAP	Prostate-specific acid phosphatase
ROS	Reactive oxygen species
rpm	Revolutions per minute
RPMI	Roswell Park Memorial Institute
S	Synthesis
SD	Standard deviation
TMRE	Tetramethylrhodamine ethyl ester
TNF	Tumour necrosis factor
TOFMS	Time-of-flight mass spectrometry
UPLC	Ultraperformance Liquid Chromatography
USA	United States of America
WHO	World Health Organization
YAP	Yes-associated protein

LIST OF UNITS

°C	Degree(s) Celsius
µg/mL	Microgram(s) per millilitre
µL	Microlitre(s)
cm	Centimetre(s)
Da	Dalton
g	Gram(s)
kV	Kilovolt(s)
m	Metre(s)

mg	Milligram(s)
mL	Millilitre(s)
mm	Millimetre(s)
mM	Millimolar
nm	Nanometre
pg/µL	Picogram(s) per microlitre
ppm	Parts per million
V	Volt(s)
µA	Microampere
µL/min	Microlitre(s) per minute
µm	Micrometre(s)
µM	Micromole

LIST OF CHEMICAL SYMBOLS

CO_2	Carbon dioxide
Fe	Iron
H_2O	Water
MeOH	Methanol

RESEARCH OUTPUTS

Part of the work in this dissertation was presented at the following:

- 50th Conference Anniversary of the Physiology Society of Southern Africa (PSSA), University of Limpopo, 25-28 August 2024
- XXXV International Academy of Pathology Congress (IAP 2024), Cancun, Mexico, 27-31 October 2024

ABSTRACT

Prostate cancer remains a significant health challenge globally, with growing interest in alternative treatment options. Once the safety and efficacy of alternative medicine are proven, it transitions from being “alternative” to mainstream. In Southern Africa, medicinal plants are widely available and form a crucial part of healthcare, with approximately 80% of the population relying on them for primary care. This rich botanical diversity offers potential for discovering novel treatments for prostate cancer, and the integration of such remedies into conventional medicine may provide safer, more holistic approaches to cancer care.

The aim of this study was to evaluate the effectiveness of the corms of *Hypoxis hemerocallidea* (African potato), *Helichrysum caespititium*, and *Dicoma anomala* on the proliferation of DU145 prostate cancer cell line in vitro. Plants were collected, dried, ground, and extracted using methanol and distilled water as solvents. Extracts from the corms of *H. hemerocallidea*, *H. caespititium*, and *D. anomala* were screened for their phytochemicals using high-resolution mass spectrometry. For the identification of compounds, using the negative and positive ion modes analysis allowed for mass fragments and molecular formula peaks recognition. The anti-oxidant activities of the corms were determined using 2,2-diphenyl-1-picrylhydrazyl (DPPH), 2, 2'-azino-bis (3-ethylbenzothiazoline-6-sulfonic acid) (ABTS), and Ferric reducing ability of plasma (FRAP) assays. The in vitro antiproliferative activity screening was evaluated using fluorescent stains, namely bisBenzamide H 33342 trihydrochloride and propidium iodide. Moreover, the antiproliferative effects mechanisms were studied by investigating the phosphatidylserine translocation and mitochondrial membrane depolarisation after treating the cells with the extracts.

The extracts demonstrated 75% (DPPH) and 95% (FRAP) anti-oxidant activities, showing a strong positive correlation with the presence of phytochemicals such as phytosterols, phenolic acids, flavonoids, and terpenoids. *D. anomala* methanolic extracts exhibited an antiproliferative effect against the prostate cancer cell line DU145 with an IC_{50} value of 18.98 µg/mL. Cell cycle analysis showed DU145 prostate cancer cell death through cell arrest at the early M phase and S phase respectively. Depolarisation of mitochondrial membrane and cleaved caspase-3 increased after 48 hours of being exposed to *D. anomala* methanolic extracts. Cell cycle arrest,

phosphatidylserine translocation, caspase activation, and mitochondrial membrane depolarisation suggested that the *D. anomala* methanolic extract can induce cell death through apoptosis observed from the Annexin V-FITC and propidium iodide stain, with melphalan as a positive control. The methanolic and aqueous extracts from *H. hemerocallidea* (African potato) and *H. caespititium* did not exhibit any cell proliferation. The extracts were thus not used for further investigation on the DU145 prostate cancer cell line.

In conclusion, this study showed that *D. anomala* has the ability to induce apoptosis on the DU145 prostate cancer cell line. Conversely, *H. hemerocallidea*. and *H. caespititium* did not exhibit inhibitory effects on the DU145 prostate cancer cell line compared to *D. anomala.*

Apoptotic activities and antioxidants properties of *D. anomala* highlight its potential as a therapeutic agent for treatment of prostate cancer. Further evaluation of *D. anomala* extracts on non-cancerous cell line and in vivo studies are recommended for safety profiling of the extract.

Keywords: *Hypoxis hemerocallidea* (African potato), *Helichrysum caespititium*, *Dicoma anomala,* Prostate cancer, DU145 cell line, Cell cycle arrest, apoptosis, antiproliferation, medicinal plants.

CHAPTER 1:
BACKGROUND

1.1 Introduction

More than 100 million people are reportedly using traditional complementary medicine, with a ratio of one traditional healthcare practitioner for every 500 patients across the African continent (Zhang, 2018). In South Africa, traditional medicine usage is seen as a tool that may aid in ensuring that Sustainable Development Goal 3, namely good health and well-being, is achieved as the healthcare system is experiencing increased levels of chronic illnesses such as cancer, in particular prostate cancer. The growing use of traditional complementary medicine is particularly relevant in the context of prostate cancer, as the ageing population and rising healthcare costs are driving more individuals to seek alternative treatments.

Medicinal plants, widely available in Africa, offer a cost-effective option for managing prostate cancer symptoms and other age-related conditions. As healthcare systems face increasing financial pressure, integrating these plant-based remedies into mainstream cancer care could provide affordable and accessible treatment solutions for the ageing population. Plant-derived metabolites have potent potential to clear free radicals; hence the increased interest in identifying their biologically active compounds (Kupe et al., 2021).

1.2 Normal prostate

The prostate is defined as an exocrine male accessory sex gland consisting of branched ducts and secretory acini. Embryologically, it is said to develop from the endodermal urogenital sinus, a process that is dependent on circulating foetal androgens (Prins, 2021). Androgens, male sex hormones such as testosterone, are produced by Leydig cells in the testes and regulated by the luteinising hormone, which is produced in the anterior pituitary gland. The complete absence of an androgen receptor (AR) or irregular-functioning AR results in failures in male sexual differentiation (Tan et al., 2015).

The prostate gland is histologically composed of epithelium and stromal components. Epithelium is critical in the development of benign and malignant disorders (El-Alfy

et al., 2000). The presence of physiologic androgens means that the normal prostate is in a steady state. The glands' self-renewing maintenance condition is composed of androgen-independent, androgen-sensitive, and androgen-dependent epithelial cells (Arnold & Isaacs, 2002).

1.3 Prostate cancer

Prostate cancer is a heterogeneous disease that leads to death in men worldwide. Cancers developing from the prostate gland are 95% adenocarcinomas with less common sarcomas and neuroendocrine tumours (El-Alfy et al., 2000). Most malignancies arise in the peripheral zone portion of the gland, the major glandular component of the prostate away from the prostatic urethra (Arnold & Isaacs, 2002).

A closer examination of the prostate's anatomical structure reveals that the stratified epithelium consists of two distinct layers: the basal layer, which is composed of low cuboidal cells, and the luminal layer, which is made up of columnar secretory cells, also known as luminal cells (Arnold & Isaacs, 2002). The luminal cells function as a synthesiser and secreter of the products of seminal plasma, including prostatic-specific antigen (PSA) and prostate-specific acid phosphatase (PAP), polyamines, and prostaglandins (Arnold & Isaacs, 2002). The protein PSA is commonly used as a biomarker for prostate cancer screening as their elevated levels can indicate prostate cancer or other prostate conditions. PAP is an enzyme historically used as a marker for prostate cancer, although its diagnostic role has decreased with the rise of PSA testing. Prostaglandins are lipid compounds involved in inflammation and cell signalling that play a role in prostate function and potentially in the progression of prostate cancer.

Prostate cancer risk factors include, but are not limited to, age, ethnicity, familial, genetic mutation, and dietary factors. The incidence has increased recently, largely due to better and earlier detection, but also because of the general ageing of the world's population and thus an increase in the proportion of men aged over 65 years old in whom the disease is known to be prevalent (Vashchenko & Abrahamsson, 2005). Figure 1.1 illustrates a histological cross-section of a normal prostate gland compared to one affected by prostate cancer, with the blue arrows indicating prostate cancer tissue and the yellow circle showing the narrowing of the urethra.

Figure 1.1: Histological cross-section of a prostate gland; (A) prostate cancer, and (B) normal prostate gland

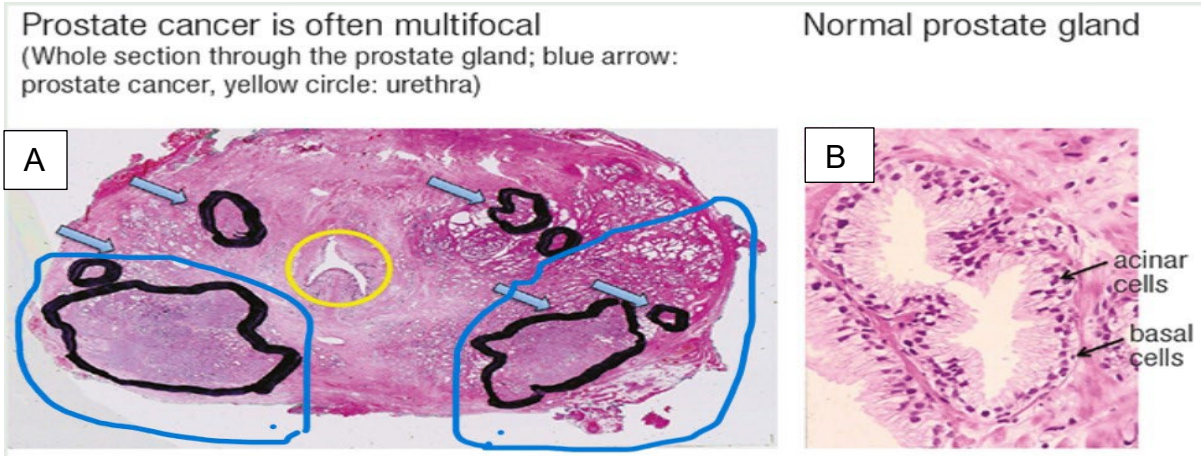

Source: Merrimen et al. (2013)

1.4 DU145 prostate cancer cell line

DU145 cells are a hypotriploid, epithelial, and adherent cell line derived from the brain lesion of a patient with metastatic prostate carcinoma. Figure 1.2 displays the characteristic morphology of the DU145 prostate cancer cell line. These cells serve as a model for AR-independent prostate cancer known to express estrogen receptor beta (ERβ), while lacking both the estrogen receptor alpha (ERα) and AR (Vashchenko & Abrahamsson, 2005). Although AR expression is observed in both AR-dependent and AR-independent prostate cancer cells (Arnold & Isaacs, 2002), the DU145 cells are unresponsive to AR deprivation therapy and AR-signalling pathways (Liao et al., 2013). This makes DU145 cells a crucial tool for studying advanced prostate cancer that does not respond to traditional hormone-based therapies and gaining insight into potential alternative therapeutic strategies.

Figure 1.2: High- and low-density morphology of the ATCC DU145 prostate cancer cell line

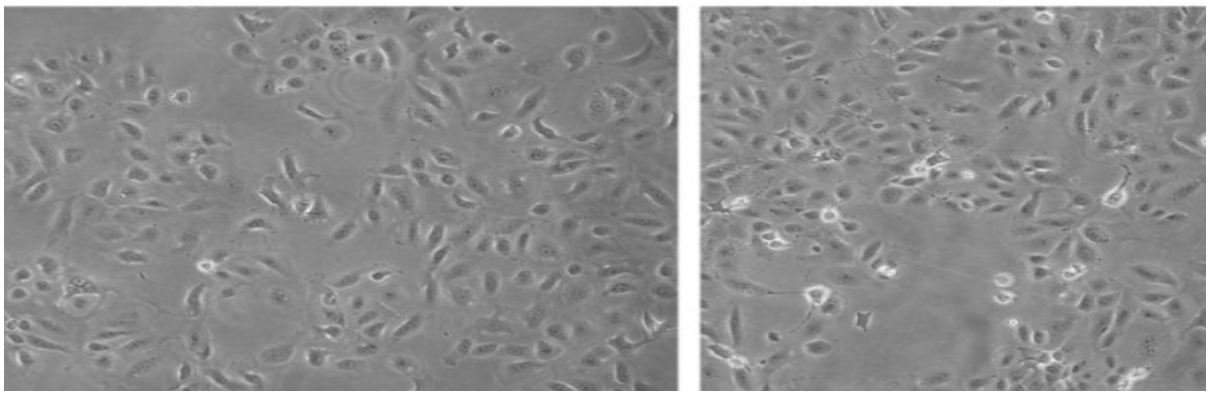

Source: Adopted from Stone et al. (1978)

1.5 Traditional medicine

The contribution of traditional medicine to the overall health management of patients has been acknowledged by societies and organisations, including the World Health Organization (WHO). Traditional medicine is said to provide preventative, curative, and palliative care to humans (Mothibe & Sibanda, 2019). Their usage can be traced to long before the advent of conventional medicine usage, and to this day it still serves the healthcare needs of the majority of the world population (Mothibe & Sibanda, 2019). Mothibe and Sibanda (2019) mention that African traditional healing is interwoven with cultural practices and religious beliefs, and it should therefore be regarded as holistic. Equally, socio-economic status and the accessibility and popularity of traditional medicine are factors that cause many people in Africa to prefer this route in their overall health management (Mothibe & Sibanda, 2019).

1.5.1 Traditional medicinal plants in South Africa

In South Africa, a health plan that includes traditional medicine is integrated within the healthcare system (Mothibe & Sibanda, 2019). Recent cases highlight the dualism in health-seeking behaviours, which are often driven by barriers in conventional healthcare, such as overcrowded facilities and the severe side effects associated with prolonged use of conventional medicine. As a result, the *Hypoxis hemerocallidea* (African potato), *Helichrysum caespititium*, and *Dicoma anomala* plants were chosen for this study based on anecdotal evidence. These plant extracts are commonly used when benign prostatic hyperplasia or prostate cancer is suspected, offering alternative treatment options rooted in traditional practices.

1.6 Research rationale

Prostate cancer is one of the most common cancers in males worldwide and is said to be the second most prevalent cancer that leads to deaths in males of all races (Ferlay et al., 2015). However, mortality rates are predominantly high in black populations, low in Asian populations, and intermediate in European regions (Ekwere & Egbe, 2002). Prostate cancer commonly affects elderly males with a mean age of 60 years. The management of prostate cancer is complex because of its biological diversity. Treatment consequences have been acknowledged by Dal Pra et al. (2010) in a

clinical study where patients with localised prostate cancer and treated by AR deprivation were associated with numerous side effects. These included sexual dysfunction, gynecomastia, and bone mineral loss.

New therapeutic targets are sought for locally advanced and metastasised prostate cancer. Developing novel complementary treatment options for prostate cancer has thus become an important medical need (Lin et al., 2012). There appear to be increasing recommendations to explore traditional herbal alternatives as they have numerous phytochemicals with pharmacological activities.

The corms of *H. hemerocallidea*, as well as *H. caespititium* and *D. anomala*, have traditionally been used in Southern Africa for managing prostate ailments such as benign prostatic hyperplasia and prostate cancer. *H. hemerocallidea* is valued for its anti-inflammatory and immune-boosting properties, while *H. caespititium* is known for its anti-oxidant and anti-inflammatory effects. *D. anomala,* recognised for its antitumour potential, is used to reduce swelling and inflammation. These plants, rich in beneficial phytochemicals, are commonly employed in traditional medicine as complementary therapies for prostate health.

This study hypothesizes that the corms of *H. hemerocallidea*, *H. caespititium*, and *D. anomala* have high yields of phenolic compounds and anti-oxidants. Moreover, extracts from these corms will inhibit DU145 cell proliferation because of their anticancer activity.

1.7 Aim

The aim of this study was to evaluate the effects of *H. hemerocallidea*, *H. caespititium*, and *D. anomala* corms on the proliferation of the DU145 prostate cancer cell line in vitro.

1.8 Objectives

The study sought to achieve the following objectives:

- To screen the phytochemicals present in *H. hemerocallidea*, *H. caespititium*, and *D. anomala*.

- To evaluate the anti-oxidant activities of *H. hemerocallidea*, *H. caespititium*, and *D. anomala*.
- To evaluate the in vitro antiproliferative effects of *H. hemerocallidea*, *H. caespititium*, and *D. anomala* on the DU145 prostate cancer cell line.
- To investigate the mechanism of action of *H. hemerocallidea*, *H. caespititium*, and *D. anomala* corms' anticancer activity on the DU145 cell line in vitro.

1.9 Methodology

1.9.1 Plant collection

All three plant species, namely *H. hemerocallidea, H. caespititium*, and *D. anomala*, were collected at the same time in April 2023 from the Bojanala district in the Rustenburg Local Municipality and the Mamerotse and Mogajane villages in the Bafokeng area from habitat along the plain roadside, where the plants were fully exposed to the sun and moderately to abundantly distributed. The bulk was sampled from sandy soil that had a well-drained moisture regime.

The plants were allocated the following herbarium specimen voucher numbers: ***Toona01:*** *H. hemerocallidea*, ***Toona02:*** *H. caespititium*, and ***Toona03:*** *D. anomala*. Specimens were deposited in the University of Johannesburg's Department of Botany and Plant Biotechnology, Faculty of Science, Auckland Park Kingsway Campus.

Figure 1.3: Google Maps view of Mamoretse, Mogajane village, Bojanala district

1.9.2 Plant extraction

In extracting the corm of plants, selecting a suitable extraction method is crucial to preserve the desired phytochemicals or bioactive metabolites. The method followed in extracting corms from *H. hemerocallidea*, *H. caespititium*, and *D. anomala* is defined as the procedure of changing one phase of a solute to another phase. There are multiple procedures in extraction, namely maceration, Soxhlet extraction, modern supercritical fluid extraction, ultrasound-assisted extraction, and microwave-assisted extraction (Fonmboh et al., 2020).

Extraction procedures allow for bioactive compounds, also referred to as natural secondary metabolites, from various parts of a plant to be isolated as they have been proven to possess a spectrum of health benefits for humans and animals. Furthermore, a suitable extraction method, given the type of environment and genetics, is known to contribute to the amount of secondary metabolites found in plants (Kupe et al., 2021). However, there are noteworthy limitations with some extraction procedures, such as lack of prescribed sets of operations and the increasing pressure of looking for eco-friendlier extraction substitutes (Uwineza & Waśkiewicz, 2020).

Multiple ways may be utilised to ensure that bioactive metabolites are preserved, and careful attention should be paid to ensuring that the analytes that are suspected to be present in the compound are accurately identified. These ways include optimisation of cultivation conditions to improve specific yields of specific metabolites and the actual processing of the bioactive analytes that are being targeted.

This study focused on the single-step maceration procedure as it resembles daily life usage and mimics the pattern that traditional or spiritual healers use (Fonmboh et al., 2020). The sonication method was especially preferred to be used in conjunction with single-step maceration in preparing aliquot for analysing compounds for phytochemical screening and anti-oxidation activities.

The corms were cut from the main plant and distilled water (dH_2O) was used to wash the corms of *H. hemerocallidea*, *H. caespititium*, and *D. anomala*. *H. hemerocallidea* needed to be cut into smaller pieces to aid with the drying. Pieces of corms were left at room temperature (22 to 25 ˚C) to allow them to dry. All corms were crushed using

a miller to obtain a fine powder, which was subsequently kept in the dark (in brown paper bags) until further use.

1.9.2.1 Direction maceration method

Methanolic extract corm, comprising 5 g of dried, powdered corm, was macerated in 50 mL of methanol (MeOH) for four hours. A Labcon shaker at 180 revolutions per minute (rpm) at room temperature was used and the extracts were then filtered using Whatman filter paper. The extraction solvents were removed from the filtrate by evaporation under reduced pressure in a rotary evaporator at the maximum temperature of 40 ˚C. The concentrated extracts were stored in small glass bottles at 4 ˚C until further use (Ghomari et al., 2019). Similarly, aqueous (deionised water [ddH_2O]) extract corm, comprising 5 g of dried, powdered corm, was macerated in 50 mL of ddH_2O for four hours. A Labcon shaker at 180 rpm at room temperature was used and the extracts were filtered using Whatman filter paper. The extraction solvents were removed from the filtrate by freeze drying. The concentrated extracts were stored in small glass bottles at 4 ˚C until further use (Ghomari et al., 2019).

1.10 Thesis outline

This thesis is organised into seven chapters. Chapter 1 provides an overview of the research, while Chapter 2 offers a concise literature review. Chapter 3 focuses on the phytochemical screening of the extracts, while Chapter 4 details their anti-oxidant activities. Chapter 5 addresses the antiproliferative effects of the extracts, followed by an exploration of their anticancer mechanisms of action in Chapter 6. Finally, Chapter 7 presents the concluding evidence and findings of the study.

REFERENCES

Arnold, J., & Isaacs, J. (2002). Mechanisms involved in the progression of androgen-independent prostate cancers: It is not only the cancer cell's fault. *Endocrine-Related Cancer*, *9*(1), 61-73.

Dal Pra, A., Cury, F. L., & Souhami, L. (2010). Combining radiation therapy and androgen deprivation for localized prostate cancer – A critical review. *Current Oncology*, *17*(5), 28-38.

Ekwere, P. D., & Egbe, S. (2002). The changing pattern of prostate cancer in Nigerians: Current status in the southeastern states. *Journal of the National Medical Association*, *94*(7), 619.

El-Alfy, M., Pelletier, G., Hermo, L. S., & Labrie, F. (2000). Unique features of the basal cells of human prostate epithelium. *Microscopy Research and Technique*, *51*(5), 436-446.

Ferlay, J., Soerjomataram, I., Dikshit, R., Eser, S., Mathers, C., Rebelo, M., Parkin, D. M., Forman, D., & Bray, F. (2015). Cancer incidence and mortality worldwide: Sources, methods and major patterns in GLOBOCAN 2012. *International Journal of Cancer*, *136*(5), E359-E386.

Fonmboh, D. J., Abah, E. R., Fokunang, T. E., Herve, B., Teke, G. N., Rose, N. M., Borgia, N. N., Fokunang, L. B., Andrew, B. N., & Kaba, N. (2020). An overview of methods of extraction, isolation and characterization of natural medicinal plant products in improved traditional medicine research. *Asian Journal of Research in Medical and Pharmaceutical Sciences, 9*(2), 31-57.

Ghomari, O., Sounni, F., Massaoudi, Y., Ghanam, J., Kaitouni, L. B. D., Merzouki, M., & Benlemlih, M. (2019). Phenolic profile (hplc-uv) of olive leaves according to extraction procedure and assessment of antibacterial activity. *Biotechnology Reports, 23*, e00347.

Kupe, M., Karatas, N., Unal, M. S., Ercisli, S., Baron, M., & Sochor, J. (2021). Phenolic composition and antioxidant activity of peel, pulp and seed extracts of different clones of the Turkish grape cultivar 'karaerik'. *Plants*, *10*(10), 2154.

Liao, R. S., Ma, S., Miao, L., Li, R., Yin, Y., & Raj, G. V. (2013). Androgen receptor-mediated non-genomic regulation of prostate cancer cell proliferation. *Translational Andrology and Urology*, *2*(3), 187-196.

Lin, H. H., Chan, K. C., Sheu, J. Y., Hsuan, S. W., Wang, C. J., & Chen, J. H. (2012). *Hibiscus sabdariffa* leaf induces apoptosis of human prostate cancer cells *in vitro* and *in vivo*. *Food Chemistry*, *132*(2), 880-891.

Merrimen, J. L., Evans, A. J., & Srigley, J. R. (2013). Preneoplasia in the prostate gland with emphasis on high grade prostatic intraepithelial neoplasia. *Pathology Journal of the RCPA*, *45*(3), 251-263.

Mothibe, M. E., & Sibanda, M. (2019). African traditional medicine: South African perspective. *Traditional and Complementary Medicine*, *2019*, 1-27.

Prins, G. S. (2021). Developmental estrogenization: Prostate gland reprogramming leads to increased disease risk with aging. *Differentiation*, *118*, 72-81.

Stone, K. R., Mickey, D. D., Wunderli, H., Mickey, G. H., & Paulson, D. F. (1978). Isolation of a human prostate carcinoma cell line (DU145). *International Journal of Cancer*, *21*(3), 274-281.

Tan, M. E., Li, J., Xu, H. E., Melcher, K., & Yong, E. L. (2015). Androgen receptor: Structure, role in prostate cancer and drug discovery. *Acta Pharmacologica Sinica*, *36*(1), 3-23.

Uwineza, P. A., & Waśkiewicz, A. (2020). Recent advances in supercritical fluid extraction of natural bioactive compounds from natural plant materials. *Molecules, 25*(17), 3847.

Vashchenko, N., & Abrahamsson, P. A. (2005). Neuroendocrine differentiation in prostate cancer: Implications for new treatment modalities. *European Urology*, *47*(2), 147-155.

Zhang, Q. (2018). Global situation and WHO strategy on traditional medicine. *Traditional Medicine and Modern Medicine*, *1*(01), 11-13.

CHAPTER 2:
LITERATURE REVIEW

2.1 Cancer statistics

In 2019, the WHO considered cancer as the first or second leading cause of death before the age of 70 years in 112 of 183 countries and ranked third or fourth in 23 countries (Sung et al., 2021). It is estimated that the number of new cancer cases reached 19.3 million globally, and nearly 10 million people died from cancer in 2020 (Cao et al., 2021). Worldwide, the incidence rate for all cancers combined was 19% higher in men (222 per 100 000) than in women (186 per 100 000) in 2020, although rates varied widely across regions (Sung et al., 2021). This disease is said to be the main cause of morbidity and mortality in every world region, irrespective of the level of human development (Sung et al., 2021). Over time, in both developed and developing countries, due to multiple reasons, the disease has remained a burden, and factors such as ageing, burgeoning populations, and accelerating socio-economic development contribute to its prevalence (Cao et al., 2021). The South African provincial cancer mortality rate was found to be 95% (68 to 70 deaths per 100 000 individuals) around the year 2014 (Made et al., 2017).

Figure 2.1: Global prevalence of cancer

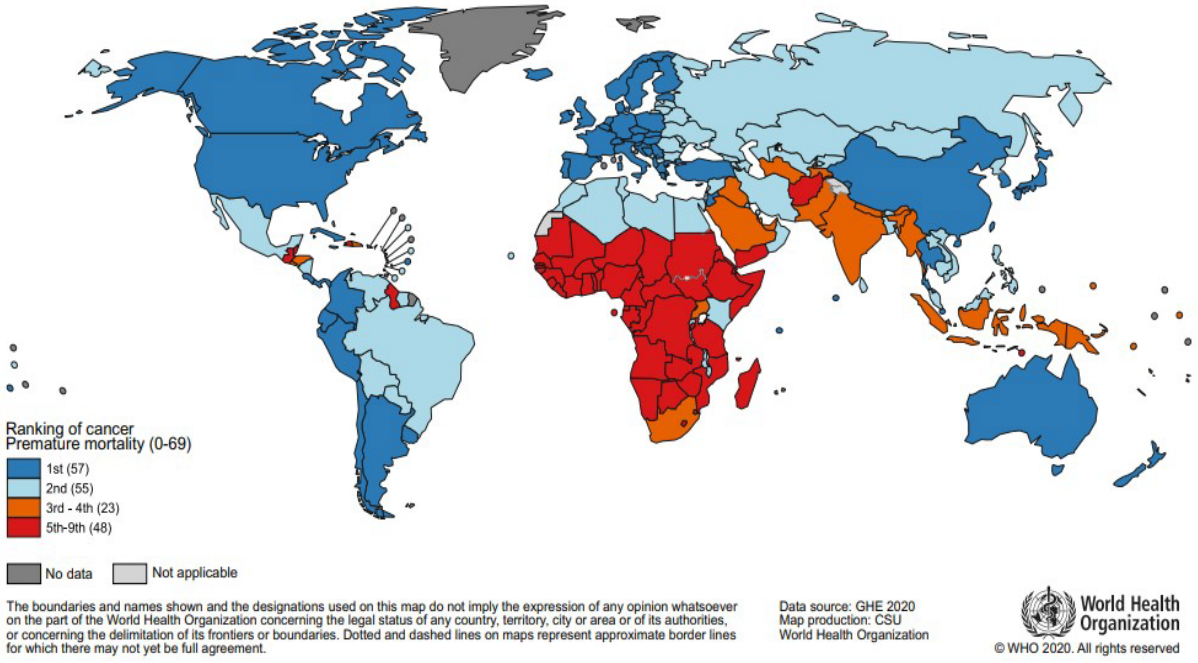

Source: Sung et al. (2021)

2.2 Prostate cancer statistics

Prostate cancer was the second most frequent cancer and the fifth leading cause of cancer death among men in 2020 (WHO, 2021). Incidence rates are said to be three times higher in developed countries than in developing countries (Sung et al., 2021). It is the most frequently diagnosed cancer in men in over one-half (112 of 185) of the countries of the world. Incidence rates vary from 6.3 to 83.4 per 100 000 men across regions, with the highest rates found in Northern and Western Europe, the Caribbean, Australia and New Zealand, North America, and Southern Africa (Sung et al., 2021). Accordingly, Torre et al. (2016) ranked prostate cancer as the most frequently diagnosed cancer in 112 countries, followed by lung cancer.

Table 2.1: Summary of incidence across cancers: 2019 to 2030

Incidence (No. of new cases per year)	2019	2022	2025	2028	2030
Female breast	19 860	22 148	24 685	27 534	29 593
Cervical	8 149	10 198	12 692	15 699	18 008
Prostate	17 554	22 110	27 989	35 728	42 181
Lung	5 985	6 877	7 924	9 169	10 120
Hodgkin lymphoma	794	986	1 232	1 546	1 804
Non-Hodgkin lymphoma	3 180	4 159	5 459	7 198	8 661
Leukaemia	2 074	2 440	2 893	2 457	3 907
Multiple myeloma	1 314	1 591	1 933	2 361	2 703
Other haematological cancers	1 580	1 687	1 797	1 913	1 991
Paediatric	1 466	1 550	1 630	1 691	1 727
Total	**61 957**	**73 744**	**88 234**	**106 296**	**120 696**

Source: Sung et al. (2021)

2.3 Current prostate cancer treatments

Cancer treatment has shown major improvements since the days of conventional surgery, radiation therapy, and chemotherapy, as single treatments or in combination. Compared to the current targeted combinational strategies that involve chemotherapeutics such as taxanes and platinum compounds, which have been found to have synergistic effects (Debela et al., 2021), modern modalities include hormone therapy, anti-angiogenic therapy, stem cell therapies, immunotherapy, and dendritic cell-based immunotherapy as some of several advancements made (Debela et al., 2021).

Several chemotherapeutic agents are available and are used in the management of prostate cancer, including abiraterone, enzalutamide, apalutamide, darolutamide, docetaxel, cabazitaxel, radium-223, and sipuleucel-T (Charmsaz et al., 2019).

The latter has been approved for advanced prostate cancer. However, advanced prostate cancers do not respond well to anticancer drug therapy comprising docetaxel and prednisolone. The recommendation of administering the medication continuously, frequently in low dosages, in order to decrease tumour growth is another challenge to cancer patients (Debela et al., 2021).

Additionally, prostate cancer patients who underwent castration or androgen ablation as a form of treatment experience insufficient androgen. The importance of androgen in male patients cannot be overlooked (Charmsaz et al., 2019). Insufficient androgen contributes to the amplification of cells that are maintained at the rate of proliferation equal to the rate of cell death and therefore remain limited and differentiate into transit cells (Arnold & Isaacs, 2002). In addition to the presented challenges is the overall funding that is directed towards communicable diseases such as HIV/AIDS and recently COVID-19. Cancer treatment resources remain limited to the population that needs it the most; hence the need for novel complementary traditional medicine (Debela et al., 2021).

2.4 Medicinal plants

The traditional use of plants dates back thousands of years. It comes with the legacy of the Neanderthal who valued herbs as medicinal agents 60 000 years ago, where the evidence is based on a grave in Iran in which pollen grains of eight medicinal plants were found (Aliya et al., 2016). Furthermore, plants with medicinal qualities were processed some 5 000 years ago and used to heal illnesses and injuries by ancient Sumerians (Aliya et al., 2016). Compiled recipes and the process of medicine on the Ebers Papyrus, for physicians' reference among the ancient Egyptians, were recorded 3 000 BCE (Aliya et al., 2016). The Indian system of medicine, the Rig-Veda, a sacred Hindu text, lists herbal medicines, and so too the Ayurvedic system for treatment. The Ayurvedic system is an ancient Chinese Pun-Tsao text that was found written in the 1600s listing herbal medicines. Similarly, in Greece, Hippocrates (considered the father of medicine) sought herbal remedies in the sixth century BCE as cures for illness and disease (Aliya et al., 2016).

Furthermore, nowadays traditional Chinese herbal medicines constitute a system of theories and therapies that were first documented in ancient Chinese classic literature dating back 2 100 years, and Africa, particularly Southern Africa, is no different (Zhou et al., 2017).

Medicinal plants' effectiveness depends on the numerous anti-oxidants that are known to help with protection against free radicals associated with diseases. The anti-oxidant compounds are regarded to be produced in plants in the form of secondary metabolites (Debela et al., 2021). In addition, there are phytochemicals, which can be referred to as "plant chemicals", which are described as non-nutritive chemical components possessing numerous health benefits and disease-prevention properties (Nwozo et al., 2023).

Phytochemicals are classified as primary constituents, including the common sugars, amino acids, chlorophylls, purines, and pyrimidines of nucleic acids, and proteins. Others are classified as secondary constituents, namely the chemicals that consist of alkaloids, flavonoids, terpenes, phenolics, lignans, plant steroids, curcumins, saponins, and glucosides, which are responsible for many functions in the body. It has been alluded by Aliya et al. (2016) that they have pharmacological effects such as anti-inflammatory, antispasmodic, anti-allergic, anti-oxidant, antibacterial, antifungal, chemo-preventative, neuroprotective, hypotensive, and anti-ageing properties, and, as such, most conventional Western medications are derived from medicinal plants (Nwozo et al., 2023).

2.4.1 *H. hemerocallidea* (African potato)

H. hemerocallidea belongs to the Hypoxidaceae family, representing the African branch of the Asparagales. The genus name *Hypoxis* is derived from the Greek word "hypo", which means "below", and "oxy", which means "sharp", which describes the pointed base of the capsule (Mofokeng et al., 2022).

This plant is commonly referred to as African potato, star flower, yellow star, star lily, or magic muthi (English), *inkomfe* or *ilabetheka* (isiZulu), *sterblom*, *sterretjie*, or *gifbol* (Afrikaans), *moli kharatsa* or *lotsane* (Sesotho), *inongwe*, *ilabatheka*, *ixhalanxa*, or *ikhubalo lezithunzela* (isiXhosa), and *tshuka-ya-poo* (Setswana) (Mofokeng et al., 2022).

Morphologically, *H. hemerocallidea* appears as smooth, black, glossy seeds, ovoid in shape, and about 2 mm in length. The plant has large, oblong, dark fibrous corms and tuberous roots that are bright yellow inside when freshly cut, but rapidly change colour after being cut. They are the focus of this study (Sikhakhane, 2013).

The plant grows as a stemless, perennial geophyte that reaches a height of up to 500 mm. It is characterised by six to 12 linear-lanceolate leaves, which are typically organised into three ranks and are hairy. The silhouette of the plant is scythe-shaped, while the leaves are usually surrounded by a dense mass of fibrous bristles resulting from the remains of dead leaves (Sikhakhane, 2013).

H. hemerocallidea is a wild tuberous plant that is native to the southern parts of Africa. It grows in the wild and is most prevalent in Southern Africa (mainly South Africa, Lesotho, Mozambique, and Zimbabwe).

The plant is said to have several medicinal uses and is considered the best-known medicinal plant among South Africans (Matyanga et al., 2020). It has been claimed that *H. hemerocallidea* can be used as an immune modulation phytotherapy in the management of immune-related diseases such as the common cold, flu, rheumatic arthritis, cancer, and HIV/AIDS (Elbagory et al., 2019). However, there are insufficient prostate cancer facts related to the corm's extracts of *H. hemerocallidea*.

Figure 2.2: (A) Photographic view of macroscopic plant *H. hemerocallidea*; (B) corm of *H. hemerocallidea*

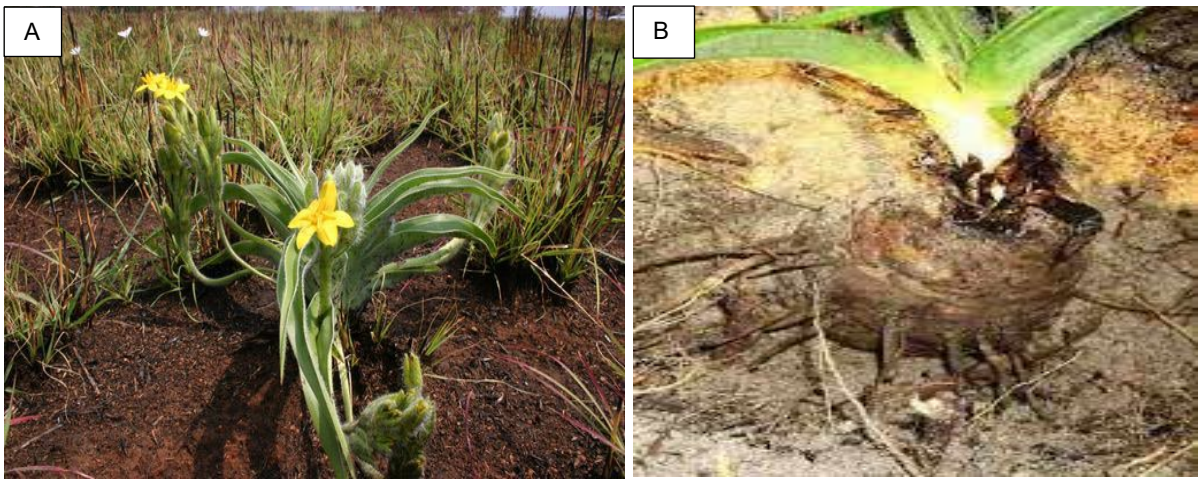

Source: Maroyi (2019)

2.4.2 *H. caespititium*

The species name *caespititium* is derived from the Latin word “caespitose”, which means “very much tufted and matted”, in reference to the cushion-forming or mat-forming growth habit of the species (Maroyi, 2019). It belongs to the Asteraceae or Compositae family. It is a perennial creeping herb that is known by several vernacular names in Southern Africa, which include golden everlasting (English), *sewejaartjies* or *speelwonderboom* (Afrikaans), *phate-ea-naha*, *boriba*, *moriri-oa-lefatse*, *lelulaphooko*, or *botsiki-nyane* (SeSotho), and *mabjana*, *matšana*, or *mmetse* (Northern Sotho) (Maroyi, 2019).

The height of *H. caespititium* ranges from 10 to 20 cm as recorded in open spaces in the grassland and savanna biomes, particularly disturbed areas at an average altitude range of 650 to 2 440 m above sea level.

The leaves are linear, clasping at the base, and hairy on both sides. The leaves are orange and gland-dotted with margins rolled under and densely crowded along the stems. The flowers of *H. caespititium* are white to yellow and pale and furry underneath. The plant has been used since ancient times for the treatment of several diseases such as broncho-pneumonia, tuberculosis, and intestinal ulceration (Mamabolo et al., 2018). Moreover, it is used in styptic wound dressing, particularly during circumcision rites (Mamabolo et al., 2018). A concoction of *H. caespititium* was taken by Bakwena and Bakgatla populations in ancient times for the treatment of gonorrhoea and other prostate-related ailments (Mamabolo et al., 2018). Maroyi (2019) alluded to pharmacological evaluations conducted on the plant, which found antibacterial and antifungal activities. The anticancer mechanisms of the extracts, however, have not been explored.

Figure 2.3: (A) Photographic view of macroscopic plant *H. caespititium*; (B) blue circle: corm of *H. caespititium*

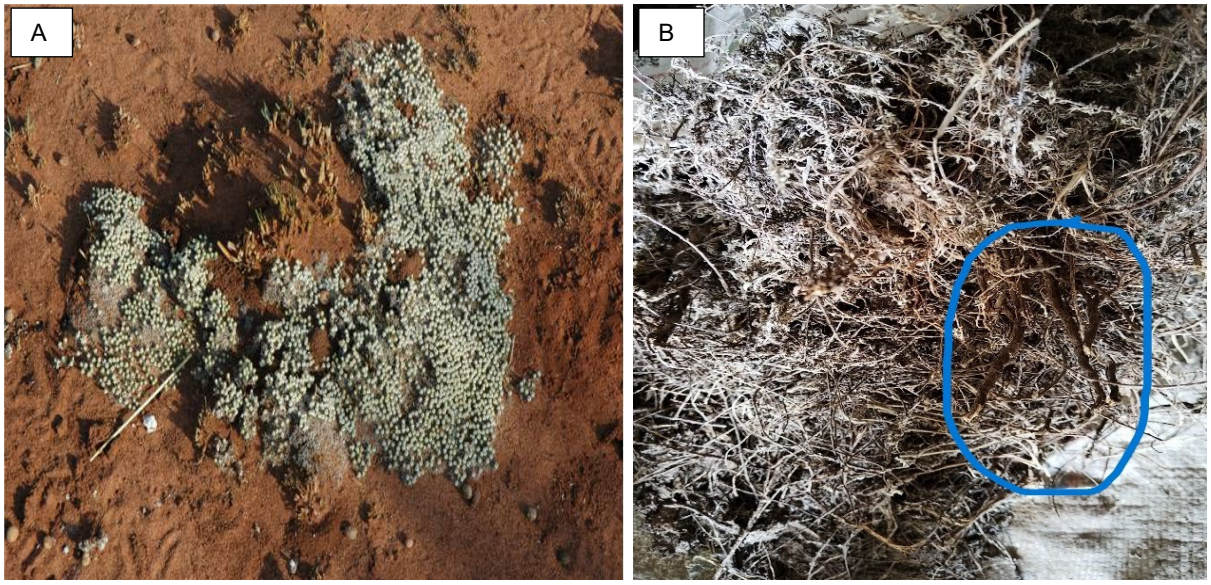

Source: Matyanga et al. (2020)

2.4.3 *D. anomala*

The word *Dicoma* is derived from two Greek words, “di” (two) and “kome” (tuft hair), and the word “anomala” is of Latin origin, which means “irregular”. *D. anomala* is a perennial herb that belongs to the family Asteraceae and they are commonly called fever or stomach bush (English), *hloenya* (Sesotho), or *tlhonya* (Setswana). It is a prostrate, decumbent, or erect perennial herb with an underground tuber. The stems are erect, thinly covered with hairs, and originate from a woody rootstock (Balogun & Ashafa, 2017). The leaves are simple, alternate, stalkless, linear, or narrowly lanceolatus. The flower heads are terminal, solitary or in small pairs, narrow, sharply pointed bracts and slender, white, mauve, purple, or pink tubular florets (Chota et al., 2020).

D. anomala leaves are narrow, stalkless, and positioned on the stem. The leaves can be described as rough and green, but mostly appear grey. The flower appears like a cup with terminal heads that look white or pinkish in colour. The plant is native to sub-Saharan Africa and is widely distributed across the country and predominantly found in the Limpopo, Gauteng, North West, Mpumalanga, KwaZulu-Natal, Free State, and Northern Cape provinces (Chota et al., 2020).

The ethnomedicinal uses of *D. anomala* are wide; its roots are extensively used in the therapy of at least 66 diseases that are known to affect humans and animals. However, South Africa has the highest number of ethnomedicinal uses of *D. anomala*, with at least 37 records for the treatment of various human illnesses (Balogun & Ashafa, 2017).

It is widely distributed in sub-Saharan Africa and is used in the treatment of cancer, malaria, fever, diabetes, ulcers, colds, and coughing (Chota et al., 2020). According to the literature, anticancer activity has been performed on *D. capensis*, which belongs to the same family as *D. anomala.* The findings demonstrated that *D. capensis* exhibited fewer side effects when compared to many chemotherapeutic agents such as androgen deprivation therapy (Rasethe et al., 2013). Chota et al.'s (2020) study further indicated that this plant species possesses novel chemicals that act as anticancer agents against three different breast cancer cell lines, namely MCF-7, MDA-MB-231, and MCF-12A (Chota et al., 2024).

The plant has an erect stem that is covered with thin hairs and bears an underground tuber (Chota et al., 2020). *D. anomala* is widely distributed across all nine provinces of South Africa.

Figure 2.4: (A) Photographic view of macroscopic plant *D. anomala*; (B) corm of *D. anomala*

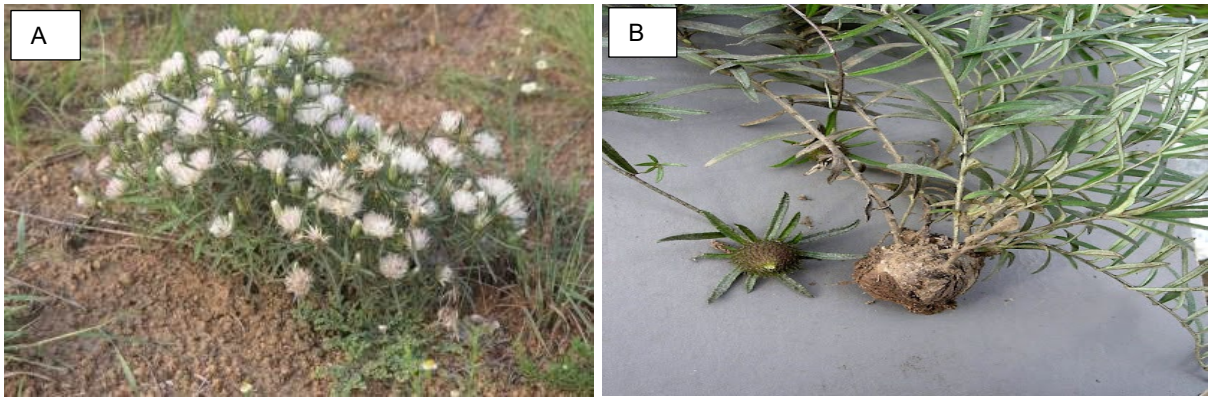

Source: Chota et al. (2020)

Notable benefits of *H. hemerocallidea* extracts are linked to the treatment of a variety of ailments, such as tuberculosis, testicular tumours, and cancers. In South Africa, the plant has been associated with HIV treatment. Extracts of *H. hemerocallidea* are taken as tonics to increase immune functions, for burn wound treatment, and prostate hypertrophy (Matyanga et al., 2020).

In addition, *H. caespititium* has demonstrated antimicrobial properties. The extracts have demonstrated treatment of several medical conditions from respiratory infections, sexually transmitted infections, wounds, to ulceration and it is also used as an aphrodisiac (Mathekga et al., 2000). Moreover, *D. anomala* herbs possess anticancer properties and have been used to treat various cancers in different parts of the world, including Europe and the Middle East. It has been shown to exhibit fewer side effects compared to many chemotherapeutic agents (Chota et al., 2020). The availability and affordability of medicinal plants and the favourable factor of its usage being aligned with inherited knowledge of the practice in local communities motivated this study. Additionally, the goal was to contribute to the current attention paid to quality control, especially of the finished product, of traditional medicinal plants.

REFERENCES

Aliya, S., Devi, Y., & Uma, A. U. (2016). Plants as potential resources of anticancer drugs. *Current Trends in Biotechnology and Pharmacy*, *10*(1), 92-107.

Arnold, J., & Isaacs, J. (2002). Mechanisms involved in the progression of androgen-independent prostate cancers: It is not only the cancer cell's fault. *Endocrine-Related Cancer*, *9*(1), 61-73.

Balogun, F., & Ashafa, A. (2017). Aqueous root extracts of *Dicoma anomala* (Sond.) extenuates postprandial hyperglycaemia in vitro and its modulation on the activities of carbohydrate metabolizing enzymes in streptozotocin-induced diabetic Wistar rats. *South African Journal of Botany*, *112*, 102-111.

Cao, W., Chen, H. D., Yu, Y. W., Li, N., & Chen, W. Q. (2021). Changing profiles of cancer burden worldwide and in China: A secondary analysis of the global cancer statistics 2020. *Chinese Medical Journal*, *134*(7), 783-791.

Charmsaz, S., Collins, D. M., Perry, A. S., & Prencipe, M. (2019). Novel strategies for cancer treatment: Highlights from the 55th IACR annual conference. *Cancers*, *11*(8), 1125.

Chota, A., Abrahamse, H., & George, B. P. (2024). Green synthesis and characterization of AgNPs, liposomal loaded AgNPs and $ZnPcS_4$ photosensitizer for enhanced photodynamic therapy effects in MCF-7 breast cancer cells. *Photodiagnosis and Photodynamic Therapy*, *48*, 104252.

Chota, A., George, B. P., & Abrahamse, H. (2020). Potential treatment of breast and lung cancer using *Dicoma anomala*, an African medicinal plant. *Molecules*, *25*(19), 4435.

Debela, D. T., Muzazu, S. G., Heraro, K. D., Ndalama, M. T., Mesele, B. W., Haile, D. C., Kitui, S. K., & Manyazewal, T. (2021). New approaches and procedures for cancer treatment: Current perspectives. *SAGE Open Medicine*, *9*, 20503121211034366.

Elbagory, A. M., Hussein, A. A., & Meyer, M. (2019). The in vitro immunomodulatory effects of gold nanoparticles synthesized from *Hypoxis hemerocallidea* aqueous extract and hypoxoside on macrophage and natural killer cells. *International Journal of Nanomedicine*, *14*, 9007-9018.

Made, F., Wilson, K., Jina, R., Tlotleng, N., Jack, S., Ntlebi, V., & Kootbodien, T. (2017). Distribution of cancer mortality rates by province in South Africa. *Cancer Epidemiology*, *51*, 56-61.

Mamabolo, M. P., Muganza, F. M., Olivier, M. T., Olaokun, O. O., & Nemutavhanani, L. D. (2018). Evaluation of antigonorrhea activity and cytotoxicity of *Helichrysum caespititium* (DC) Harv. whole plant extracts. *Biology and Medicine*, *10*(1), 1C.

Mofokeng, M. M., Prinsloo, G., Araya, H. T., Amoo, S. O., Du Plooy, C. P., & Mashela, P.W. (2022). Nades compounds identified in *Hypoxis hemerocallidea* corms during dormancy. *Plants*, *11*(18), 2387.

Maroyi, A. (2019). *Helichrysum caespititium* (DC.) Harv.: Review of its medicinal uses, phytochemistry and biological activities. *Journal of Applied Pharmaceutical Science, 9*(6), 111-118.

Mathekga, A. D., Meyer, J. M., Horn, M. M., & Drewes, S. E. (2000). An acylated phloroglucinol with antimicrobial properties from *Helichrysum caespititium*. *Phytochemistry*, *53*(1), 93-96.

Matyanga, C. M., Morse, G. D., Gundidza, M., & Nhachi, C. F. (2020). African potato (*Hypoxis hemerocallidea*): A systematic review of its chemistry, pharmacology and ethno medicinal properties. *BMC Complementary Medicine and Therapies*, *20*, 1-12.

Nwozo, O. S., Effiong, E. M., Aja, P. M., & Awuchi, C. G. (2023). Antioxidant, phytochemical, and therapeutic properties of medicinal plants: A review. *International Journal of Food Properties*, *26*(1), 359-388.

Rasethe, M. T., Semenya, S. S., Potgieter, M. J., & Maroyi, A. (2013). The utilization and management of plant resources in rural areas of the Limpopo province, South Africa. *Journal of Ethnobiology and Ethnomedicine*, *9*, 1-8.

Sikhakhane, X. (2013). Evaluating the anticancer and antimicrobial properties of extracts from *Hypoxis hemerocallidea* (African potato). University of Johannesburg.

Sung, H., Ferlay, J., Siegel, R. L., Laversanne, M., Soerjomataram, I., Jemal, A., & Bray, F. (2021). Global cancer statistics 2020: Globocan estimates of incidence and mortality worldwide for 36 cancers in 185 countries. *CA: A Cancer Journal for Clinicians*, *71*(3), 209-249.

Torre, L. A., Siegel, R. L., Ward, E. M., & Jemal, A. (2016). Global cancer incidence and mortality rates and trends – An update. *Cancer Epidemiology, Biomarkers & Prevention*, *25*(1), 16-27.

World Health Organization (WHO). (2021). *WHO guidelines for screening and treatment of precancerous lesions for cervical cancer prevention*. WHO.

Zhou, Z. H., Yang, J., & Kong, A. N. (2017). Phytochemicals in traditional Chinese herbal medicine: Cancer prevention and epigenetics mechanisms. *Current Pharmacology Reports, 3*, 77-91.

CHAPTER 3:
PHYTOCHEMICAL SCREENING OF THE PLANTS' CORMS

3.1 Phytochemical screening: High-resolution mass spectrometry (HRMS)

An analysis was done to identify critical components of the corms of *H. hemerocallidea*, *H. caespititium*, and *D. anomala*. Mass spectrometry is an analytical technique based on the measurement of the mass to charge ratio of ionic species related to the analyte being screened. The technique used allowed for molecular mass and elemental composition of analytes, as well as the structural elucidation of analytes to be determined (Pratima & Gadikar, 2018).

3.2 Sample preparation for HRMS

Solvents, namely MeOH and ddH_2O, were added to a pure dry sample of ~1 mg of each extract. A 50:50 mixture was then sonicated for five minutes to ensure there were no traces of particles. The mixture was diluted 10 times into Eppendorf vials of 100 µL sample and 900 µL of solvent each. The mixture was centrifuged for five minutes to remove any remaining particulates. Further dilution of X10 into sample vials was conducted, which comprised a 100 µL sample of supernatant and 900 µL solvent and used solvent as a blank (or control).

3.3 Materials and method for HRMS

3.3.1 Waters Acquity Ultra-Performance Liquid Chromatography (UPLC) Synapt G2 High Definition Mass Spectrometer (HDMS)

Figure 3.1: UPLC Synapt G2 HDMS

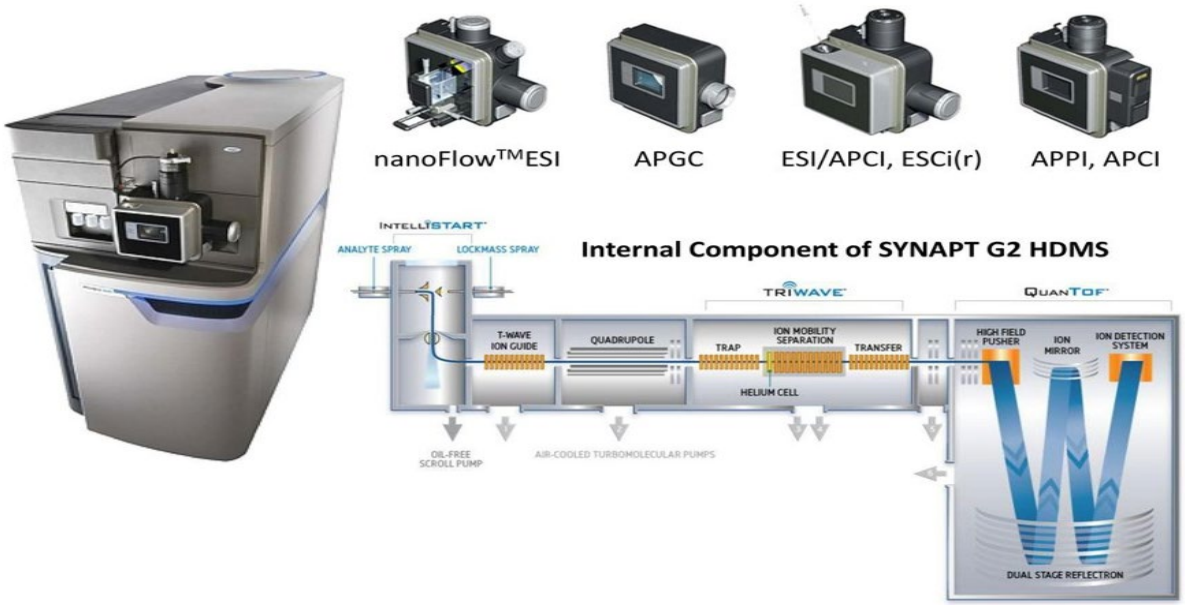

Source: Dit Fouque *et al.* (2021); Physical components of Instrument SYNAPT G2 HDMS (n.d.)

Liquid chromatography separates compounds according to their polarity by moving them through a stationary column using a polar or non-polar solvent. The mobile phase travels through the system and carries sample components with it once the sample has been injected. The stationary phase is held within the system by a support and does not move. As sample components pass through the system, components that have the strongest interactions with the stationary phase are highly retained by this phase and move through the system more slowly than components that have weaker interactions with the stationary phase and spend more time in the mobile phase (Hage, 2018).

Prepared extracts (see Section 3.2) were analysed using the Waters Acquity UPLC Synapt G2 High Definition Mass Spectrometer (Waters Inc., Milford, Massachusetts, United States of America [USA]). MassLynxTM (version 4.1) software (Waters Inc., Milford, Massachusetts, USA) was used to acquire and process data. Selective ionisation of polar species was achieved with an electrospray combined ion source (ESCI), which allows for quasi-simultaneous analysis alternating between electrospray ionisation (ESI) and atmospheric pressure chemical ionisation (APCI). The extracts

were infused at a flow rate of 5 µL/min. Capillary voltages of +4 kV and -2.5 kV were used to collect positive and negative ions respectively. The sampling cone was set to 40 V, while the extraction cone was set to 5 V. The source temperature was 120 °C and the desolvation temperature was 300 °C. A current of 20 µA was applied to the corona needle during the APCI experiments (Smit *et al.*, 2018).

The acquisition of ESI and APCI was done in separate functions and processed separately. Raw data were collected in the form of a continuous profile by combining 200 primary mass spectral acquisitions (scans). An automatic peak detection algorithm in the software was used to integrate mass spectral peaks and to obtain data where the area of each peak is represented by its height. Automated background subtraction was applied prior to integration. An external calibration of the m/z scale was performed using 8 sodium formate (mass range 112.936 to 1132.688 Da). A 200 pg/µL solution of leucine enkephalin (m/z 555.2693) was infused into the ion source throughout the analysis, and internal calibration was performed automatically by the software based on the measured and exact mass of this peptide. A resolution of 20 000 at m/z 200 (full width at half-maximum) was obtained. Elemental compositions were assigned to mass spectral peaks with an absolute intensity above 3 000 and 300 for the ESI and APCI respectively.

These arbitrary values were chosen based on close inspection of noise levels in the raw mass spectra. Both odd and even electron configurations were allowed, with a double bond equivalent (DBE) range of -1.5 to 30 and mass accuracy was specified to be within 5 ppm.

The following limits were applied to the range of atoms allowed: carbon: 0 to 50, hydrogen: 0 to 100, nitrogen: 0 to 2, oxygen: 0 to 5, and sulphur: 0 to 5. For positive ion mass spectra, sodium atoms (0 to 1) were also included to account for the formation of adducts.

3.4 HRMS analysis

The Waters Acquity UPLC® system was used to perform hydrophilic interaction liquid chromatography (HILIC). An XBridge BEH HILIC XP column (2.5 µm × 2.1 mm × 100 mm) was used together with an in-line pre-column filter (Phenomenex, KrudKatcher, 0.5 µm depth filter × 0.004 inch inner diameter). The column temperature

was kept constant at 25 °C and the injection volume was 5 µL. All the (ionisable) compounds eluted within three minutes. The same parameters were used for the ESCI time-of-flight mass spectrometry (TOFMS) as discussed above. Mass spectral scans (primary acquisitions) were collected every 0.2 seconds. Elemental compositions were assigned to mass spectral peaks with an absolute intensity above 300 for both ionisation methods, and mass accuracy was specified to be within 10 ppm.

To evaluate the separation achieved by employing HILIC, two different approaches were followed. Firstly, mass spectral scans were combined to obtain combined mass spectral scans for five retention windows for each of the chromatograms; in other words, for each window, 30 and 40 scans were combined into a single spectrum for the positive and negative ion modes, sequentially. Ideally, individual chromatographic peaks or mass spectral scans at specific retention times should be considered, but this was not possible due to low signal intensities. To investigate the effect of chromatographic pre-separation on the observable (ionisable) species, mass spectral scans collected throughout the chromatographic run (where sample peaks eluted) were combined to obtain a single mass spectrum, which was compared to the results obtained from direct mass spectrometric analysis (ESCI TOFMS).

The positive and negative ion mass spectra were collected in separate chromatographic runs (employing the same separation conditions) and consisted of a combination 10 of 150 and 200 mass spectral scans respectively. The combination of mass spectral scans was done specifically to obtain data that are directly comparable to the results obtained from analyses without chromatographic separation (i.e., direct infusion into the ion source). The ionisation efficiency of an analyte is determined by its chemical nature, as well as the presence of other (ionisable) compounds; i.e., matrix effects. Therefore, by comparing (combined) mass spectral data obtained with and without chromatographic separation, the effect of the chromatographic separation on ionisation efficiency can be evaluated.

3.5 HRMS results

3.5.1 Chromatogram profile obtained from methanolic extracts (negative mode)

Figure 3.2 demonstrates the chromatographic profile of *H. hemerocallidea* extract in negative mode, with a flow rate of 5 µL/min. in a time window of 0 to 20 minutes.

Figure 3.2: Chromatogram profile obtained from Methanolic A: *H. hemerocallidea* in negative mode

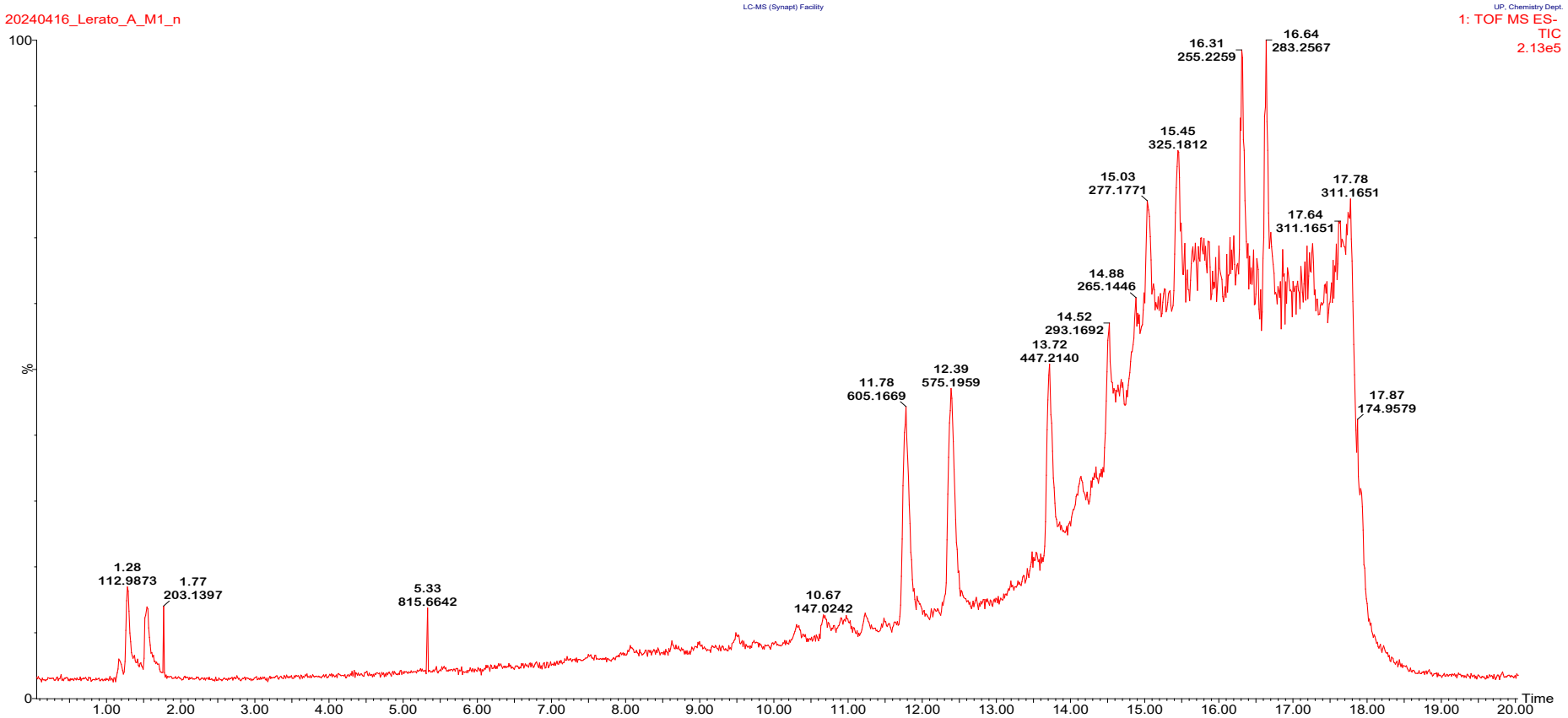

Figure 3.3 is a demonstration of the chromatographic profile of *H. caespititium* extract in negative mode, with a flow rate of 5 µL/min. in a time window of 0 to 20 minutes.

Figure 3.3: Chromatogram profile obtained from Methanolic B: *H. caespititium* in negative mode

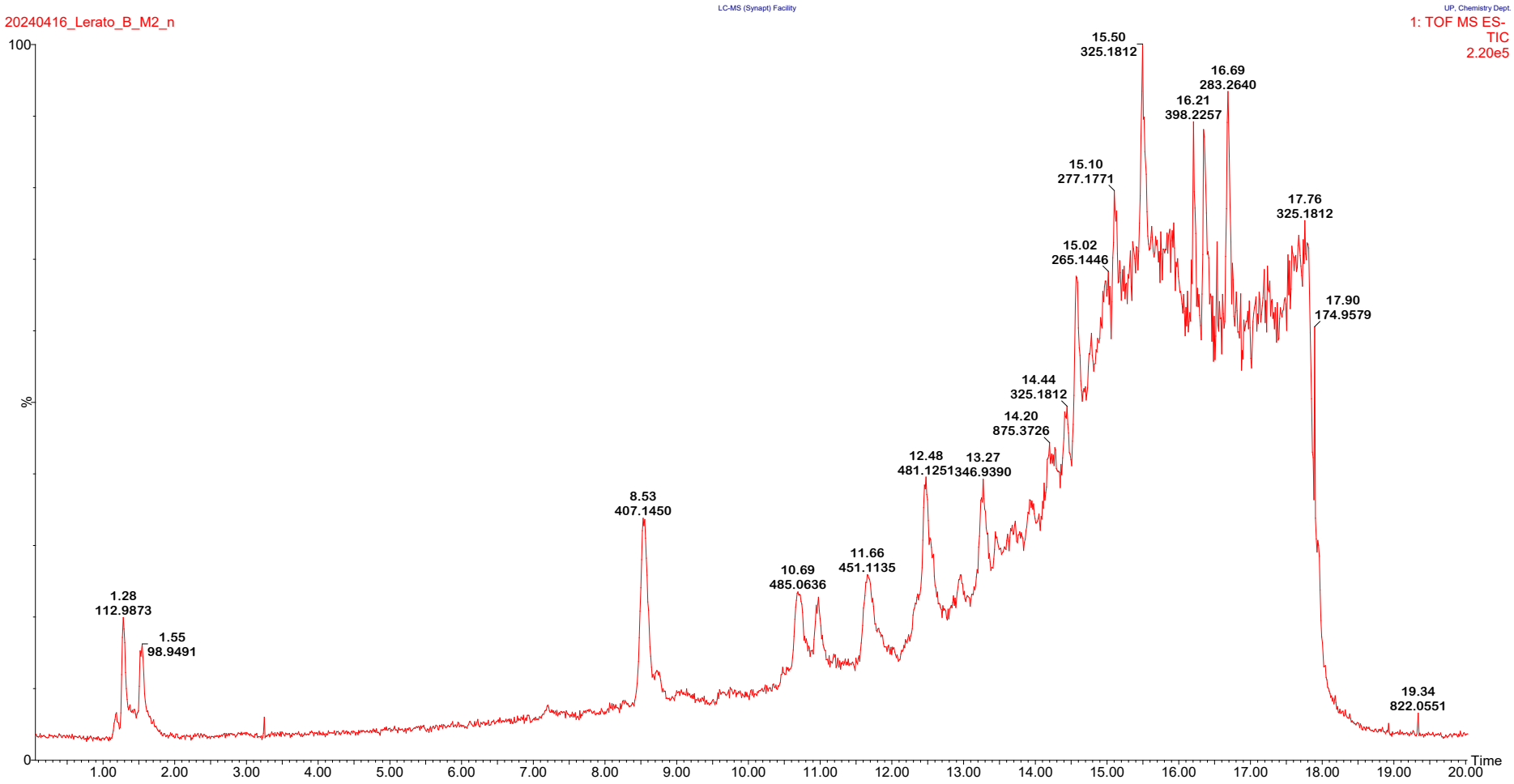

Figure 3.4 demonstrates the chromatographic profile of the *D. anomala* extract in negative mode, with a flow rate of 5 µL/min. in a time window of 0 to 20 minutes.

Figure 3.4: Chromatogram profile obtained from Methanolic C: *D. anomala* in negative mode

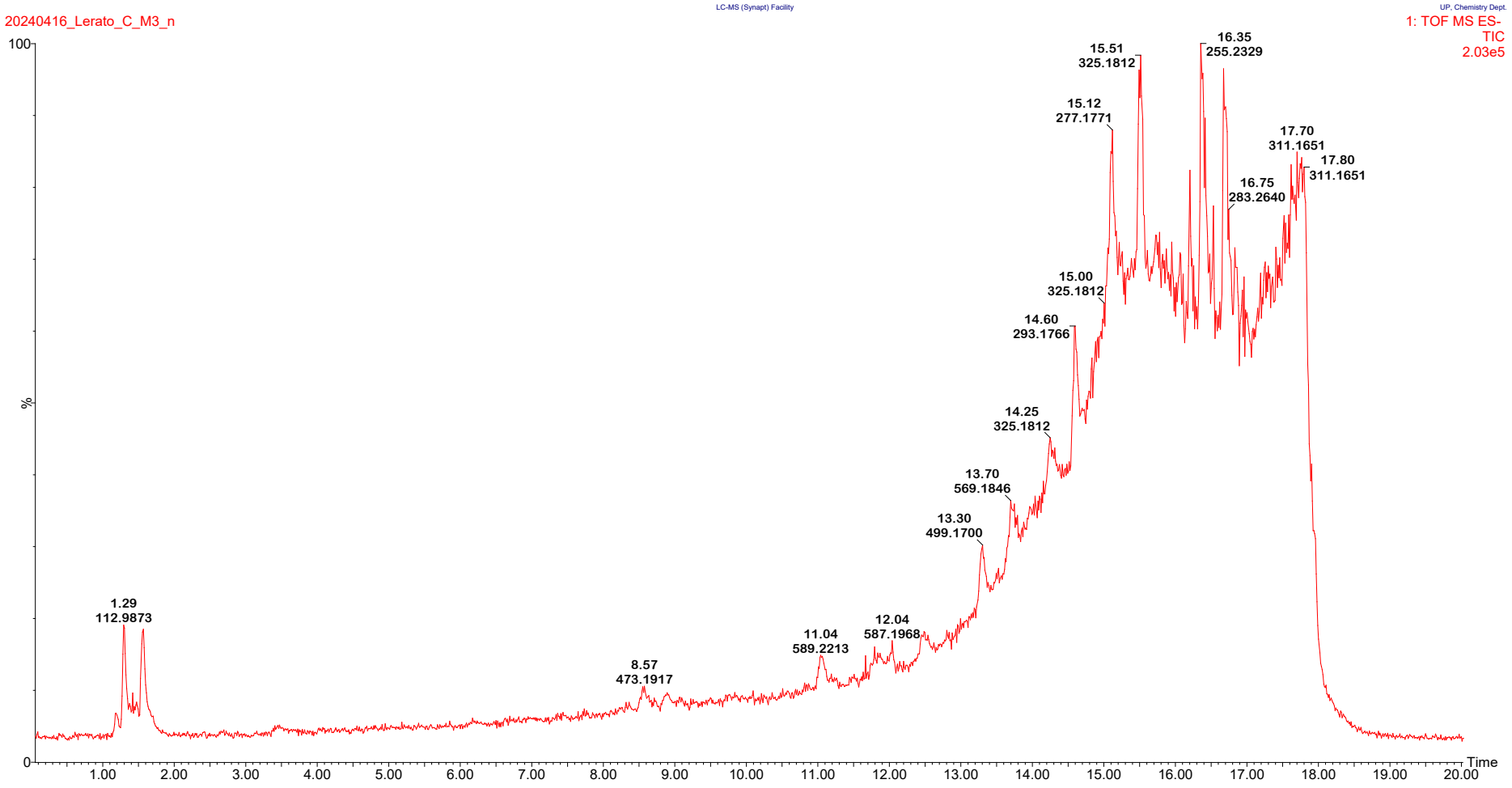

Figure 3.5 demonstrates the chromatographic profile of the *H. hemerocallidea* extract in positive mode, with a flow rate of 5 µL/min. in a time window of 0 to 20 minutes.

Figure 3.5: Chromatogram profile obtained from Methanolic A: *H. hemerocallidea* in positive mode

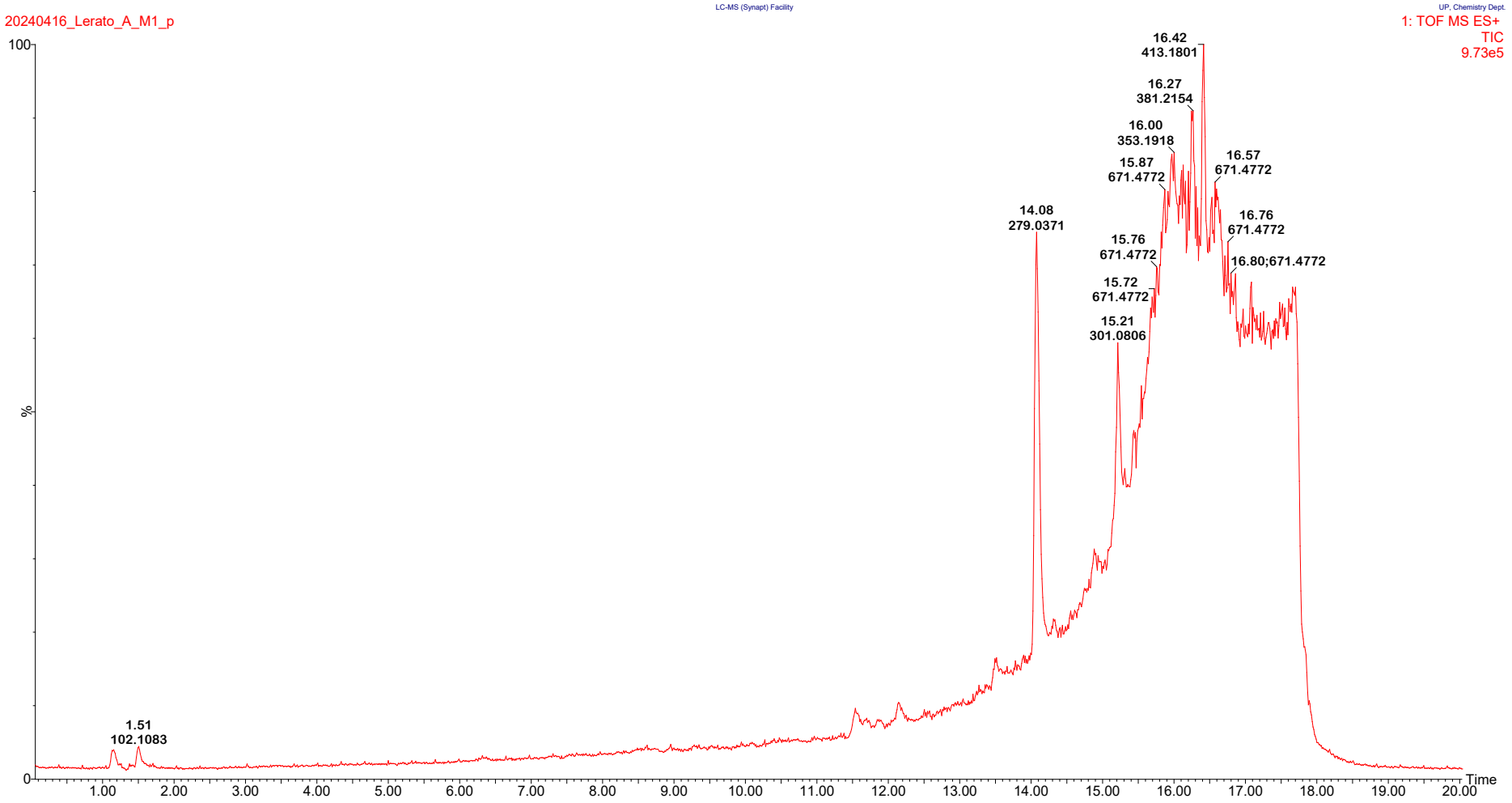

Figure 3.6 is a demonstration of the chromatographic profile of the *H. caespititium* extract in positive mode, with a flow rate of 5 µL/min. in a time window of 0 to 20 minutes.

Figure 3.6: Chromatogram profile obtained from Methanolic B: *H. caespititium* in positive mode

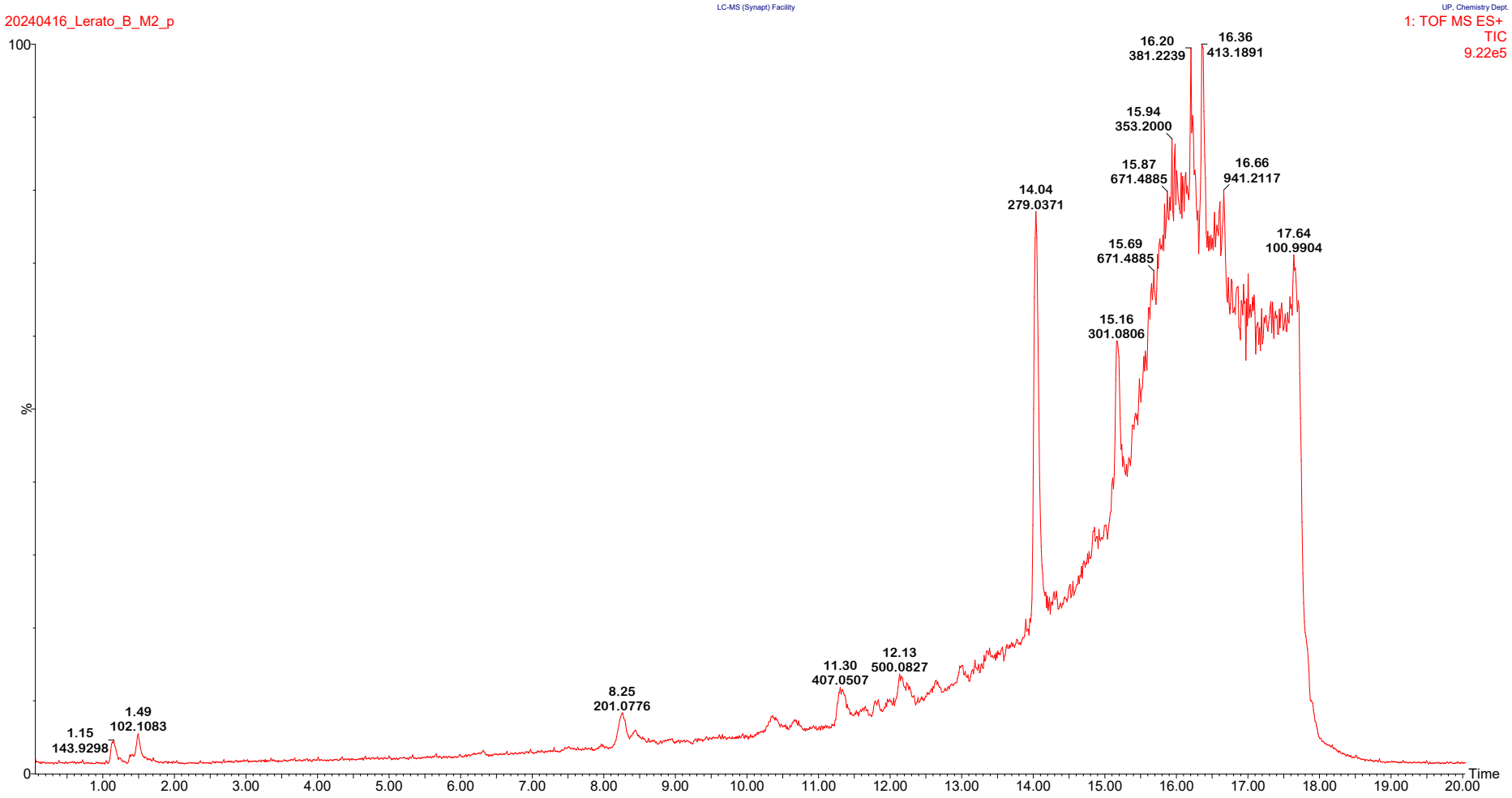

Figure 3.7 demonstrates the chromatographic profile of the *D. anomala* extract in negative mode, with a flow rate of 5 µL/min. in a time window of 0 to 20 minutes.

Figure 3.7: Chromatogram profile obtained from Methanolic C: *D. anomala* in positive mode

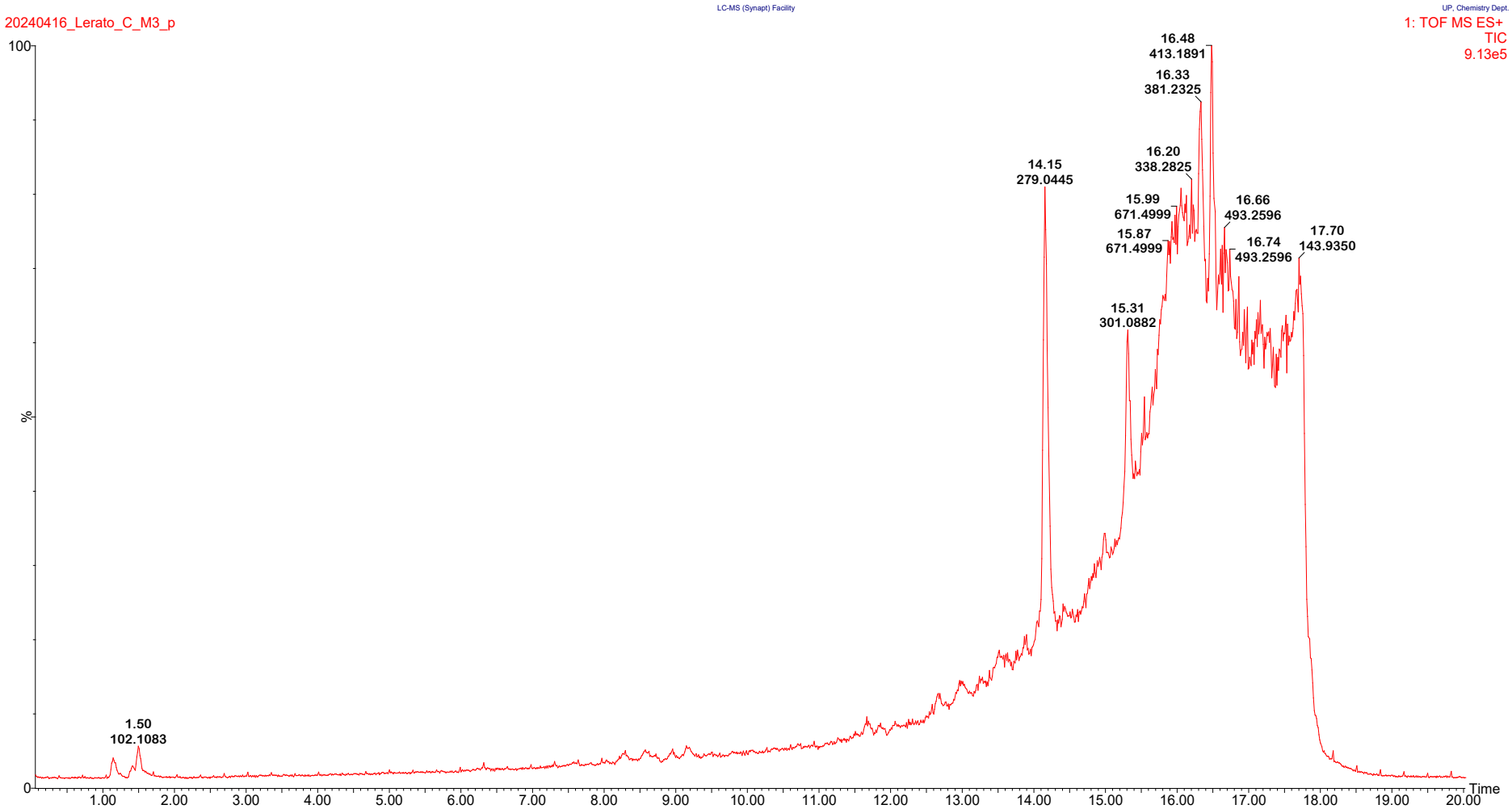

3.5.2 Chromatogram profile obtained from aqueous extracts (negative mode)

Figure 3.8. is the chromatographic profile indication of the *H. hemerocallidea* extract (aqueous) in negative mode, with a flow rate of 5 µL/min. in a time window of 0 to 20 minutes.

Figure 3.8: Chromatogram profile obtained from Aqueous A: *H. hemerocallidea* in negative mode

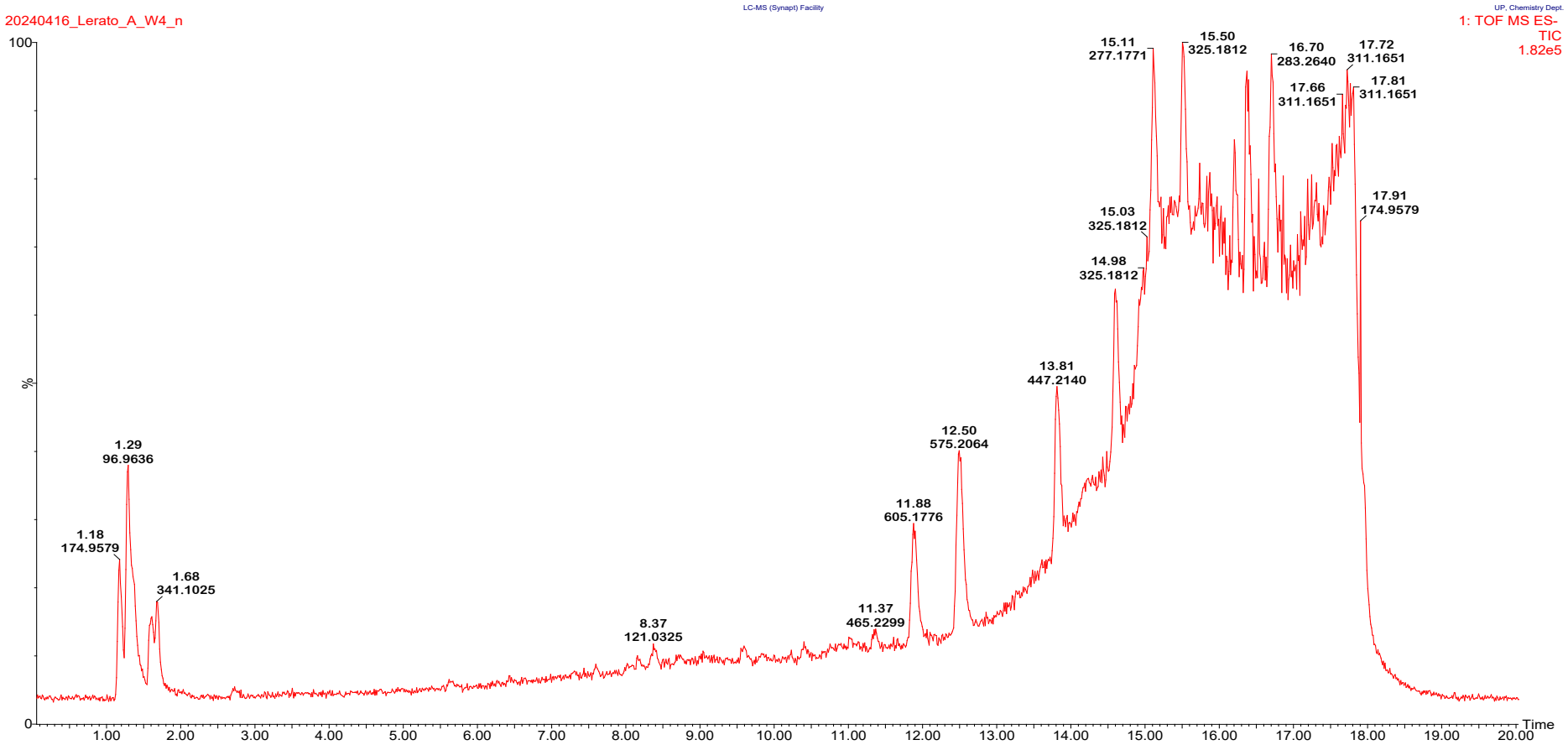

Figure 3.9 is the chromatographic profile indication of the *H. caespititium* extract (aqueous) in negative mode, with a flow rate of 5 µL/min. in a time window of 0 to 20 minutes.

Figure 3.9: Chromatogram profile obtained from Aqueous B: *H. caespititium* in negative mode

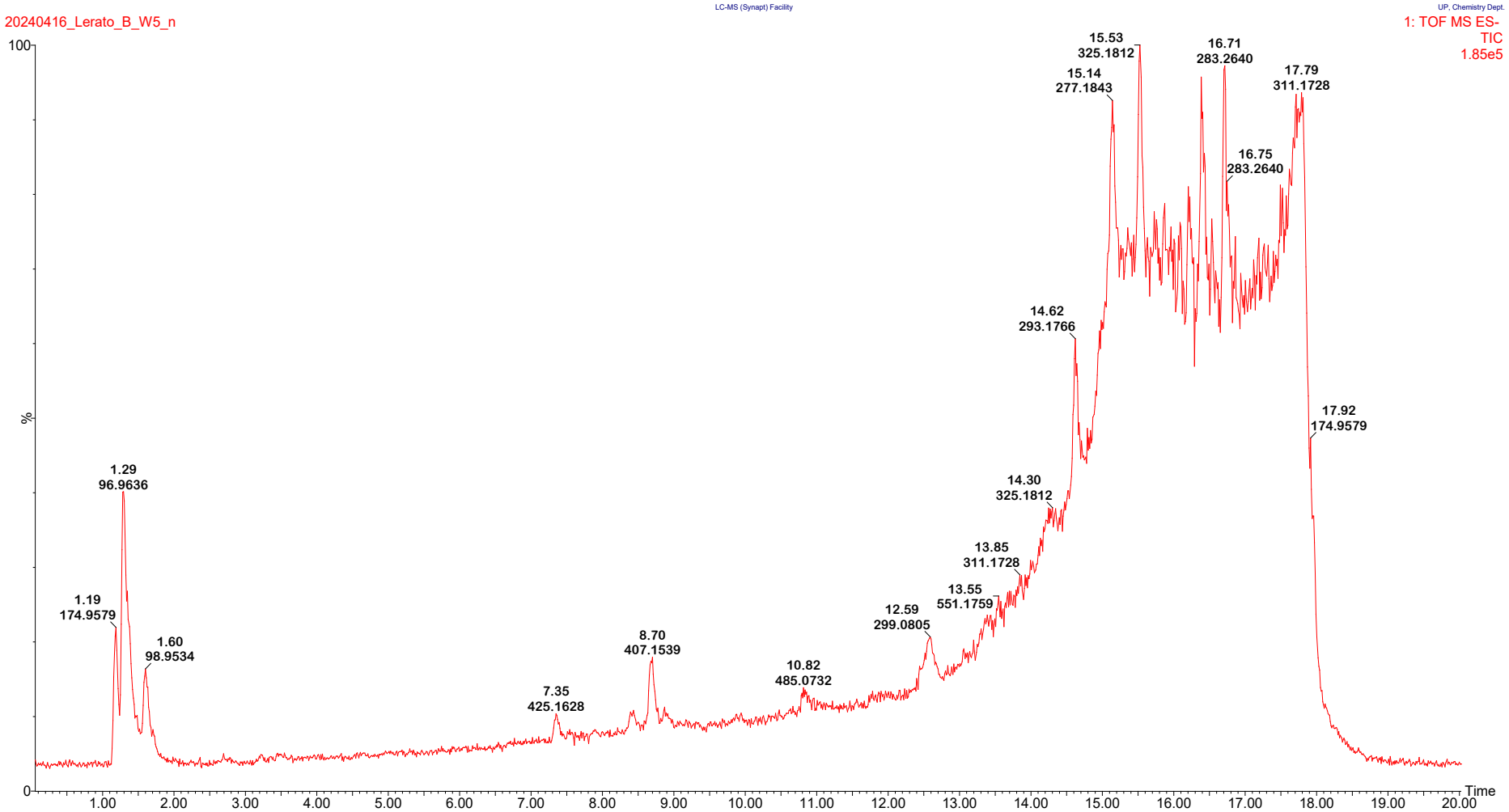

Figure 3.10 demonstrates the chromatographic profile of the *D. anomala* extract (aqueous) in negative mode, with a flow rate of 5 µL/min. in a time window of 0 to 20 minutes.

Figure 3.10: Chromatogram profile obtained from Aqueous C: *D. anomala* in negative mode

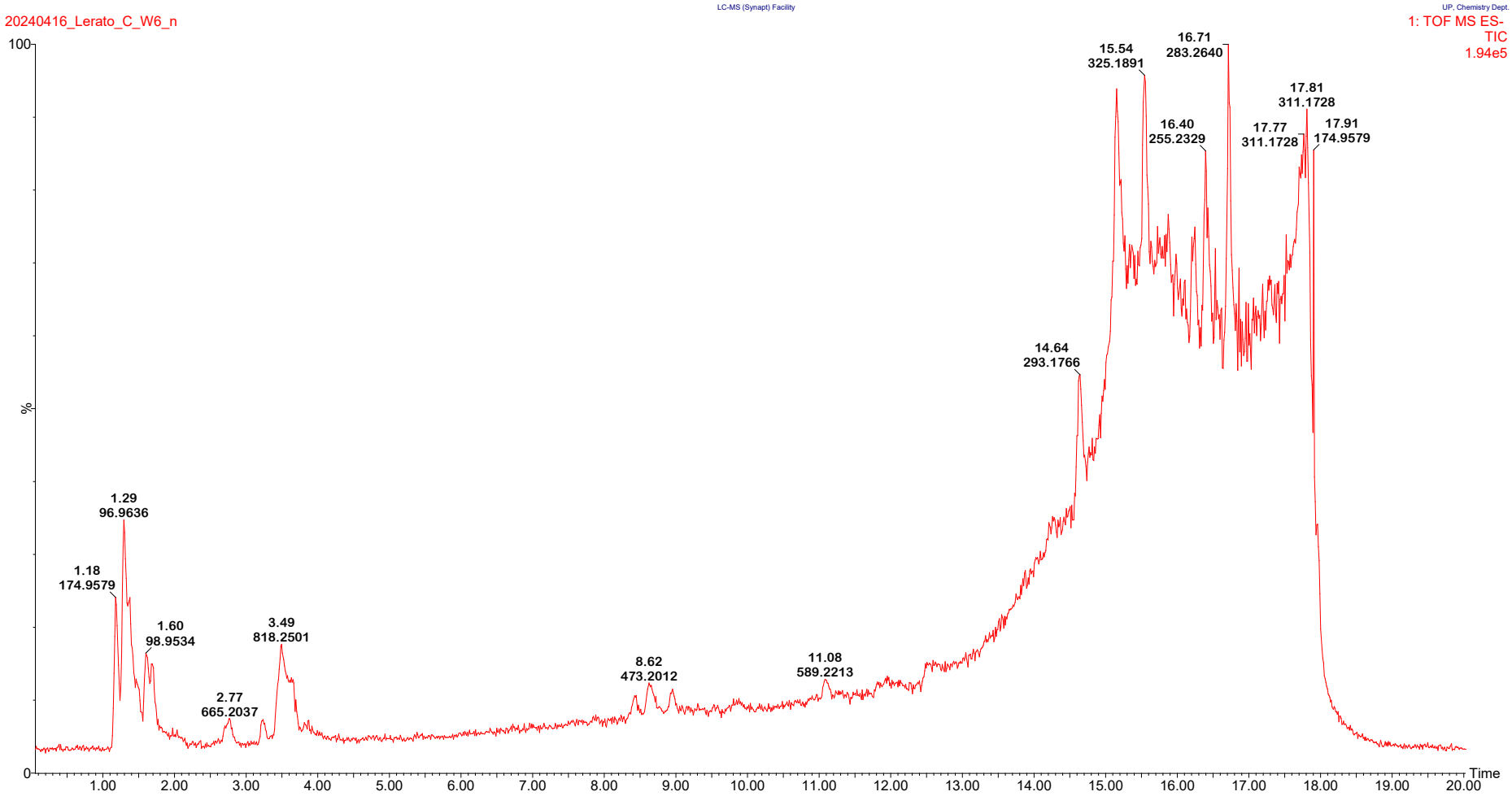

3.5.3 Chromatogram profile obtained from aqueous extracts (positive mode)

Figure 3.11 is the chromatographic profile indication of the *H. hemerocallidea* extract (aqueous) in positive mode, with a flow rate of 5 µL/min. in a time window of 0 to 20 minutes.

Figure 3.11: Chromatogram profile obtained from Aqueous A: *H. hemerocallidea* in positive mode

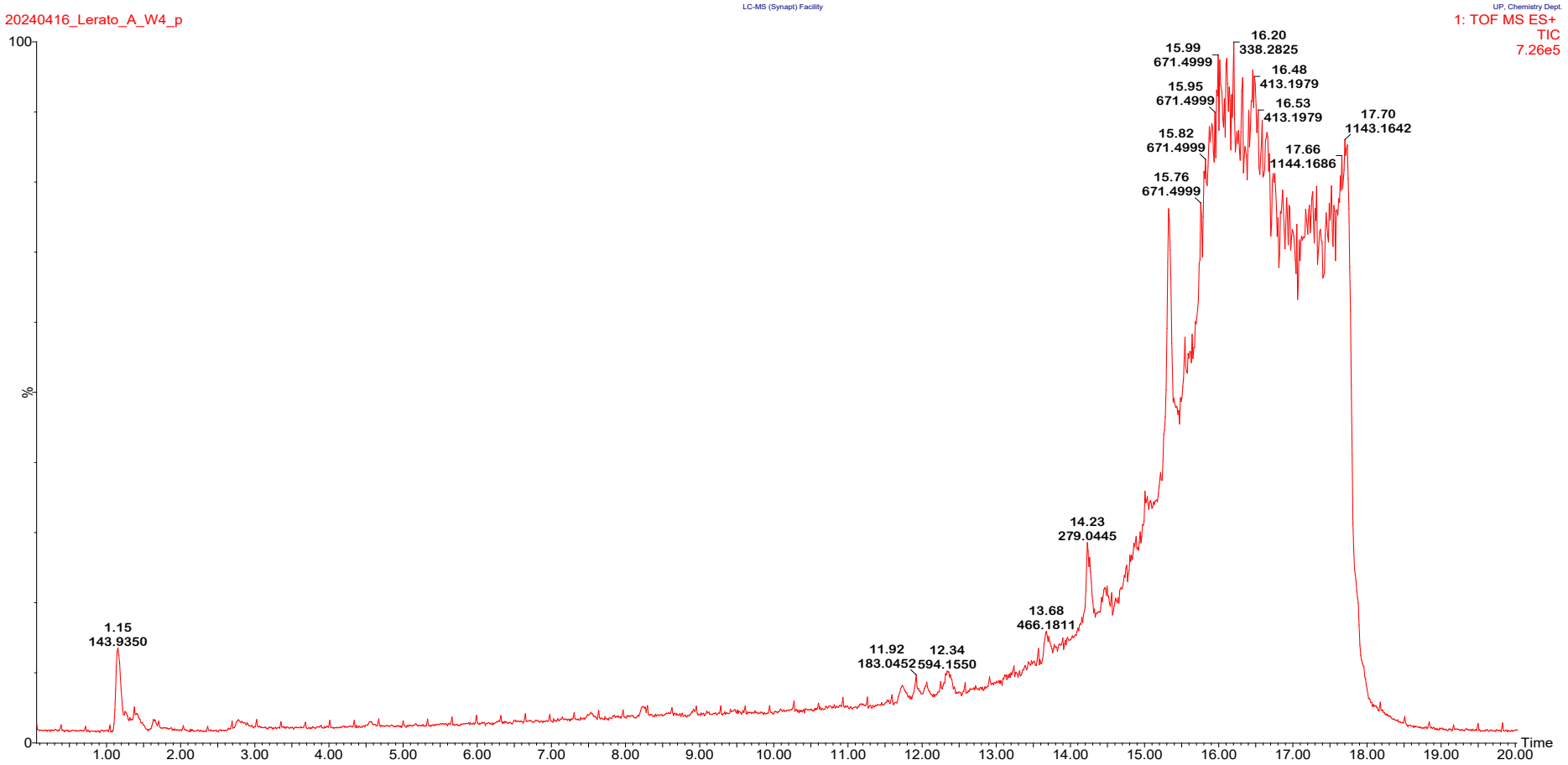

Figure 3.12 is the chromatographic profile indication of the *H. caespititium* extract (aqueous) in positive mode, with a flow rate of 5 µL/min. in a time window of 0 to 20 minutes.

Figure 3.12: Chromatogram profile obtained from Aqueous B: *H. caespititium* in positive mode

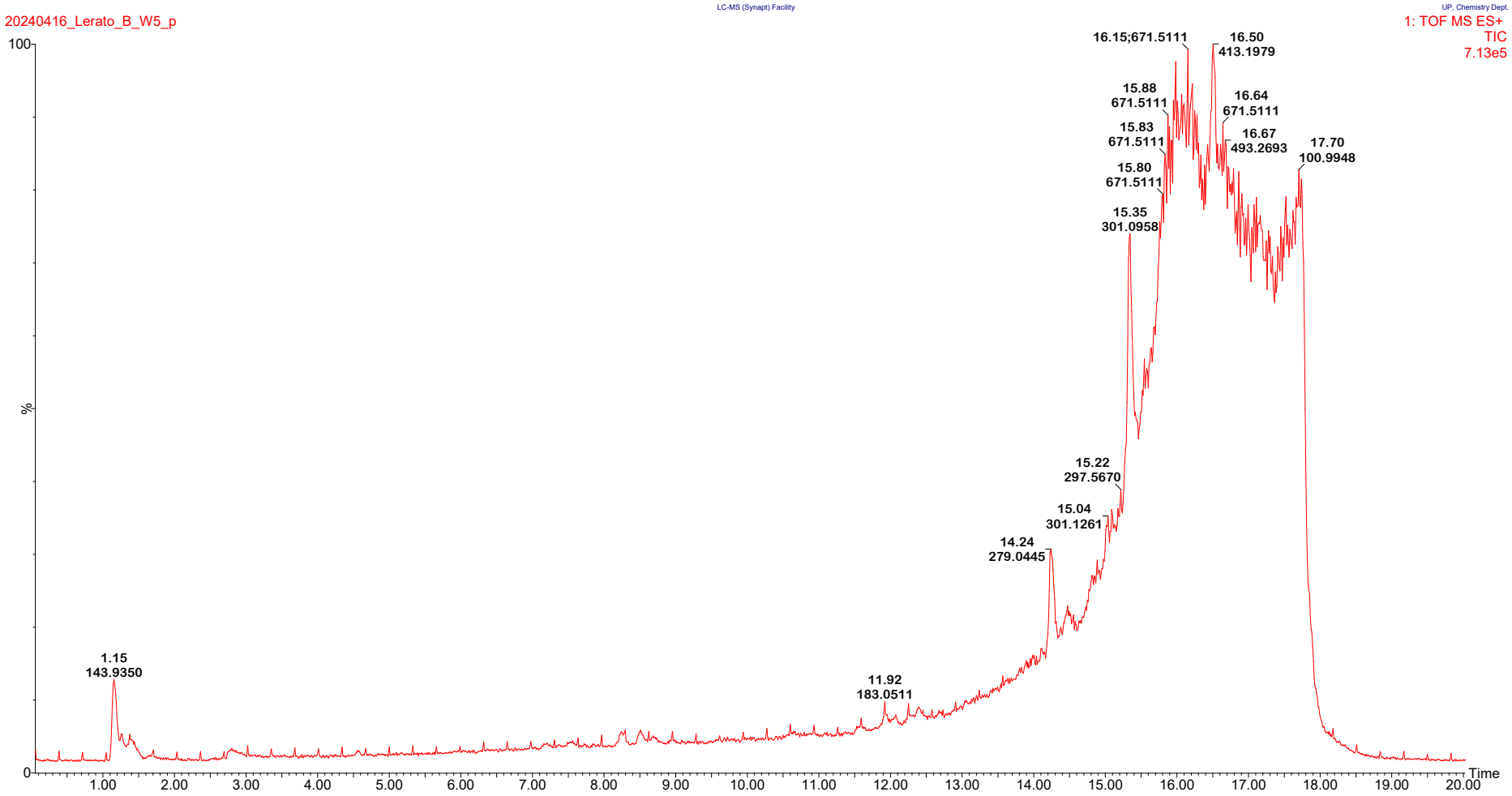

Figure 3.13 demonstrates the chromatographic profile of the *D. anomala* extract (aqueous) in positive mode, with a flow rate of 5 µL/min. in a time window of 0 to 20 minutes.

Figure 3.13: Chromatogram profile obtained from Aqueous C: *D. anomala* in positive mode

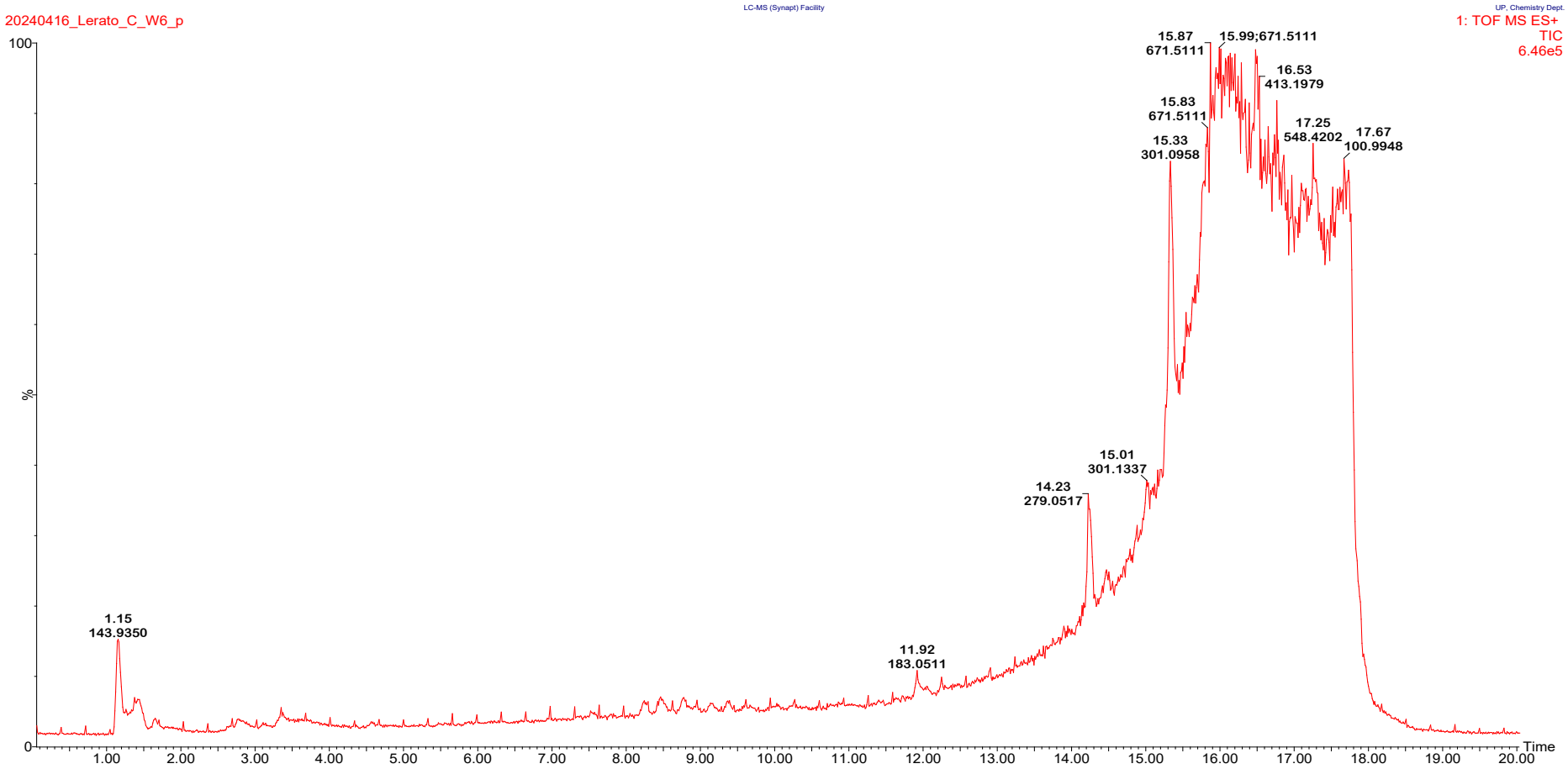

3.6 Discussion

The following was ascertained from the screening for phytochemicals in the *H. hemerocallidea*, *H. caespititium*, and *D. anomala* methanolic and aqueous extracts.

Firstly, the methanolic extracts of *H. hemerocallidea* chromatogram profile were measured in both the negative (see Figure 3.2) and positive (see Figure 3.5) ionisation modes. Based on the screening overview, cholesterol sulphate, 3beta,5alpha,6beta-trihydroxy-delta7-sterols, and 5,6-secosterols were present in the aqueous extracts (see Figures 3.8 and 3.11), resembling the same outcome as the methanolic extracts. This means that all three compounds are amphiphilic by nature as they could interact with and dissolve in both the aqueous and organic solvents. The phytochemicals identified are suggestive of the hypocholesterolemic component and similar to Matyanga et al.'s (2020) findings, which reported that all *Hypoxis* species have various sterols and glycosides. Sterols, also referred to as phytosterols, function in food as an inhibitor to the absorption of cholesterol from the diet. Additionally, phytosterols are said to possess prophylactic and therapeutic uses in hypercholesterolemia and cardiovascular disease (Matyanga et al., 2020).

Matyanga et al. (2020) also reported that phytosterols can affect different levels of tumour development and have immune-modulating properties. Applicable to this study is the claim made of the compound to initiate programmed cell death (PCD) in prostate cancer (Akuru & Amadi, 2018), which is a concept that further supports the investigation of these extracts' effects on the DU145 prostate cancer cell line; the results of which are discussed in Chapters 4 and 5.

Secondly, the methanolic extracts of the *H. caespititium* chromatogram profile measured in both the negative (see Figure 3.3) and positive (see Figure 3.6) ionisation modes displayed the following compounds: 1,3,5-trimethoxybenzene, 2,4,6-trihydroxytoluene and 2-nitrobenzene-1,3,5-triol, with the key emphasis of methoxybenzene, known as the biomarker of flavonoids. Flavonoids and phenolic components are the essence of these extracts, and the aqueous extracts' (see Figures 3.9 and Figure 3.12) outcome was similar to the methanolic counterparts.

Correspondingly, chemometric identification of chemical markers in *H. caespititium* extracts by Bassey et al. (2021) described the major marker of this plant to be 4-methyl2,4-bis(p-hydroxyphenyl)penet-1-ene, which was indicated for both the MeOH and acetone extracts, alongside 3,4-dihydroxymandelic acid.

These findings are similar to the assessment of total phenolic content estimation that showed *H. caespititium* ethanol extract to have higher total phenolic content in comparison to the aqueous extract; likewise, the estimated total flavonoids showed the MeOH extract to have a higher total flavonoid content when compared to the aqueous extract (Mfengwana, 2024). Interestingly, flavonoids are polyphenols with anticancer functions (Akuru & Amadi, 2018), which are properties that are relevant to this study.

Thirdly, the *D. anomala* methanolic extracts' chromatogram profile measured in both the negative (see Figure 3.4) and positive (see Figure 3.7) ionisation modes exhibited the following compounds: cirsimaritin, isoscutellarein 7,8,4'-trimethyl ether, scutellarein, isoscutellarein 5-O-Beta-D-Glucopyranoside, isoscutellarein 7-xyloside, and isoscutellarein 8-glucuronide, which are all categorised as flavonoids. Also noted was the presence of 10-Hydroxy-isolaurene, under the lipids category, and 1,3-Jimachaladiene, with the last two classified as isoprenoids, a terpenoids category. Similar peaks were observed in the aqueous *D. anomala* extracts (see Figures 3.10 and 3.13), with lower calculated mass in comparison to the methanolic extracts' calculated mass.

Flavonoids, terpenoids, and tannins are phytocompounds that possess the abilities of inducing tumour cell death. The molecular targets include apoptosis, cell cycle arrest, and proliferative inhibition pathways (Chota et al., 2020). Further analysis of the screened extracts is presented in Chapters 4 and 5 to evaluate the antiproliferative effects of these extracts.

In summary, based on the screening overview of the compounds, classes include those of phenolic acids, flavonoids, and tannins. This study's focus was on corm extracts of *H. hemerocallidea*, *H. caespititium*, and *D. anomala*; the expected compound to be noted during the screening was therefore phenolic acids as they are said to be concentrated in the bark (or corms) and leaves of the plants (Riaz et al., 2023). Phenolic substances are

said to be distributed throughout the entire metabolic process in the plants, and their existence in any form, particularly in the corms (roots) of *H. hemerocallidea* (African potato), *H. caespititium*, and *D. anomala* is said to be of greater medicinal value (Ghomari et al., 2019). As Riaz et al. (2023) argued that phenolic compounds inhibit enzymes that are associated with the development of human diseases, particularly cancer, these bioactive compounds have shown specific efficacy in targeting enzymes implicated in the progression of prostate cancer. Phenolics, through their anti-oxidant properties, can suppress the activity of enzymes such as 5-alpha-reductase and aromatase, both of which play critical roles in hormone regulation and cancer cell proliferation. By inhibiting these enzymes, phenolic compounds may help reduce the conversion of testosterone into dihydrotestosterone and estrogen, respectively, which are linked to the growth of prostate tumours. This enzymatic inhibition contributes to slowing down tumour progression and may offer protective benefits against the onset and advancement of prostate cancer.

REFERENCES

Akuru, U., & Amadi, B. (2018). Phytochemicals and antioxidant properties of some selected medicinal plants. *Journal of Pharmacognosy and Phytochemistry*, *7*(5), 283-285.

Bassey, K., Mamabolo, P., Mothibe, M., & Muganza, F. (2021). Phytochemical profiling and chemical marker compounds identification in *Helichrysum caespititium*: A chemometrics and 2D gas chromatography time of flight mass spectrometry (GCxGC-TOF-MS) perspective. *Pharmacognosy Journal*, *13*(2), 486-494.

Chota, A., George, B. P., & Abrahamse, H. (2020). Potential treatment of breast and lung cancer using *Dicoma anomala*, an African medicinal plant. *Molecules*, *25*(19), 4435.

Dit Fouque, K., Garabedian, A., Leng, F., & Tse-Dihn, Y. (2021). Trapped ion mobility spectrometry of native macromolecular assemblies. *Analytical Chemistry*, *93*(5), 2933-2941.

Ghomari, O., Sounni, F., Massaoudi, Y., Ghanam, J., Kaitouni, L. B. D., Merzouki, M., & Benlemlih, M. (2019). Phenolic profile (hplc-uv) of olive leaves according to extraction procedure and assessment of antibacterial activity. *Biotechnology Reports, 23*, e00347.

Gohari, A., Hajimehdipoor, H., Saeidnia, S., Ajani, Y., & Hadjiakhoondi, A. (2011). Antioxidant activity of some medicinal species using FRAP assay. *Journal of Medicinal Plants*, *10*(37), 54-60.

Hage, D. S. (2018). Chromatography. In N. Rifai, A. R. Horvath, C. T. Wittwer, & A. Hoofnagle (Eds.), *Principles and applications of clinical mass spectrometry* (pp. 1-32). Elsevier.

Matyanga, C. M., Morse, G. D., Gundidza, M., & Nhachi, C. F. (2020). African potato (*Hypoxis hemerocallidea*): A systematic review of its chemistry, pharmacology and ethno medicinal properties. *BMC Complementary Medicine and Therapies*, *20*, 1-12.

Mfengwana, P. H. (2024). Phytochemical constituents, ferric reducing and radical scavenging activities of *Helichrysm caespititium*. *Natural Product Research*, *9*, 1-6.

Munteanu, I. G., & Apetrei, C. (2021). Analytical methods used in determining antioxidant activity: A review. *International Journal of Molecular Sciences*, *22*(7), 3380.

Physical Components of Instrument SYNAPT G2 HDMS. (n.d.). https://images.app.goo.gl/7XoGfJNhpQezkLxv9

Pratima, N. A., & Gadikar, R. (2018). Liquid chromatography-mass spectrometry and its applications: A brief review. *Archives of Organic and Inorganic Chemical Sciences*, *1*, 26-34.

Riaz, M., Khalid, R., Afzal, M., Anjum, F., Fatima, H., Zia, S., Rasool, G., Egbuna, C., Mtewa, A. G., & Uche, C. Z. (2023). Phytobioactive compounds as therapeutic agents for human diseases: A review. *Food Science & Nutrition*, *11*(6), 2500-2529.

Smit, E., De Goede, S., & Rohwer, E. R. (2018). Class separation of the trace polar species present in diesel using hydrophilic interaction chromatography and high resolution mass spectrometry. *Energy & Fuels, 32*(9), 8944-8954.

CHAPTER 4:
ANTI-OXIDATION ACTIVITY OF THE CORM OF *H. HEMEROCALLIDEA* (AFRICAN POTATO), *H. CAESPITITIUM*, AND *D. ANOMALA*

4.1 Introduction

Normal cellular metabolism produces reactive oxygen species (ROS), which are reactive molecules responsible for cell structure damage and altering of cellular functions (Birben et al., 2012). Anti-oxidants, which may be classified as primary and secondary anti-oxidants, are enzymes that are expected to be the first line of cellular defence against oxidative damage (Jomova et al., 2011). Diseases such as prostate cancer develop when oxidative stress prevails over the activity of anti-oxidants. Oxidative stress is defined as a persistent imbalance between the generation of free radicals such as ROS and the ability of the intercellular anti-oxidant system to deactivate them (Rao et al., 2014). To evaluate the anti-oxidation activity of *H. hemerocallidea*, *H. caespititium*, and *D. anomala*, three methods classified under the spectrometry category were utilised for this study.

4.2 Sample preparation for anti-oxidation: Extraction by sonication method

Corms of *H. hemerocallidea*, *H. caespititium*, and *D. anomala* were extracted by dissolving 5 mL of MeOH mixed with a 0.250 g sample and 5 mL of ddH_2O as the other solvent. The mixture was vortexed for one minute, then sonicated (Argo Lab) for 30 minutes. Samples were removed for centrifugation (Eppendorf 5702R; Merck) for 10 minutes. The supernatant was steadily removed and further filtered with syringe filter (25 mm hydrophilic polytetrafluoroethylene). Anti-oxidants analysis was undertaken.

4.3 Materials and methods

4.3.1 2,2-diphenyl-1-perylhydrazyl (DPPH) anti-oxidant capacity assay

To determine the anti-oxidant reaction with an organic radical, the DPPH anti-oxidant capacity assay was conducted following the method by Kewuyemi et al. (2022). The DPPH radical is scavenged by anti-oxidants through the donation of protons forming the

reduced DPPH. The colour changes from purple to yellow after reduction. The degree of discolouration indicates the free radical-scavenging potentials of the sample anti-oxidant by their hydrogen-donating ability. The electrons pair off and the solution loses colour depending on the number of electrons taken up (Kalita et al., 2013).

The DPPH radical-scavenging assay method followed with slight modification of the working solution was prepared by dissolving 4 mg of DPPH (0.1 mM) reagent (Merck) in 100 mL of MeOH (Alimirah et al., 2006).

An amount of 15 µL test sample, Trolox standard or blank (ethanol), was placed in a 96-well microplate, after which 285 µL of working DPPH solution was added and left to stand in the dark for 30 minutes. The absorbance was read against blank at 517 nm using Accuris 96 Biospectrometer Kinetic.

The percentage scavenging activity was estimated using Equation 1 to determine the anti-oxidant activity of the MeOH and aqueous extracts (Kupe et al., 2021).

Equation 1: %Scavenging activity = $\frac{(A-A_S)}{A}$ x100

A-absorbance (blank), A_s -absorbance (MeOH, aqueous extract)

The results were expressed as µM Trolox Equivalent/g dry weight using standard curve (R^2 =0.75) (see Figure B1 in Appendix B).

4.3.2 2,2-Azinobis-(3-ethylbenzthiazolin-6-sulfonic acid) (ABTS) anti-oxidant capacity assay

To observe anti-oxidant reaction with an organic radical cation, the colourless ABTS molecule is converted into the blue-green coloured radical, ABTS radical cation ($ABTS^+$) by oxidation of one electron. The degree of discolouration indicates the free radical-scavenging potential of the sample by their hydrogen-donating ability (Kalita et al., 2013). The $ABTS^+$ assay was performed following the method by Kewuyemi et al. (2022), which was followed with slight modification where a mixed solution containing 7.6 mM of $ABTS^+$ (Merck) and 2.6 mM of potassium persulphate (Merck) solutions (19 mg / 5mL and

3.5 mg / 5mL respectively) and 5 mL of dH_2O was incubated in the dark at an ambient temperature for 16 hours.

One millilitre of the reaction solution was mixed with 60 mL of dH_2O to prepare a working solution. Thirty microliters of sample were mixed with 3 mL of the prepared solution and incubated for one minute at room temperature (Labcon). The resulting absorbance of the obtained mixture was determined against a blank.

The reduction of ABTS was estimated as % decolourisation using Equation 2 to determine the anti-oxidant activity of the MeOH and aqueous extracts.

Equation 2: % decolourisation = $\frac{(A-A_S)}{A}$ x100

A-absorbance (blank), A_S -absorbance (MeOH, aqueous extract)

The results were expressed as the µM Trolox Equivalent/g dry weight using standard curve (R^2 =0.37) (see Figure B3 in Appendix B).

4.3.3 Ferric reducing ability of plasma (FRAP) anti-oxidant capacity assay

To observe anti-oxidant reaction with an iron (Fe) (III) complex, the free radical-scavenging assay FRAP measures the reduction of ferric-tripyridyltriazine (Fe (III)-TPTZ) complex to its blue-coloured form ferrous-tripyridyltriazine (Fe (II)-TPTZ) at low pH in the presence of an anti-oxidant. The test solution is mixed with a known amount of FRAP reagent and the absorbance is measured at 590 nm (Gohari et al., 2011). The results are expressed as µM Trolox Equivalent/g dry weight using standard curve (R^2 =0.97) (see Figure B5 in Appendix B).

4.4 Anti-oxidant results: DPPH, ABTS, and FRAP

Table 4.1 shows the anti-oxidant activity of the methanolic and aqueous extracts of *H. hemerocallidea*,*H. caespititium*, and *D. anomala*.

Table 4.1: Percentage of scavenging activity by *H. hemerocallidea*, *H. caespititium*, and *D. anomala* methanolic and aqueous extracts

Samples	DPPH % inhibition	ABTS % inhibition	FRAP % inhibition
H. hemerocallidea (MeOH)	86.69 [0.07]	60.68 [0.26]	78.62 [0.35]
H. caespititium (MeOH)	89.09 [0.09]	89.19 [0.07]	59.50 [0.41]
D. anomala (MeOH)	89.79 [0.08]	82.09 [0.12]	50.00 [0.42]
H. hemerocallidea (dH_2O)	89.49 [0.06]	94.99 [0.03]	49.82 [0.43]
H. caespititium (dH_2O)	89.59 [0.06]	86.17 [0.35]	69.82 [0.42]
D. anomala (dH_2O)	89.69 [0.06]	79.38 [0.14]	49.99 [0.40]

*Mean values are different ($p \leq 0.05$). Values in square brackets are the standard deviations of the respective means.

4.5 Discussion

To evaluate *H. hemerocallidea*, *H. caespititium*, and *D. anomala*'s ability to neutralise free radicals, DPPH and ABTS assays were used. FRAP was used to directly measure the reducing capacity of the extracts (Kewuyemi et al., 2022). Conspicuous percentage inhibitions were observed in the aqueous *H. hemerocallidea* extracts (ABTS of 95% inhibition), followed by methanolic *D. anomala* (DPPH of 90% inhibition), and methanolic *H. hemerocallidea* (FRAP of 79% inhibition). The lowest percentage inhibition was from the aqueous *H. hemerocallidea* (FRAP of 49%) and aqueous *D. anomala* (FRAP of 50% inhibition) extracts respectively (see Table 4.1.).

The anti-oxidant components of the extracts resulted in the purple colour of the DPPH radical changing to yellow (see Figure B2 in Appendix B). The DPPH assay operates on the principle that DPPH, a stable free radical with an intense violet colour due to its unpaired electron, can be neutralised by anti-oxidants. When an anti-oxidant donates an electron or hydrogen atom, the DPPH radical is reduced to its stable, non-radical form (DPPH-H), leading to a noticeable colour change. This reduction causes the solution to shift from deep violet to pale yellow, with the extent of discolouration reflecting the anti-oxidant's effectiveness. In addition, the anti-oxidant capacity variability of the methanolic extracts from *H. hemerocallidea*, *H. caespititium*, and *D. anomala* was not substantial and mirrored the aqueous extracts.

Extracts or natural products are considered effective to prevent destructive processes caused by oxidative stress such as mutation in prostate cancer if they exhibit high percentages of anti-oxidants ideally as seen in DPPH assay high scavenging activity (Das

et al., 2014). Furthermore, phytosterols in *H. hemerocallidea*, phenolic acids in *H. caespititium*, and flavonoids, phenolic acids, and terpenoids seen in *D. anomala* support high anti-oxidant activity demonstrated by DPPH percentage inhibition. However, these high percentages should be regarded as highlighting the anti-oxidant activity of extracts or natural products in vitro, and not as a reflection of the actual anti-oxidant activity post-consumption (Tan et al., 2015).

Correspondingly, the cation radical colourless ABTS molecule was not converted to the blue-green coloured radical, $ABTS^{+}$ as expected; however, there was a colour change to lime green (see Figure B4 in Appendix B).

The highest anti-oxidant activity of aqueous extracts from *H. hemerocallidea* (ABTS of 95%) and the higher overall anti-oxidant scavenging activity, especially when compared to the FRAP results, was noticeable. However, the standard curve observed in ABTS (see Figure B3 in Appendix B) underpins the possibility of variables such as the pH and solubility of a compound in an environment to interfere with the analysis (Munteanu & Apetrei, 2021).

The assay is known to not take into account the reaction rates, which makes it difficult to accurately quantify anti-oxidant capacity; it is therefore recommended to perform multiple assays (Skowyra, 2014). Additionally, solvent polarity and pH exhibited some interferences with the rate of chemical reaction; thus impacting the extracts' ability to reduce ABTS and making the assay solvent and pH dependent (Tan & Lim, 2015). Nonetheless, the extracts from the *H. hemerocallidea*, *H. caespititium*, and *D. anomala* corms expressed favourable anti-oxidant properties.

In addition, the FRAP scavenging activity of the methanolic and aqueous extracts of *H. hemerocallidea*, *H. caespititium*, and *D. anomala* corms was the lowest in comparison to the DPPH and ABTS assays, particularly aqueous *H. hemerocallidea* (FRAP of 49%). An indication of the extracts' low reducing power and the possibility that anti-oxidants are slow to reduce the FRAP reagent (Moyo, 2016) may also have implications in the context of prostate cancer prevention or treatment. Prostate cancer cells are characterised by altered oxidative stress dynamics, and anti-oxidants play a critical role in modulating

these processes. Extracts with low reducing power may indicate the presence of anti-oxidants that are either less bioavailable or less effective under the assay's specific conditions. However, these same anti-oxidants could still provide beneficial effects in the prostate cancer microenvironment by selectively modulating ROS levels. For instance, some anti-oxidants may function indirectly by stabilising other bioactive compounds or enhancing the efficacy of therapeutic agents. Optimising the extraction and understanding the bioavailability of these compounds could help in developing plant-based therapies or supplements that target prostate cancer.

Secondary metabolites such as phytosterols, phenolic acids, flavonoids, and terpenoids are said to assist in elevating ROS even further and causing cell death. These compounds can elevate ROS levels in cancer cells beyond their tolerance threshold, which will lead to oxidative damage and apoptosis (PCD). This mechanism is particularly significant in prostate cancer treatment, as cancer cells often have heightened baseline oxidative stress. By further increasing ROS levels selectively in cancer cells, these compounds can induce cell death without harming normal cells, which makes them promising agents for therapeutic interventions. Moreover, Kumar et al. (2020) reported on gallic acid mediated cell death that was due to elevated ROS in DU145 human prostate cancer cells.

Moreover, anti-oxidants play an integral role in maintaining human health by preventing and treating diseases such as prostate cancer by their abilities to reduce oxidative stress (Munteanu & Apetrei, 2021). Similarly, the enormous role of anti-oxidants' properties has been recognised in overcoming the adverse effects of chemotherapeutic agents through the manipulation of the pharmacokinetics (Kupe et al., 2021). This is supported by the greater release or the enzymatic synthesis of bioactive compounds in the extracts.

Phenolic acids and flavonoids are known to be responsible for anti-oxidant enzyme cofactors and oxidative enzyme inhibitors that possess the ability to scavenge free radicals. Subsequently, DPPH's and ABTS's higher percentage inhibition was expected since both assays' principle depends on anti-oxidant reaction with an organic radical cation. The above results thus support the anti-oxidative benefits of corms from *H. hemerocallidea*, *H. caespititium*, and *D. anomala*.

REFERENCES

Alimirah, F., Chen, J., Basrawala, Z., Xin, H., & Choubey, D. (2006). DU-145 and PC-3 human prostate cancer cell lines express androgen receptor: Implications for the androgen receptor functions and regulation. *FEBS Letters*, *580*(9), 2294-2300.

Bassey, K., Mamabolo, P., Mothibe, M., & Muganza, F. (2021). Phytochemical profiling and chemical marker compounds identification in *Helichrysum caespititium*: A chemometrics and 2D gas chromatography time of flight mass spectrometry (GCxGC-TOF-MS) perspective. *Pharmacognosy Journal*, *13*(2), 486-494.

Birben, E., Sahiner, U. M., Sackesen, C., Erzurum, S., & Kalayci, O. (2012). Oxidative stress and antioxidant defense. *World Allergy Organization Journal*, *5*, 9-19.

Chota, A., George, B. P., & Abrahamse, H. (2020). Potential treatment of breast and lung cancer using *Dicoma anomala*, an African medicinal plant. *Molecules*, *25*(19), 4435.

Das, N., Islam, M. E., Jahan, N., Islam, M. S., Khan, A., Islam, M. R., & Parvin, M. S. (2014). Antioxidant activities of ethanol extracts and fractions of *Crescentia cujete* leaves and stem bark and the involvement of phenolic compounds. *BMC Complementary and Alternative Medicine*, *14*, 1-9.

Fonmboh, D. J., Abah, E. R., Fokunang, T. E., Herve, B., Teke, G. N., Rose, N. M., Borgia, N. N., Fokunang, L. B., Andrew, B. N., & Kaba, N. (2020). An overview of methods of extraction, isolation and characterization of natural medicinal plant products in improved traditional medicine research. *Asian Journal of Research in Medical and Pharmaceutical Sciences, 9*(2), 31-57.

Ghomari, O., Sounni, F., Massaoudi, Y., Ghanam, J., Kaitouni, L. B. D., Merzouki, M., & Benlemlih, M. (2019). Phenolic profile (hplc-uv) of olive leaves according to extraction procedure and assessment of antibacterial activity. *Biotechnology Reports, 23*, e00347.

Gohari, A., Hajimehdipoor, H., Saeidnia, S., Ajani, Y., & Hadjiakhoondi, A. (2011). Antioxidant activity of some medicinal species using FRAP assay. *Journal of Medicinal Plants*, *10*(37), 54-60.

Jomova, K., Jenisova, Z., Feszterova, M., Baros, S., Liska, J., Hudecova, D., Rhodes, C., & Valko, M. (2011). Arsenic: Toxicity, oxidative stress and human disease. *Journal of Applied Toxicology*, *31*(2), 95-107.

Kalita, P., Tapan, B. K., Pal, T. K., & Kalita, R. (2013). Estimation of total flavonoids content (TFC) and anti-oxidant activities of methanolic whole plant extract of *Biophytum sensitivum* linn. *Journal of Drug Delivery and Therapeutics*, *3*(4), 33-37.

Kewuyemi, Y. O., Kesa, H., & Adebo, O. A. (2022). Biochemical properties, nutritional quality, colour profile and techno-functional properties of whole grain sourdough and malted cowpea and quinoa flours. *International Journal of Food Science & Technology*, *57*(3), 1527-1543.

Kumar, M., Sharma, A., & Kumar, P. (2020). *Pharmacotherapeutic botanicals for cancer chemoprevention*. Springer.

Kupe, M., Karatas, N., Unal, M. S., Ercisli, S., Baron, M., & Sochor, J. (2021). Phenolic composition and antioxidant activity of peel, pulp and seed extracts of different clones of the Turkish grape cultivar 'karaerik'. *Plants*, *10*(10), 2154.

Mfengwana, P. H. (2024). Phytochemical constituents, ferric reducing and radical scavenging activities of *Helichrysm caespititium*. *Natural Product Research*, *9*, 1-6.

Moyo, S. M. (2016). *Effects of cooking and drying on the phenolic compounds, antioxidant activity and antibacterial activity of Cleome gynandra (spider plant)* (Master's thesis). University of Johannesburg.

Munteanu, I. G., & Apetrei, C. (2021). Analytical methods used in determining antioxidant activity: A review. *International Journal of Molecular Sciences*, *22*(7), 3380.

Pratima, N. A., & Gadikar, R. (2018). Liquid chromatography-mass spectrometry and its applications: A brief review. *Archives of Organic and Inorganic Chemical Sciences*, *1*, 26-34.

Rao, L., Kang, N., & Rao, A. (2014). Lycopene and other antioxidants in the prevention and treatment of osteoporosis in postmenopausal women. In V. R. Preedy (Ed.), *Aging* (pp. 247-258). Elsevier.

Riaz, M., Khalid, R., Afzal, M., Anjum, F., Fatima, H., Zia, S., Rasool, G., Egbuna, C., Mtewa, A. G., & Uche, C. Z. (2023). Phytobioactive compounds as therapeutic agents for human diseases: A review. *Food Science & Nutrition*, *11*(6), 2500-2529.

Skowyra, M. (2014). *Antioxidant properties of extracts from selected plant materials (Caesalpinia spinosa, Perilla frutescens, Artemisia annua and Viola wittrockiana) in vitro and in model food systems* (Doctoral dissertation). Polytechnic University of Catalonia.

Tan, J. B. L., & Lim, Y. Y. (2015). Critical analysis of current methods for assessing the in vitro antioxidant and antibacterial activity of plant extracts. *Food Chemistry*, *172*, 814-822.

Tan, M. E., Li, J., Xu, H. E., Melcher, K., & Yong, E. L. (2015). Androgen receptor: Structure, role in prostate cancer and drug discovery. *Acta Pharmacologica Sinica*, *36*(1), 3-23.

Uwineza, P. A., & Waśkiewicz, A. (2020). Recent advances in supercritical fluid extraction of natural bioactive compounds from natural plant materials. *Molecules, 25*(17), 3847.

CHAPTER 5:
PROSTATE CANCER CELL PROLIFERATION

5.1 Introduction

Plants' indispensable properties are the secondary metabolites that are said to have therapeutic potential when extracted (Riaz et al., 2023). The phytobioactive activities of extracts from the corms of *H. hemerocallidea*, *H. caespititium*, and *D. anomala* on cell proliferation of the DU145 prostate cancer cell line were of interest in this study. This chapter focuses on evaluating the effects of *H. hemerocallidea*, *H. caespititium*, and *D. anomala* extracts as agents that are capable of inhibiting cell proliferation. This is arguably an important initial step for any plant to be considered safe before it can be added to combinations that are considered as agents for targeting prostate cancer (Liu et al., 2000).

The main feature in cell proliferation is cell division. There are two forms of cell division, namely meiosis and mitosis, as illustrated in Figure 5.1. Upsetting the intricate balance of these cellular processes is known to have dramatic or tragic outcomes. Dysregulation of meiosis manifests as a genetic disorder, while any impairment during mitosis results in malignant disorders (Koss & Melamed, 2006).

Figure 5.1: Two forms of cell division: Mitosis and meiosis

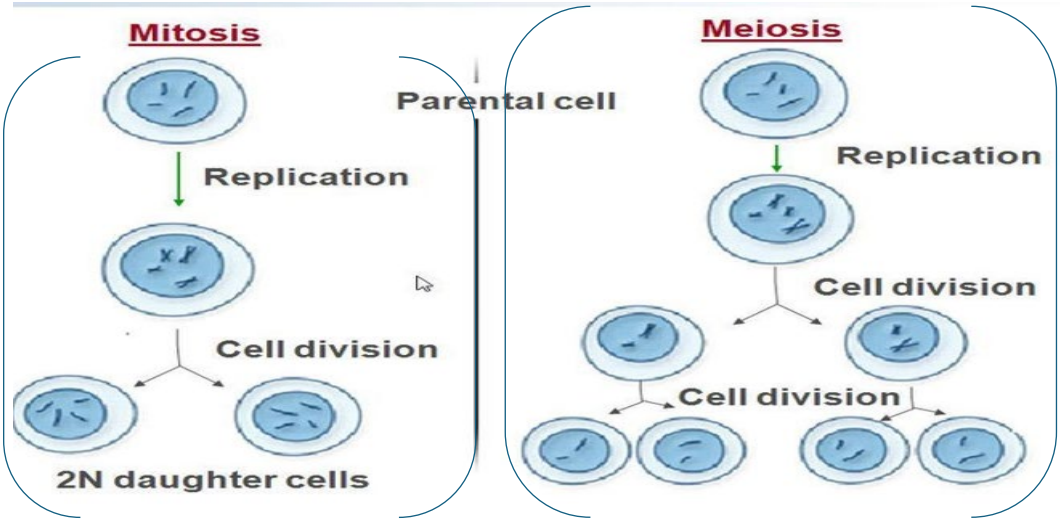

Source: Adopted from Knox (2018)

Cell proliferation can be focal, limited, and unable to invade adjacent tissue or metastasise. It can also be autonomous proliferation with the ability to invade and form metastatic disease, as with prostate cancer (Koss & Melamed, 2006).

5.2 Prostate gland proliferation: The role of androgen

Normal prostate proliferation is directly dependent on androgen for growth and survival, similarly with prostate cancer (Vashchenko & Abrahamsson, 2005). AR functions by way of regulating the total prostatic cell number by continuously stimulating the rate of cell proliferation while at the same time inhibiting the rate of cell death (Arnold & Isaacs, 2002).

Prostate cancer progression is initially AR dependent; however, cancer cells that do not depend on AR for growth are influenced by the hormonal milieu of the host, and the serum levels of gonadal and adrenal ARs, as well as cortisol and cytokines (Arnold & Isaacs, 2002). Pravettoni et al.'s (2007) study focused on the role that ER may have in the progression of prostate cancer. The study noted that ER has opposite effects on cell proliferation, which may result in a complex mechanism of action, whereby either one or the other ER receptors, namely ERα and ERβ, interact with estrogen-responsive elements on the deoxyribonucleic acid (DNA).

Furthermore, the study found that ERβ receptors can behave as a negative regulator of ERα activity in the prostate, ERβ's presence seems to be linked to a reduction of the epithelial cell proliferation coupled with an increased differentiation not only in the normal gland, but also in the carcinoma (Pravettoni et al., 2007).

5.3 Prostate gland regulators: Positive regulator in prostate cancer cell proliferation

ERβ's role as a negative regulator focused attention on the epithelial cell proliferation of prostate carcinoma and the need to probe the opposite regulator. It thus became relevant to note the kidneys and brain's role in prostate cancer cell proliferation, which is associated with ERβ functions. The kidney and brain associated protein (KIBRA) is defined as a memory performance and cognition-associated protein that is expressed in

the kidneys and brain. It functions as a positive regulator of the Hippo yes-associated protein (YAP) pathway, which plays a critical role in tumorigenesis (Stauffer et al., 2016).

The Hippo YAP pathway's role has been found to be part of a network of interlinked signalling pathways that regulate cell transformation, proliferation, invasion, migration, metastasis, and, ultimately, cancer progression (Koinis et al., 2022); hence the association of this protein with resistance to treatment. This suggests that more attention must be paid to new strategies of treating prostate cancer. Since this study's focus is on complementary traditional medicine, it is worth noting the contribution that it makes to prostate cancer cell proliferation (Koinis et al., 2022).

Similarly, the ectopic expression of KIBRA enhances cell proliferation, migration, and invasion in both immortalised and cancerous prostate epithelial cells (Stauffer et al., 2016), where findings reveal a pro-tumour function for KIBRA in prostate cancer.

5.4 Downstream targets: Androgen-responsive proliferative pathway

In addition to regulating cell proliferation, androgen has been found to exert significant effects on the cell cycle, particularly by influencing the transition from the G1 phase to the S phase. ARs stimulate the expression of cyclin D1 and other cyclin-dependent kinases (CDKs), which are crucial for driving the cell past the G1 checkpoint and into the DNA synthesis phase (S phase). By modulating these proteins, ARs promote the progression of the cell cycle by facilitating cellular growth and division (Arnold & Isaacs, 2002). Furthermore, ARs can downregulate CDK inhibitors such as p21 and p27, which further enhances the cell's ability to bypass cell cycle checkpoints. This ability to push cells through the G1 to S phase transition is particularly relevant in the context of prostate cancer, where AR signalling is often amplified, which leads to uncontrolled cellular proliferation and tumour growth (Tan et al., 2015).

Androgen is responsible for specifically driving G1 progression through cross-communication with the cell cycle machinery and regulation of the transcription of genes that control the G1-S transition, whereby, during G1, cells are said to interpret signals from the external and internal environments and the S phase is known to be dominated

by duplication and segregation events. This is further illustrated in Figure 6.4 (Koryakina et al., 2015).

Extracellular signals ultimately impinge on CDKs, which dictate transitions into and within the proliferative cell cycle. Knudsen et al. (1998) reported on the distinct elements that are responsible for controlling the G1-S transition, by acting on the downstream of the AR-signalling pathways to promote G1 progression in AR-dependent cells after studying elements that control the AR-dependent proliferation in the LNCaP prostate cell line (Knudsen et al., 1998). All these signals the complex and intricate nature of prostate cancer cell proliferation.

5.5 Extracellular matrix microenvironment

In exploring cell proliferation, especially of prostate cancer, its environment cannot be overlooked. It has been shown that the stroma mediates many androgenic effects seen in the epithelium. In addition, stromal cells' role is to secrete paracrine peptide growth factors such as epidermal growth factor, fibroblast growth factor, keratinocyte growth factor, and nerve growth factor. These paracrine factors can diffuse from the stromal compartment to the epithelial cells and in time influence epithelial growth and differentiation (Arnold & Isaacs, 2002). The normal stroma and microenvironment may play a regulatory role in the cell proliferation of cancers.

Kumar et al. (2020) state that cancer treatments circulating in the markets target the abnormal functional pathways that halt the proliferation of cancer cells but there are no targeted agents that focus on the environment. Consequently, the examination of any alternative cancer treatment's initial step must pass the cytotoxicity mark. Cytotoxicity is defined as the ability of an agent to produce a toxic effect on a cell and the determination of their harmful effects (Pringle et al., 2018). In this regard, the study focused on carrying out cytotoxicity testing of the effect of crude extracts from *H. hemerocallidea*, *H. caespititium*, and *D. anomala* on the DU145 human prostate cancer cell line. The assays were used to assess the ability of the DU145 prostate cell line to continue proliferating in the presence of a test compound or substance (Pringle et al., 2018).

5.6 Materials

The cell line (DU145 cell line) was purchased from Highveld Biological, Cellonex, South Africa (see Figure 1.1). RPMI 1640, low glucose cell culture medium, and foetal bovine serum (FBS) were purchased from GE Healthcare Life Sciences (Logan, Utah, USA). Trypsin-Ethylenediamine tetraacetic acid (EDTA), Dulbecco's phosphate buffered saline (DPBS) with Ca^{2+} and Mg^{2+} and DPBS without $Ca^{2+}$and Mg^{2+}, and Trypan blue, cisplatin, penicillin/streptomycin, bovine serum albumin (BSA) Fraction V were purchased from Lonza (Wakersville, Maryland, USA).

Cells were maintained in 10-cm culture dishes in RPMI supplemented with 10% FBS (Biowest) and incubated at 37 °C in a humidified incubator with 5% CO_2. Fifty milligrams of dry extracts, as outlined in Chapter 3, were weighed and prepared (according to bioassay guidelines) and transported to Nelson Mandela University Laboratories for further cell-based analysis. Samples were solubilised in dimethyl sulfoxide and diluted to the desired concentrations of 15, 31, 62.5, 125, 250, and 500 µg/mL in the medium. They were added to wells with exponentially growing cells, and all experiments were done in triplicate.

The extracts and solvents were labelled as follows:

Labelling of extracts: A: *H. hemerocallidea*, **B:** *H. caespititium*, **C:** *D. anomala.*

Labelling of solvents: W: Aqueous (ddH_2O), **M:** MeOH

5.7 Method

Cells were seeded in 96-well plates at densities of 5 000 cells per well (DU145) and 10 000 cells per well using 100-µL aliquots and left overnight to attach. For treatment, an additional 100 µL of the treatments at varying concentrations of extracts (0.1 to 300 µg/mL and compounds 0.1 to 200 µM) were added. Treated cells were incubated at 37 °C in a humidified 5% CO_2 incubator for 48 hours. The treatment medium was removed and replaced with 100 µL DPBS with Ca^{2+} and Mg^{2+} containing Hoechst33342 at a final concentration of 5 µg/mL. Propidium iodide (PI) was added at a final concentration of

10 µg/mL using 10 µL per well of a 110 µg/mL stock just before image acquisition, which was done using and ImageXpress Micro XLS fluorescent microscope and evaluated with Meta Xpress software.

5.8 Antiproliferation results

Figure 5.2 (cell proliferation percentage) and Figure 5.3 (average live cell line) are dose-responsive column/bar charts resulting from the DU145 prostate cell line treated with aqueous *H. hemerocallidea*, *H. caespititium*, and *D. anomala* extracts respectively (as labelled in Section 5.6).

In comparison to the untreated cells and melphalan control, cessation of the DU145 cell line was seen in *D. anomala* aqueous extracts of 15 µL/mg and 62.5 µL/mg. Conversely, the *H. hemerocallidea* and *H. caespititium* extracts did not result in significant DU145 cell line inhibition. The aqueous extracts therefore did not exhibit any cytotoxicity even at the maximum extract concentration of 500 µL/mg, although at this concentration *D. anomala* aqueous extracts still proved to be potent.

Figure 5.2: Control: untreated cell line; solvent: aqueous (ddH_2O); melphalan: cell line treated with melphalan

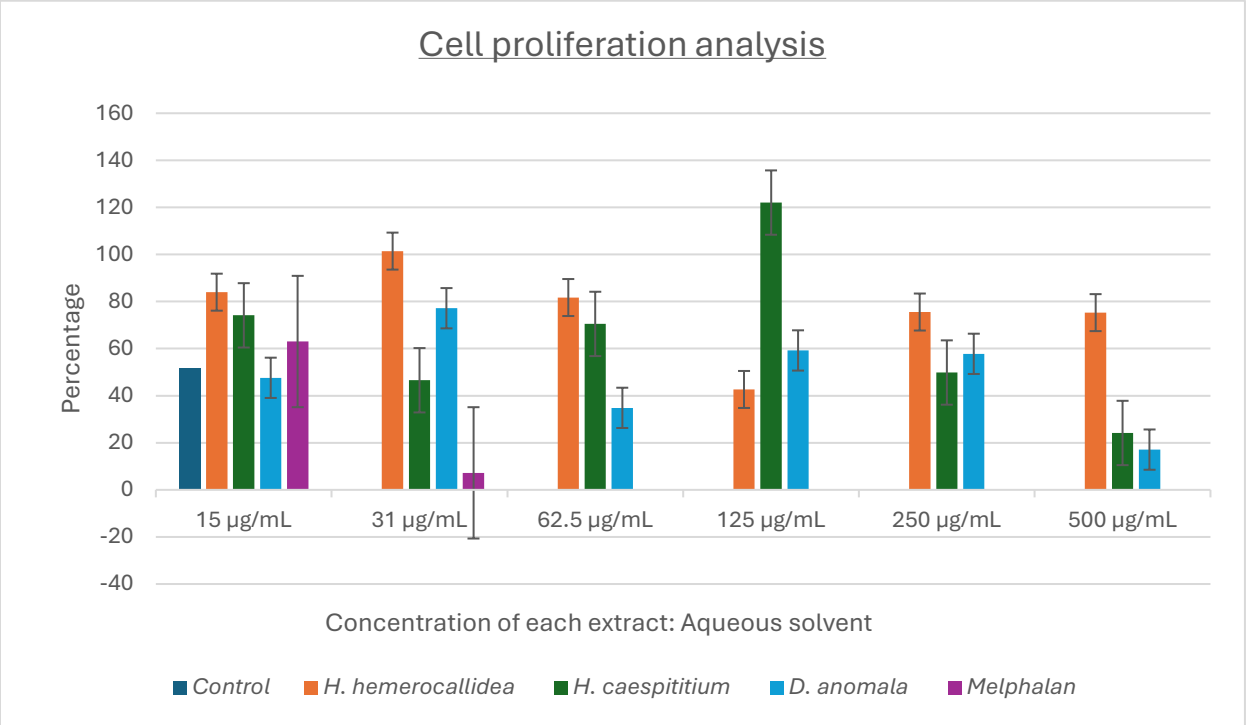

The bar graph represents the average of one individual experiment performed in quadruplicate. Standard deviation (SD) is represented as the error bar.

Figure 5.3 shows on average the proliferation of the DU145 cell line post dose-dependent aqueous extract treatment of *H. hemerocallidea*, *H. caespititium*, and *D. anomala* extracts respectively.

Figure 5.3: Control: untreated cell line; solvent: aqueous (ddH_2O); melphalan: cell line treated with melphalan

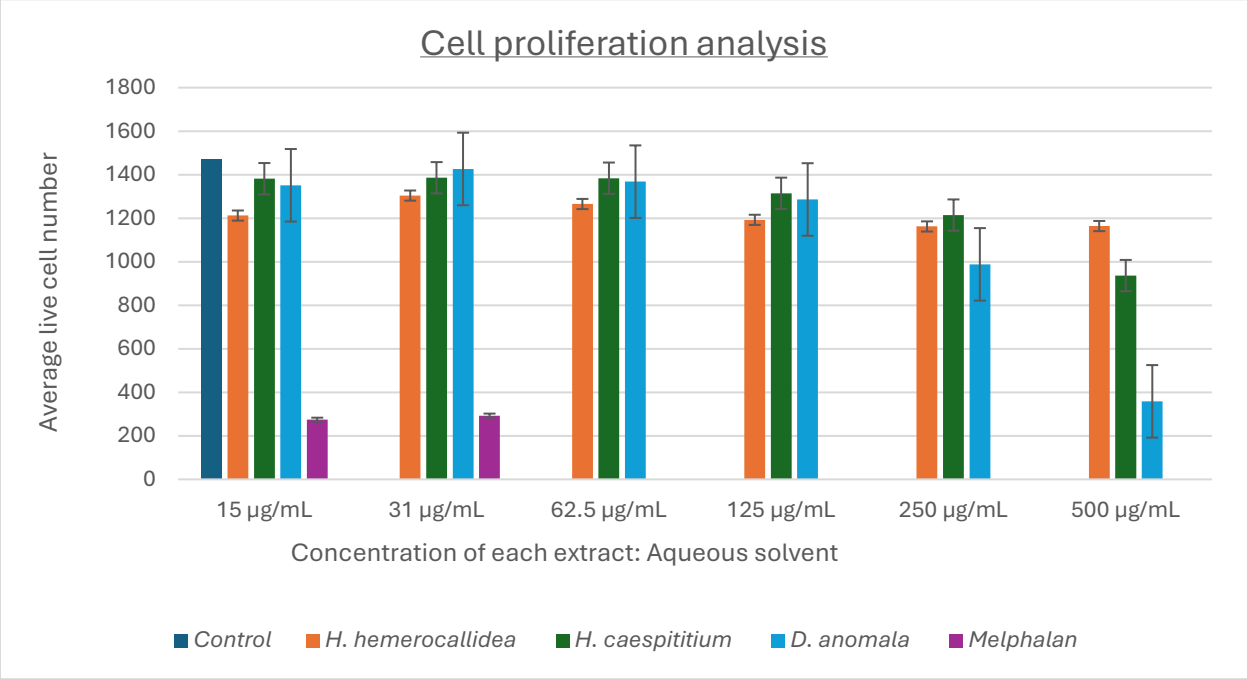

The bar graph represents the average of one individual experiment performed in quadruplicate. SD is represented as the error bar.

The DU145 prostate cell line was treated with methanolic *H. hemerocallidea*, *H. caespititium*, and *D. anomala* extracts; see Figure 5.4 (cell proliferation percentage) and Figure 5.5 (average live cell line) indicating dose-responsive changes.

Figure 5.4: Control: untreated cell line; solvent: MeOH; melphalan: cell line treated with melphalan

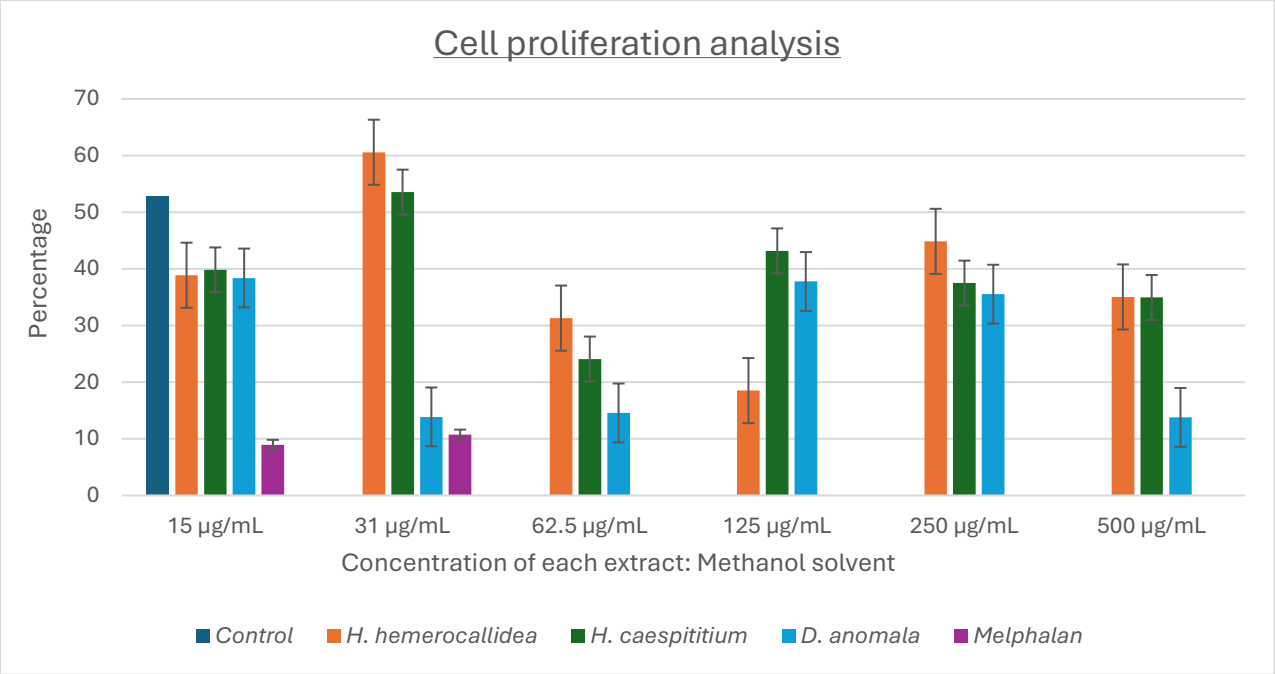

The bar graph represents the average of one individual experiment performed in quadruplicate. SD is represented as error bars.

The methanolic extracts from *H. caespititium* and *D. anomala* arrested the DU145 cell line at 15 µL/mg and 31 µL/mg concentrations in comparison to the untreated cell line and melphalan treatment control, although not much termination was noticeable because of the methanolic extracts of *H. hemerocallidea*. Furthermore, when comparing methanolic extracts with the aqueous extracts at the same dosages of 15 µL/mg and 31 µL/mg, the DU145 cell proliferation percentage was mostly affected by the methanolic extracts. *H. caespititium* and *D. anomala*'s methanolic effect thus halted the DU145 cell line at 40% and 38%. The DU145 cell proliferation was arrested at 15 µL/mg.

Cell proliferation was noted to be 54% after *H. caespititium* methanolic extract at 31 µL/mg and14% of cells proliferated because of *D. anomala* at 31 µL/mg. This suggests that the methanolic extract of *D. anomala* was more cytotoxic to the DU145 prostate cancer cell line. Aqueous extracts of *H. hemerocallidea*, *H. caespititium*, and *D. anomala* were not used for further investigation. In comparison with the methanolic extracts of

H. hemerocallidea and *H. caespititium*, the DU145 cell line was treated with methanolic *D. anomala* as it showed more cytotoxicity.

Figure 5.5 demonstrates the average DU145 cell line proliferation post dose-dependent methanolic extract treatment from the *H. hemerocallidea*, *H. caespititium*, and *D. anomala* extracts respectively.

Figure 5.5: Control: untreated cell line; solvent: MeOH; melphalan: cell line treated with melphalan

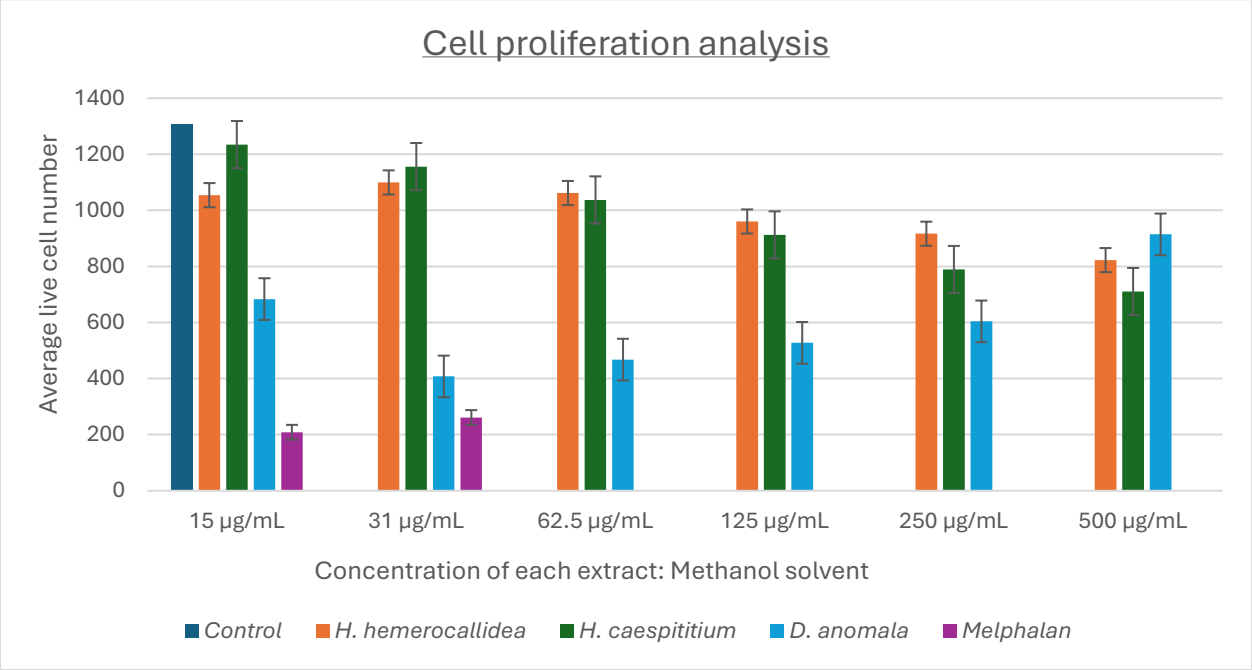

The bar graph represents the average of one individual experiment performed in quadruplicate. SD is represented as error bars.

5.8.1 Half-maximal inhibitory concentration (IC_{50}) determination

The inhibition concentration (IC) was determined in the cytotoxic evaluation of the methanolic extracts of *D. anomala*.

Figure 5.6 indicates the dose-response curve resulting from treatment of the DU145 cell line with methanolic *D. anomala* extracts. Methanolic extracts of *D. anomala* proved to be cytotoxic against the DU145 cell line, with an IC value of 18.98 µg/mL (R^2 = 94%).

Figure 5.6: Dose-response curves for the MeOH *D. anomala* extract

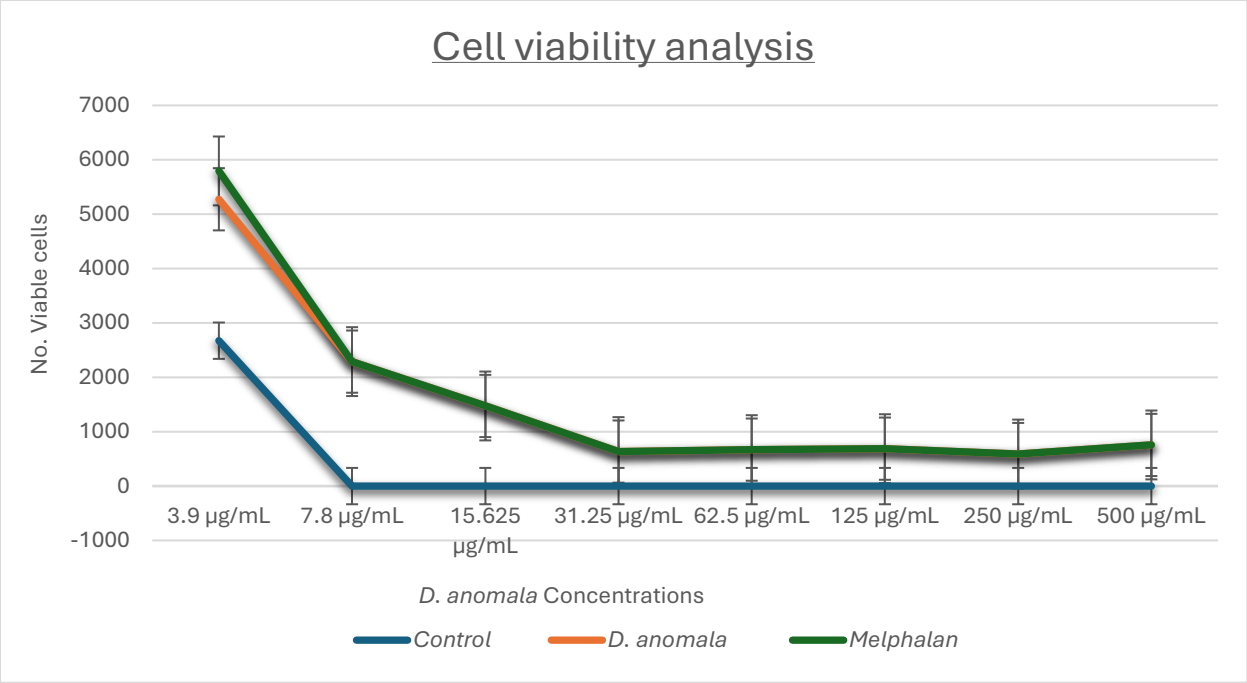

Data represent the mean ± SD for replicate wells at each of the indicated concentrations.

5.9 Discussion

Cell viability data indicate that the MeOH-extracted *D. anomala* concentrations reduced the proliferation of the DU145 prostate cell line at the concentrations of 15 µg/mL and 30 µg/mL (see Figure 5.6) when compared to the positive control of melphalan.

The results revealed that the two concentrations of *D. anomala* possessed significant cytotoxic activity against the DU145 prostate cancer cell line. The two optimum concentrations of *D. anomala* of 15 µL and 30 µL were selected for further study (see Chapter 6). Suitable agents are regarded as effective at concentrations of up to 100 µg/mL. *D. anomala*'s activity identified is therefore below the 100 µg/mL range (Mfengwana et al., 2019).

The study hypothesised that all extracts, particularly the methanolic ones, would have cytotoxic effects on the DU145 prostate cancer cell line. The unforeseen outcome was for only methanolic extract of *D. anomala* to be effective in cessation of the prostate cancer cell line proliferation, especially considering the consumption and advocacy of the

combined three plant extracts. Adequate focus on characterising the mechanism of cytotoxicity from the *H. hemerocallidea*, *H. caespititium*, *and D. anomala* extracts on the DU145 prostate cancer cell line proliferation was done and aided in the perception of all these extracts. This follows that *H. hemerocallidea* was specifically constituted of phytosterols, as demonstrated in Chapter 3. Phytosterols' main role is seen in inhibiting cholesterol.

In comparison to the cytotoxicity screening done by Boukes and Van de Venter (2011), the outcome is similar as they found that the aqueous extract of *H. hemerocallidea* stimulated the growth of prostate carcinoma (DU145) and non-malignant breast (MCF-12A) cell line. Likewise, with an aqueous extract of *H. hemerocallidea* at 15 µg/mL and 30 µg/mL, the cells continued to proliferate from 84% and 100% (see Figure 5.2). However, the literature indicates that *H. hemerocallidea* has previously shown capabilities to inhibit the MCF-7 cancer cell growth (Steenkamp & Gouws, 2006). It can be argued that there may be few carcinoma cell lines where aqueous extracts can halt their stimulation. Steenkamp and Gouws (2006) mentioned that the cytotoxicity of the plants investigated has been reported by other authors, and it is evident that different cell lines exhibit different sensitivities towards the plant extracts.

Additionally, this study contributes to the minimal work done previously on *Helichrysum* species. Methanolic extracts are less cytotoxic to prostate cancer cell line proliferation. Specific attention paid to *H. caespititium* was needed as Akaberi et al. (2021) alluded to the limited number of plants such as *H. italicum, H. arenarium,* and *H. stoechas* that have been investigated, yet the ongoing consumption of *H. caespititium* in the country is notable (Lourens et al., 2008). Accordingly, Mamabolo et al. (2018) concluded that *H. caespititium* aqueous extracts were far less toxic and may be used without any hindrances. It must be stated that the investigation was done on rats' hepatocytes H411E, where in comparison aqueous extracts' high cytotoxicity to the cancer cell line would have been the preferable outcome.

A concentration 18.98 µg/mL of *D. anomala* MeOH extract inhibited 50% of the DU145 prostate cell population (see Figure 5.6). Conversely, *H. hemerocallidea* and *H. caespititium* did not produce toxic effects that are significant to the cell proliferation of

the DU145 cell line. Chota et al.'s (2020) study stated that *D. anomala* extracts exhibited anticancer properties that may widely be used in the treatment of breast and lung cancers. In the same way, it has been stated that *D. anomala* plays an important role in the development of new potent anticancer agents (Chota et al., 2020).

An anticipated outcome from plant-derived phytochemicals is to induce apoptotic cell death in cancer cell lines. The *D. anomala* MeOH extracts exhibited bioactive compounds (as reported in Chapter 3) with the potential to halt cell proliferation but their ability to increase apoptotic effects with less necrosis is yet to be demonstrated. Bioactive compounds extracted from *D. anomala* have the ability to promote apoptotic pathways, or autophagy, and inhibit different phases of the cell cycle, as well as the migration and invasion of cancerous cell (Chota et al., 2020). Finding alternative anticancer agents aims to reduce cancer incidence and resistance caused by conservative therapies (Chota et al., 2020).

Flavonoids, alkaloids, terpenoids, and phenolic compounds have been widely studied for their antiproliferative effects on prostate cancer cells, targeting key pathways involved in tumour growth. Flavonoids, such as quercetin and apigenin, have demonstrated the ability to suppress AR signalling, a critical driver of prostate cancer progression, thereby inhibiting cancer cell proliferation. Alkaloids, such as vinblastine, are known to disrupt microtubule formation, effectively arresting the cell cycle and preventing cancer cell division. Terpenoids, including limonene and ursolic acid, act by inhibiting the PI3K/AKT pathway, which is a pathway that is often hyperactivated in prostate cancer, and thus reducing cellular growth and promoting apoptosis. Phenolic compounds, such as resveratrol, exert their antiproliferative effects by modulating oxidative stress and inhibiting enzymes such as 5-alpha-reductase, which is linked to prostate cancer cell growth.

Together, these plant-derived secondary metabolites offer a multifaceted approach to decelerating prostate cancer cell proliferation by targeting multiple cancer-related pathways and cellular mechanisms.

Thus, to treat prostate cancer, combined therapy is the proposed direction that should be taken to combat cancer, and not just a single approach that includes chemotherapy, prostatectomy, and radiation therapy (Chota et al., 2020).

REFERENCES

Akaberi, M., Najaran, Z. T., Azizi, N., & Emami, S. A. (2021). Metabolite profiling and antiprotozoal activity of three endemic Iranian helichrysum species. *Industrial Crops and Products*, *174*, 114196.

Arnold, J., & Isaacs, J. (2002). Mechanisms involved in the progression of androgen-independent prostate cancers: It is not only the cancer cell's fault. *Endocrine-Related Cancer*, *9*(1), 61-73.

Boukes, G. J., & Van de Venter, M. (2011). Cytotoxicity and mechanism(s) of action of *Hypoxis* spp. (African potato) against HeLa, HT-29 and MCF-7 cancer cell lines. *Journal of Medicinal Plants Research*, *5*(13), 2766-2774.

Chota, A., George, B. P., & Abrahamse, H. (2020). Potential treatment of breast and lung cancer using *Dicoma anomala*, an African medicinal plant. *Molecules*, *25*(19), 4435.

Knox, S. S. (2018). Wave/particle duality and biomedical research designs. *Molecular Biology: Open Access*, *2018*(7), 3. https://pdfs.semanticscholar.org/b1a6/0d2b81caee8832ad75f487cae0e03c5b995a.pdf

Knudsen, K. E., Arden, K. C., & Cavenee, W. K. (1998). Multiple G1 regulatory elements control the androgen-dependent proliferation of prostatic carcinoma cells. *Journal of Biological Chemistry*, *273*(32), 20213-20222.

Koinis, F., Chantzara, E., Samarinas, M., Xagara, A., Kratiras, Z., Leontopoulou, V., & Kotsakis, A. (2022). Emerging role of yap and the Hippo pathway in prostate cancer. *Biomedicines, 10*(11), 2834.

Koryakina, Y., Knudsen, K. E., & Gioeli, D. (2015). Cell-cycle-dependent regulation of androgen receptor function. *Endocrine-Related Cancer*, *22*(2), 249-264.

Koss, L. G., & Melamed, M. R. (2006). *Koss' diagnostic cytology and its histopathologic bases*. Lippincott Williams & Wilkins.

Kumar, M., Sharma, A., & Kumar, P. (2020). *Pharmacotherapeutic botanicals for cancer chemoprevention*. Springer.

Liu, W., Xu, S., & Che, C. T. (2000). Anti-proliferative effect of ginseng saponins on human prostate cancer cell line. *Life Sciences*, *67*(11), 1297-1306.

Lourens, A., Viljoen, A. M., & Van Heerden, F. (2008). South African *Helichrysum* species: A review of the traditional uses, biological activity and phytochemistry. *Journal of Ethnopharmacology*, *119*(3), 630-652.

Mamabolo, M. P., Muganza, F. M., Olivier, M. T., Olaokun, O. O., & Nemutavhanani, L. D. (2018). Evaluation of antigonorrhea activity and cytotoxicity of *Helichrysum caespititium* (DC) Harv. whole plant extracts. *Biology and Medicine*, *10*(1), 1C.

Mfengwana, P. H., Mashele, S. S., & Manduna, I. T. (2019). Cytotoxicity and cell cycle analysis of *Asparagus laricinus Burch*. and *Senecio asperulus DC*. on breast and prostate cancer cell lines. *Heliyon*, *5*(5), e01666.

Pravettoni, A., Mornati, O., Martini, P., Marino, M., Colciago, A., Celotti, F., Motta, M., & Negri Cesi, P. (2007). Estrogen receptor beta (erbeta) and inhibition of prostate cancer cell proliferation: Studies on the possible mechanism of action in du145 cells. *Molecular and Cellular Endocrinology*, *263*(1-2), 46-54.

Pringle, N. A., Koekemoer, T. C., Holzer, A., Young, C., Venables, L., & Van de Venter, M. (2018). Potential therapeutic benefits of green and fermented rooibos (*Aspalathus linearis*) in dermal wound healing. *Planta Medica*, *84*(09/10), 645-652.

Riaz, M., Khalid, R., Afzal, M., Anjum, F., Fatima, H., Zia, S., Rasool, G., Egbuna, C., Mtewa, A. G., & Uche, C. Z. (2023). Phytobioactive compounds as therapeutic agents for human diseases: A review. *Food Science & Nutrition*, *11*(6), 2500-2529.

Stauffer, S., Chen, X., Zhang, L., Chen, Y., & Dong, J. (2016). KIBRA promotes prostate cancer cell proliferation and motility. *The FEBS Journal*, *283*(10), 1800-1811.

Steenkamp, V., & Gouws, M. (2006). Cytotoxicity of six South African medicinal plant extracts used in the treatment of cancer. *South African Journal of Botany*, *72*(4), 630-633.

Tan, M. E., Li, J., Xu, H. E., Melcher, K., & Yong, E. L. (2015). Androgen receptor: Structure, role in prostate cancer and drug discovery. *Acta Pharmacologica Sinica*, *36*(1), 3-23.

Vashchenko, N., & Abrahamsson, P. A. (2005). Neuroendocrine differentiation in prostate cancer: Implications for new treatment modalities. *European Urology*, *47*(2), 147-155.

CHAPTER 6:
ANTICANCER MECHANISM ACTIVITY

6.1 Introduction

Plant secondary metabolites have garnered significant attention for their ability to induce cancer cell death through various mechanisms. These bioactive compounds, including flavonoids, alkaloids, terpenoids, and phenolics, exhibit anticancer properties by targeting multiple pathways that regulate cell survival, proliferation, and apoptosis. One of the preferred mechanisms of action involves the induction of oxidative stress within cancer cells, which leads to the generation of ROS. Elevated ROS levels disrupt cellular homeostasis and damage critical components such as DNA, proteins, and lipids, and eventually triggering PCD (apoptosis).

Additionally, plant metabolites can inhibit key signalling pathways such as the PI3K/AKT/mTOR and MAPK pathways, which are often dysregulated in cancer cells, thereby arresting tumour growth and promoting apoptosis. Some secondary metabolites also target specific enzymes or proteins, such as topoisomerases or heat shock proteins, and impairing cancer cell replication and survival. This multitargeted approach makes plant secondary metabolites promising candidates for cancer therapies, as they offer a natural means of selectively inducing cancer cell death while minimising damage to healthy tissues. This chapter focuses on the anticancer activity of *D. anomala* on the DU145 prostate cancer cell line as it was the only plant with high antiproliferative activity when compared to *H. hemerocallidea* and *H. caespititium* (see Chapter 5). Thus, below apoptosis, the signalling pathways and modalities of cell death will be discussed.

6.2 Apoptosis: Apoptotic programmed cell death (PCD)

The ability of an agent or crude extract to kill, destroy, or slow down the process of cancer cell proliferation may be classified under the category of “anticancer”. Anticancer agents are mainly aimed at triggering the apoptosis signalling system. Apoptosis, as defined by Obeng (2020), is a process of the sequential order of cell death, referred to as PCD, where the idea is that cell death does not occur accidentally. However, the definition was

restated by Fulda (2010) as an evolutionary highly conserved intrinsic death programme that plays a key role in maintaining tissue homeostasis during development and in adult life. Apoptosis is characterised by DNA fragmentation, chromatin compaction, plasma membrane blebbing, cell shrinkage, and collapse into small intact fragments called apoptotic bodies (Rahman et al., 2016), as illustrated in Figure 6.1. Below is an outline of pathways responsible for initiating apoptosis.

Figure 6.1: Characteristics of apoptosis

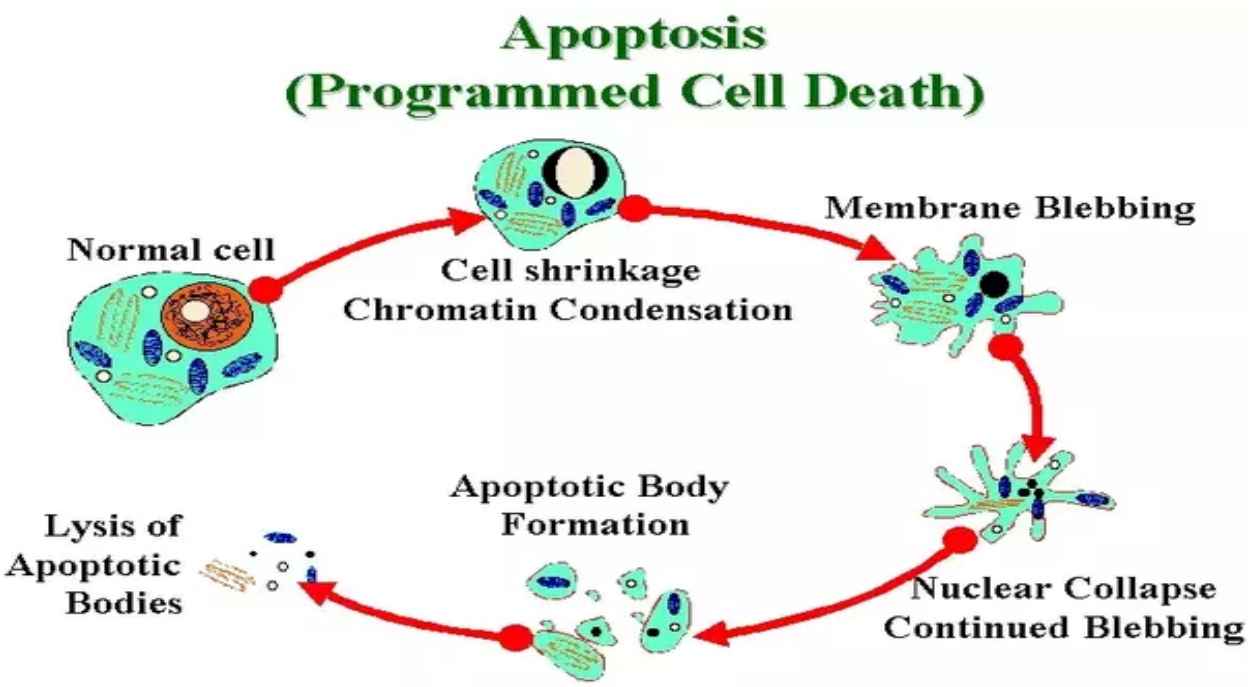

Source: Rayfield (2023)

6.3 Apoptosis signalling system

Two distinct pathways are responsible for initiating apoptosis, namely the intrinsic and extrinsic pathways, both of which converge to trigger the effector or execution phase of the cell (Obeng, 2020). Both pathways ultimately activate a cascade of caspases, particularly executioner caspases that cleave vital cellular components and dismantle the cell in a controlled manner to ensure cell death without damaging surrounding tissues.

6.3.1 Intrinsic pathway (internal stimuli)

Every cell possesses an internal signal that can initiate apoptosis at any point in time. The mitochondrial pathway is initiated by the release of apoptogenic factors such as Cytochrome C, apoptosis inducing factor, or lack of growth factors (Vermeulen et al., 2003). Biochemical stress and DNA damage (p53 gene) are also capable of initiating the pathway. Green and Kroemer (2004) focused on the controversies around mitochondrial outer membrane permeabilisation (MOMP) as many proteins can inhibit or halt it. Green and Kroemer (2004) indicated that MOMP occurs suddenly and leads to the release of proteins normally found in the space between the inner and outer mitochondrial membranes (Green & Llambi, 2015).

Members of the Bcl-2 family of apoptosis-regulating proteins act directly on the outer mitochondrial membrane by activating caspase. Anti-apoptotic Bcl-2 family members function to block MOMP, whereas the various pro-apoptotic members promote it. The balancing act is said to determine the susceptibility of the cell to apoptosis (Fulda, 2010).

Furthermore, the other subfamily, namely BH3-only proteins (that contain only the BH3 domains), can act either to activate Bax and Bak or to interfere with the anti-apoptotic Bcl-2 family members (Fulda, 2010). Bax-Bax dimers are said to increase cell susceptibility to apoptosis (Green & Kroemer, 2004).

6.3.2 Extrinsic pathway (external stimuli)

Located on the cell surface, death receptors are defined by Fulda and Debatin (2006) as members of the tumour necrosis factor (TNF) receptor gene superfamily that consists of more than 20 proteins with a broad range of biological functions, including regulation of cell death, survival, and differentiation or immune regulation; among others.

The corresponding ligands of the TNF superfamily comprise death receptor ligands such as CD95 ligand (CD95L), TNFα, and lymphotoxin-α. The latter are said to bind to tumour necrosis factor receptor, TNF-related apoptosis inducing ligand, and TWEAK, which is a ligand for death receptor 3 (Fulda & Debatin, 2006). Fulda and Debatin (2006) asserted that the CD95 ligand is produced by activated T cells and plays a crucial role in the

regulation of the immune system by triggering autocrine suicide or paracrine death in lymphocytes or other target cells (Green & Llambi, 2015). Furthermore, CD95L expression on cancer cells has been implicated in the immune escape of tumours (Fulda & Debatin, 2006).

Correspondingly, Obeng (2020) stated that the binding of the death domain/adapter protein to the receptor ligands complex allows the binding of an initiator caspase 8 or 10 through its death effector domain to form an activated complex called death inducing signalling complex. Obeng (2020) affirmed that the binding and activation allow for caspase-8 to relay the death signal to an execution caspase to bring about apoptosis, as seen in Figure 6.2.

Figure 6.2: Apoptosis signalling systems

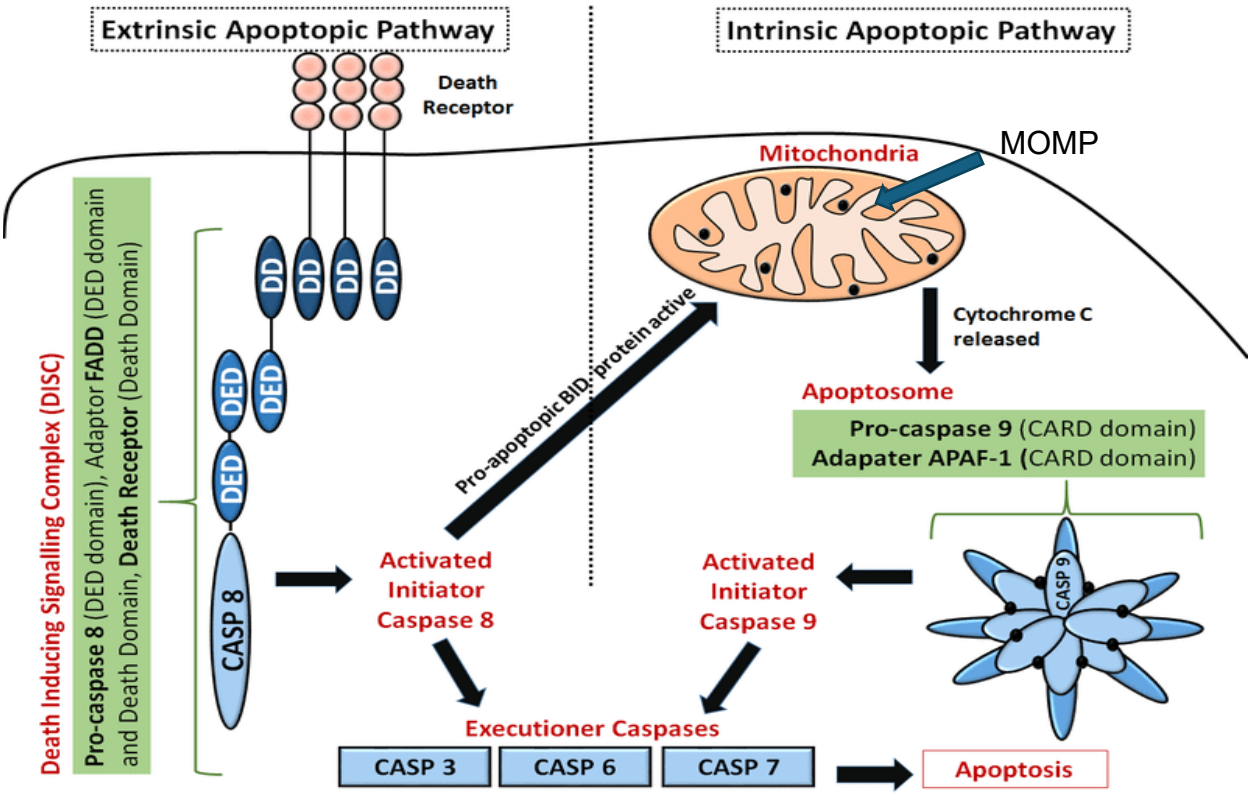

Source: Adopted from Speller (2023)

6.3.3 Effector pathway (execution phase)

Some caspases that are said to be inactive, such as caspase-8 and -29, or operate as “initiators” and transmit cell death signals by activating “executioner or effector” caspases, such as caspase-3, -26, and -27 (Oropesa Ávila et al., 2015). After activation, effector caspases cleave to several different substrates in the cytoplasm or nucleus. For example, caspase-3 activates deoxyribonuclease, which leads to DNA fragmentation. A wide range of proteins are usually required for cell survival (Green & Llambi, 2015).

The execution phase of apoptosis has been said to last approximately one hour. Oropesa Ávila et al. (2015) stated that the phase is routinely characterised by the following typical morphological features: cell shrinkage, plasma membrane blebbing, chromatin condensation, and DNA and cell fragmentation.

6.4 Modalities of cell death

Cell death is not limited to apoptosis. Modalities of cell death include apoptosis, necrosis, autophagy, and cornification. Atypical cell death modalities include mitotic catastrophe, anoikis, excitotoxicity, Wallerian degeneration, paraptosis, pyroptosis, pyronecrosis, and entosis (Kroemer et al., 2009). The list may seem endless but Yan et al. (2020) provided a summary of cell death modalities.

Green and Llambi (2015) categorised cell death into PCD or non-PCD. The grouping is said to be based on their signal dependency. PCD can be further divided into two groups, namely apoptotic cell death or non-apoptotic cell death. Furthermore, programmed apoptosis is said to consist of apoptosis, as well as anoikic. In contrast, accidental cell death is referred to as non-PCD as a result of unexpected cell injury or necrosis (Van Doorn, 2011).

The determination of the Nomenclature Committee on Cell Death sought to simplify the considerable confusion surrounding cell death determination by means of exploring multiple mechanisms and phenotypes that compose programmed non-apoptotic cell death (Van Doorn, 2011). These include, firstly, vacuole-presenting cell death (autophagy, entosis, methuosis, and paraptosis); secondly, mitochondrial-dependent cell

death (mitoptosis and parthanatos); thirdly, iron-dependent cell death (ferroptosis) and immune-reactive cell death (pyroptosis and NETosis); as well as other types, such as necroptosis (Reape & McCabe, 2010).

6.5 Autophagy: Non-apoptotic PCD

Yan et al. (2020) defined autophagy as a process that is initiated by cellular stress, for a protective response. Once the cellular stress is irreversible, the cell will be committed to death, also through excessive levels of autophagy. There are three forms of autophagy, namely macro-autophagy, micro-autophagy, and chaperone-mediated autophagy. Macro-autophagy is said to be characterised by the sequestration of cytoplasmic material within autophagosomes for bulk degradation by lysosomes, while in micro-autophagy, the cytoplasmic components are directly sequestrated into the lysosomes, where acidic hydrolases further mediate the degradation (Ravanan et al., 2017). Chaperone-mediated autophagy selectively targets KFERQ motif (Lys-Phe-Glu-Arg-Gln)-containing proteins (Kroemer et al., 2009), as shown in Figure 6.3.

Correspondingly, autophagic cell death is morphologically defined as a type of cell death that occurs in the absence of chromatin condensation but is accompanied by massive autophagic vacuolisation of the cytoplasm (Kroemer et al., 2009). It is said to also be involved in a variety of biological functions such as development, cellular differentiation, and cell defence against pathogens and nutritional starvation (Ravanan et al., 2017). Autophagic cell death is said to be characterised by the appearance of large intracellular vesicles, plasma membrane blebbing, enlarged organelles, and the depletion of cytoplasmic organelles in the absence of chromatin condensation (Ravanan et al., 2017). It was shown to function as a lever in the cell process, with some reports indicating that cells presenting features of autophagic cell death can still recover upon the withdrawal of the death-inducing stimulus (Kroemer et al., 2009). Alternatively, Green and Llambi (2015) referred to specific degradation of the mitochondria as mitophagy. The selective autophagy of foreign pathogens is called xenophagy. There are also some other selective autophagy forms, such as lipophagy, aggrephagy, and lysophagy.

6.6 Necrosis: Non-PCD

Necrosis has been commonly considered as a passive process that does not require de novo macromolecular synthesis, but minimal energy (Yan et al., 2020). Kroemer et al. (2009) asserted that necrosis has been considered merely as an accidental, uncontrolled form of cell death. However, evidence is accumulating that the execution of necrotic cell death may be finely regulated by a set of signal transduction pathways and catabolic mechanisms (Van Doorn, 2011). For instance, death domain receptors (e.g., TNFR1, Fas/CD95, and TRAIL-R) and toll-like receptors (e.g., TLR3 and TLR4) have been shown to elicit necrosis, in particular the presence of caspase inhibitors (Green & Llambi, 2015).

The process is said to be stimulated by several external factors, such as infections, toxins, and physical injury that lead to morphological alterations (Van Doorn, 2011). For instance, cytoplasmic swelling (oncosis, pre-lethal phase caused by the disruption of ionic pumps such as Ca+ influx), plasma membrane rupture, and the subsequent loss of intracellular organelles without severe chromatin condensation, but randomly degraded DNA, to mention some (see outline in Figure 6.3) (Yan et al., 2020).

Figure 6.3: Cell death morphological alteration

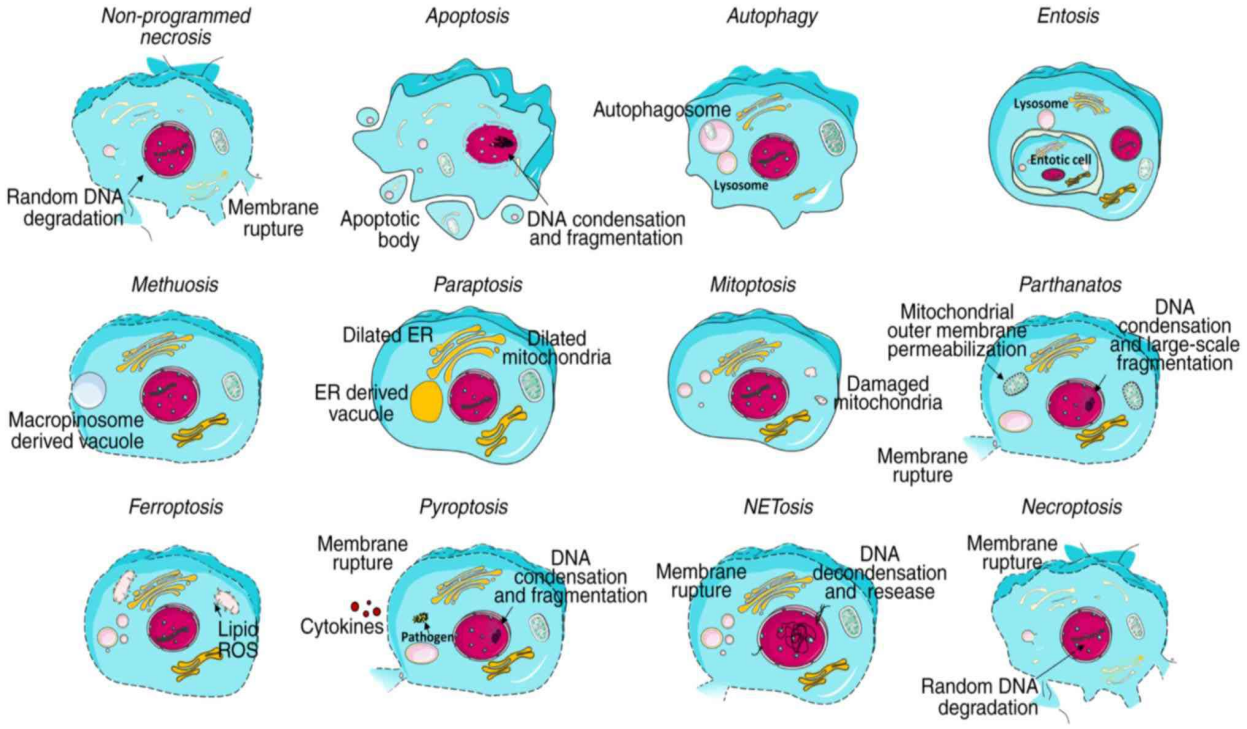

Source: Yan et al. (2020)

6.7 Secondary necrosis

Secondary necrosis, regarded as the natural result of apoptosis in unicellular eukaryotes, has also been found to occur in multicellular organisms and it has been hypothesised to participate in the genesis of many human diseases (Oropesa Ávila et al., 2015). In vivo secondary necrosis may occur in the presence of massive apoptosis whereby there are overloads in the clearance activity of macrophages, as well as deficiencies in the number of macrophages or saturation of the immune system, as seen in chronic inflammation (Nikoletopoulou et al., 2013).

Succinctly stated, cells that perform apoptosis on in vitro cell cultures are not eliminated by phagocytes and undergo a late process of secondary necrosis, which is characterised by the loss of membrane integrity and the release of cell content into the extracellular medium (Oropesa Ávila et al., 2015). Additionally, it is not only cell membrane integrity that is compromised; extensive nuclear membrane blebbing and rupture, and a lucent cytoplasm, also take place. The apoptotic cell contour may remain, whereas the nucleus disintegrates through extensive chromatolysis (Uller et al., 2004).

The summary by Fulda (2010) expressed non-apoptotic modes of cell death that are to be taken into consideration as a response to cytotoxic therapy. These alternative forms of cell death have not yet been defined precisely (Green & Llambi, 2015).

In some non-caspase proteases such as calpains or cathepsins, lysosomal enzymes or PARP-1 may be involved. In the same way, the form of cell death may depend on the context, including the cell type, the genotype of the cell, the type of DNA damage, and the dose of the agent used (Nikoletopoulou et al., 2013).

6.8 Cell cycle cell division

A cell cycle is divided into four phases, namely Gap 1 (G1), Synthesis (S), Gap 2 (G2), and Mitosis (M). The phases describe the chronological order of different events observed in normal cycling cells, as illustrated in Figure 6.4. Barnum and O'Connell (2014) asserted

that the bulk of duplication and segregation events occur in the S and M phases. Moreover, during the S phase, both DNA and centrosomes are said to be duplicated (Vermeulen et al., 2003). Typically, duplicated centrosomes separate to form the poles of the mitotic spindle responsible for segregating sister chromatids. Sister chromatid segregation is initiated during the M phase, or mitosis. G1 and G2 are termed “gap” phases, as they separate the visibly observable events of the S and M phases (Dickson & Schwartz, 2009).

Figure 6.4: Phases of the cell cycle

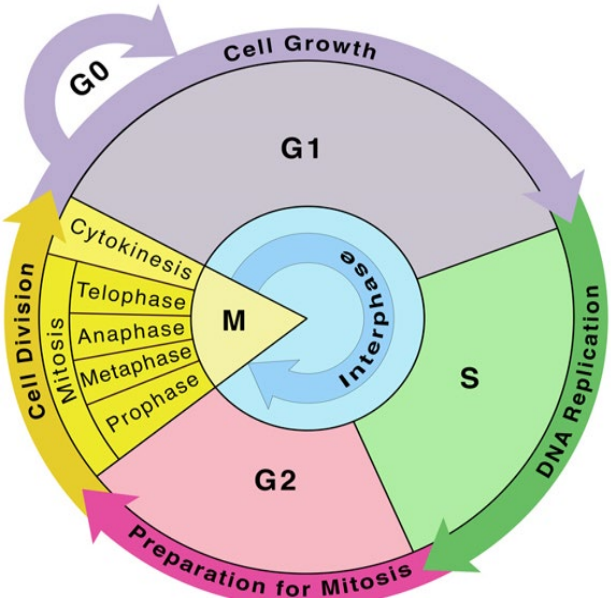

Source: Adopted from Science Facts (2024)

Barnum and O’Connell (2014) stated that although no overt cellular changes or events are observed during G1 and G2, the cells are interpreting signals from their extracellular and intracellular environments to ensure that conditions are appropriate for cellular division events. Each cell cycle event, such as DNA replication, centrosome duplication, and chromosome segregation, is therefore a complex process that requires the coordination of many different proteins acting together to complete the task at hand (Dickson & Schwartz, 2009). The cell cycle analysis of the *D. anomala* methanolic extract was evaluated to understand its mechanism of action when inhibiting the proliferation of the DU145 prostate cancer cells.

6.9 Materials

The cell line mentioned above (see Section 6.8) was purchased from Highveld Biological (DU145 ATCC® HTB-81™), Cellonex, South Africa. The RPMI 1640 cell culture medium and FBS were purchased from GE Healthcare Life Sciences (Logan, Utah, USA). Trypsin-EDTA and DPBS with $Ca^{2+}$and Mg^{2+} were purchased from Lonza (Wakersville, Maryland, USA). Trypan blue, bisBenzamide H33342 trihydrochloride (Hoechst 33342), cisplatin, penicillin/streptomycin, BSA Fraction V, anti-CASP8 polyclonal, and anti-CASP3 monoclonal antibodies were purchased from Sigma-Aldrich (St. Louis, Missouri, USA). The Annexin V-fluorescein isothiocyanate (FITC)/PI kit was purchased from MACS Miltenyi Biotec (Germany). Cleaved caspase-3 (Asp 175) (D3E9) Rabbit mAb, cleaved caspase-8 (Asp 391) (18C8) Rabbit mAb, Anti-rabbit IgG (H+L), F(ab')2 fragment (Alexa fluor® 647 conjugate), Anti-rabbit IgG (H+L), F(ab')2 fragment (Alexa fluor® 488 conjugate), and Phospho-Histone H3(Ser10) (D2C8) mAb were purchased from Cell Signalling Technology (Massachusetts, USA).

6.10 Method

6.10.1 Cell cycle analysis: Phosphatidylserine (PS) translocation

Cell cycle analysis was performed to determine the state of DNA in the DU145 prostate cancer cell line in response to *D. anomala* MeOH extracts following Riss et al.'s (2016) method.

Cells were seeded in 96-well plates at a density of 5000 cells per well using 100-µL aliquots and left overnight to attach. The cells were treated with 15 µg/mL and 30 µg/mL concentrations of *D. anomala* MeOH extract, respectively. The treated cells were incubated at 37 °C in a humidified 5% CO_2 incubator for 24 and 48 hours. The treatment medium was removed and replaced with 50-µL aliquots of a mixture of Annexin V-FITC at a final concentration of 1X the stock (50 µL) and Hoechst 33342 at a final concentration of 2 µg/mL (1 µL of 10 mg/mL stock) in 5 mL DPBS with Ca^{2+} and Mg^{2+} containing 250 µL of binding buffer (20X). The cells were incubated in the dark for 15 minutes at room

temperature. PI at a final concentration of 1 µg/mL (50 µL per well of 2 µg/mL working stock) was added to the Annexin/Hoechst33342 stain just before image acquisition.

6.11 Results for the anticancer mechanism of action

6.11.1 Hoechst 33342, Annexin V-FITC, and propidium iodide (HAPI)

The effects of the *D. anomala* MeOH extract on the integrity of the DU145 cell membrane was determined after staining with HAPI.

Figure 6.5 denotes the average cell analysis of the DU145 prostate cancer cell line using HAPI stains after 24 hours of exposure to treatments. Cells were treated with 40 µM melphalan as the positive control and untreated cells. Treatment of methanolic *D. anomala* extract comprised 15 µg/mL and 30 µg/mL respectively. Extract concentrations were dependent on the cytotoxic activity demonstrated in Chapter 5 (see Figure 5.6) on DU145 cell proliferation.

Figure 6.5: HAPI after 24 hours

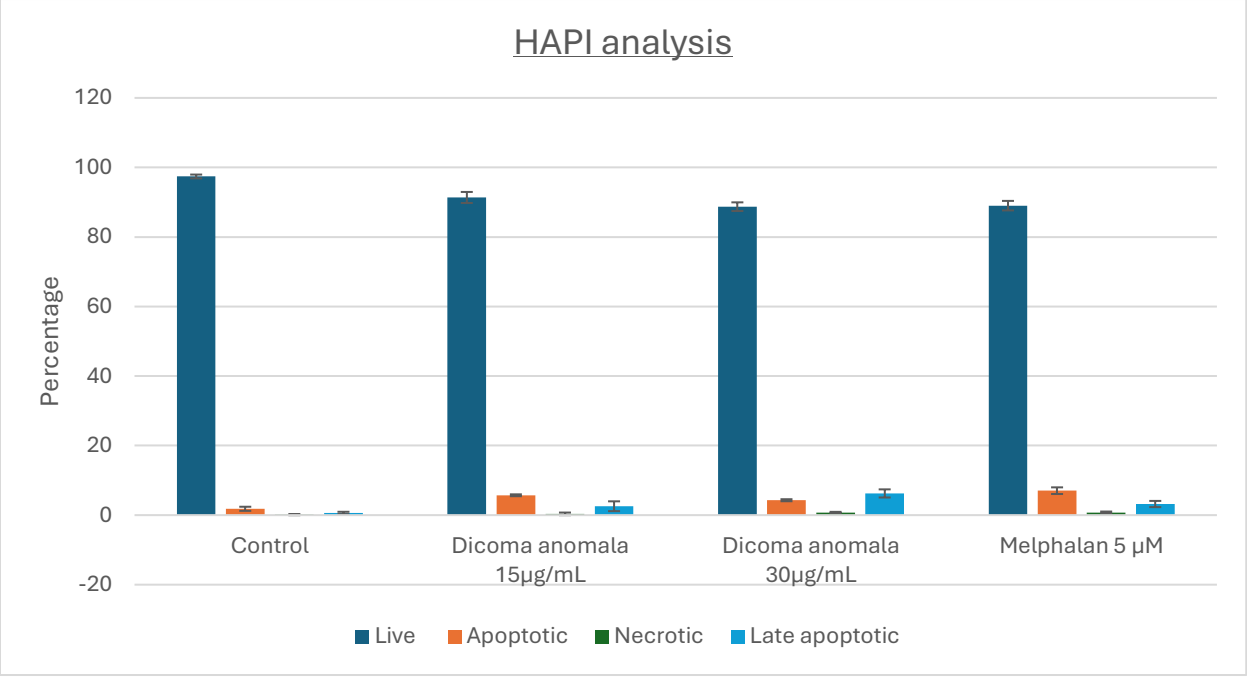

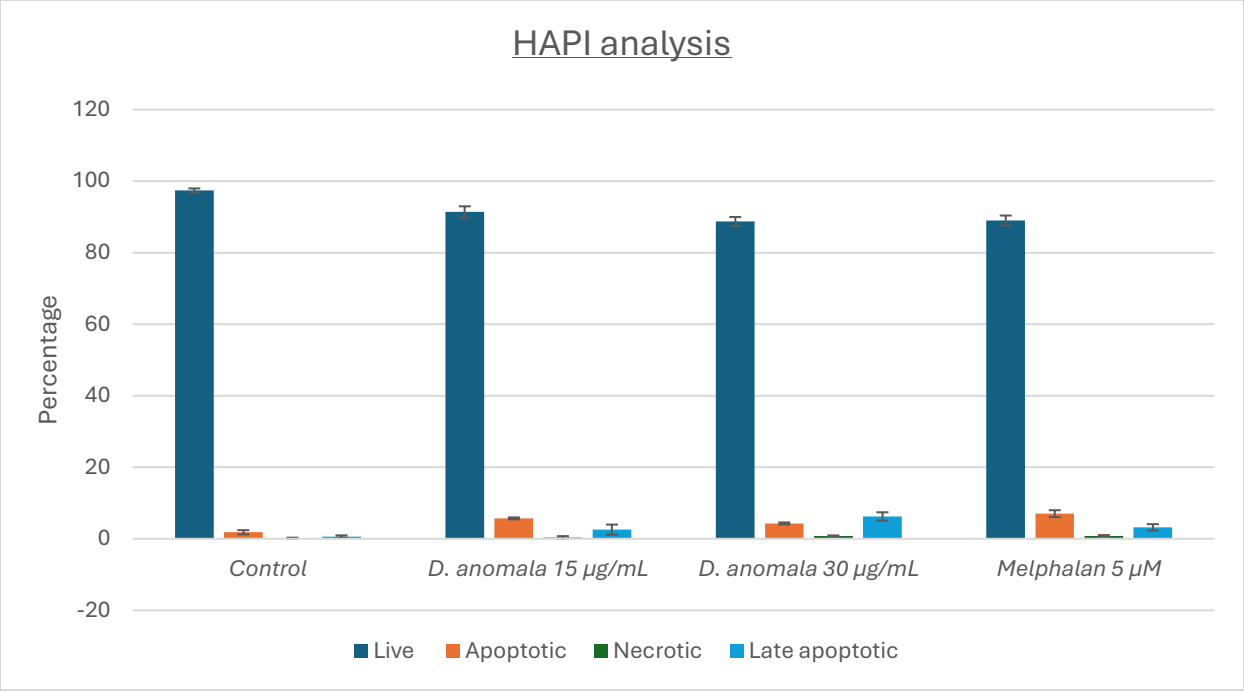

Figure 6.5 illustrates the average live, apoptotic, necrotic, and late apoptotic DU145 cells after 24 hours of treatment with MeOH-extracted *D. anomala* at 15 µg/mL and 30 µg/mL concentrations.

The bar graph represents the average of one individual experiment performed in quadruplicate. SD is represented as error bars.

Figure 6.6 represents the average cell analysis of the DU145 prostate cancer cell line using HAPI stains after 48 hours of exposure to treatments. Cells were treated with 40 µM melphalan as the positive control and untreated cells. The treatment of methanolic *D. anomala* extract comprised 15 µg/mL and 30 µg/mL respectively.

Figure 6.6: HAPI after 48 hours

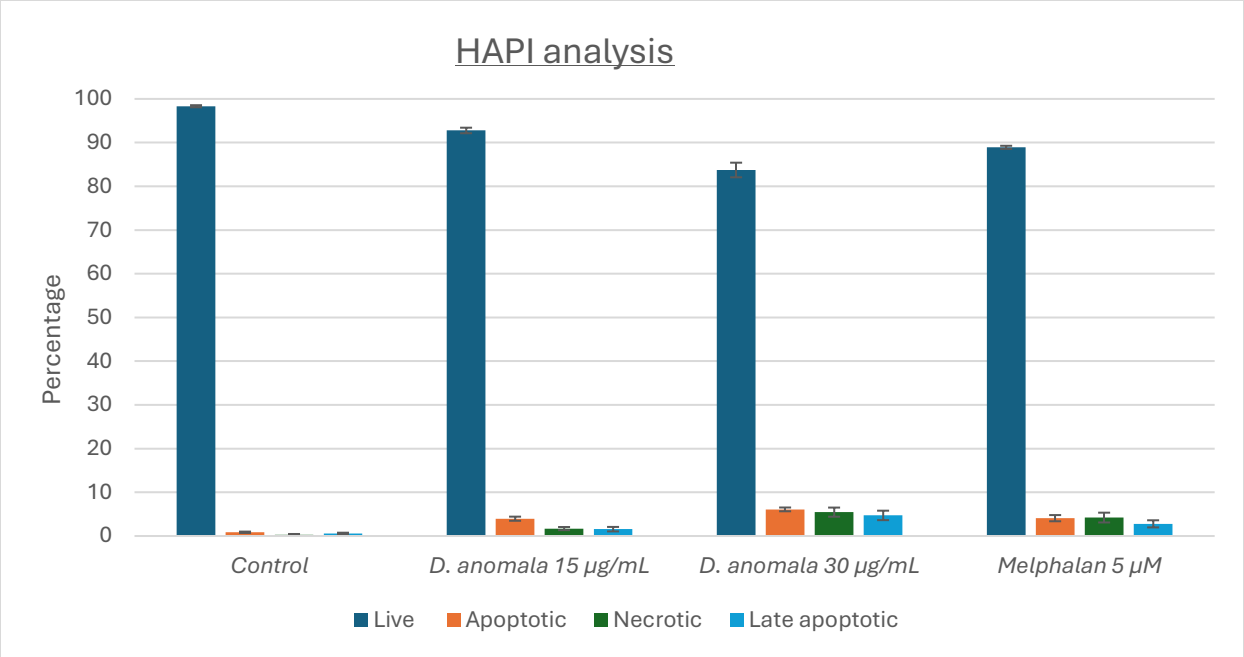

Figure 6.6 illustrates the average live, apoptotic, necrotic, and late apoptotic DU145 cells after 48 hours of treatment with MeOH-extracted *D. anomala* at 15 µg/ml and 30 µg/ml concentrations.

The bar graph represents the average of one individual experiment performed in quadruplicate. SD is represented as error bars.

The initial stage of apoptosis is denoted by loss of phospholipid asymmetry and thus results in the exposure of PS on the outer surface of the cell membrane. Therefore, an important marker of early apoptosis is the loss of phospholipid asymmetry and the resultant appearance of PS on the outer surface of the cell membrane. In necrosis, PS also becomes accessible due to the disruption of the cell lipid membrane (Venables, 2013). Figure 6.5 showed 5.71% of the cells at 15 µg/ml of *D. anomala* after 24 hours had arguably lost phospholipid and was close to the control treated cell at 7.03% of melphalan, which points to early apoptosis. Thus, in comparison to Figure 6.6 at 15 µg/ml of *D. anomala* after 48 hours exposure, 3.96% of the cells exhibited loss of early stage of apoptosis and a decline in the number of cells. Inversely, at 30 µg/ml of *D. anomala*, after 24 hours, 4.29% of the cells indicated early apoptosis, with an increase of cells after 48 hours to 6.09% of the DU145 prostate cell line (see Figure 6.6).

6.11.2 Cell cycle analysis

DNA cell cycle analysis was performed to determine the arrest of cells in a certain phase of the cell cycle. Figure 6.7 indicates the DNA cell cycle analysis that was performed to determine the arrest of cells in certain phases of the cell cycle. The DU145 prostate cancer cell line was exposed to methanolic extract at concentrations of 15 µg/mL and 30 µg/mL respectively for 24 hours.

Figure 6.7: DNA structure after 24 hours

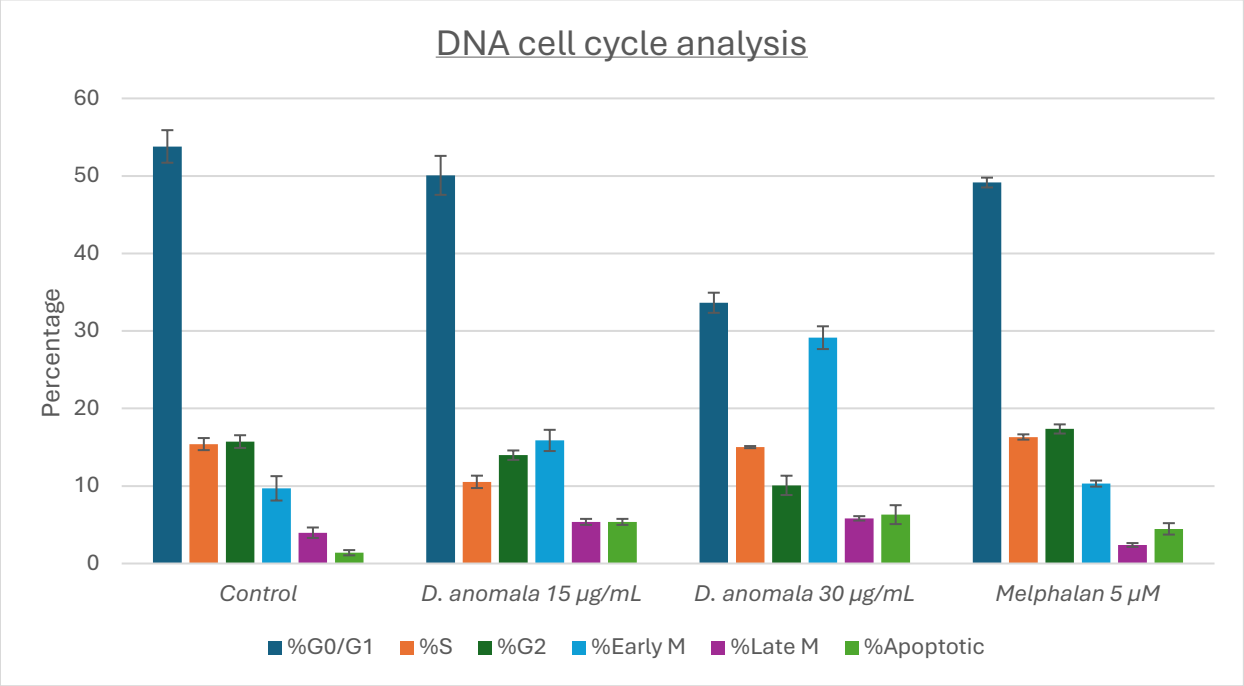

Figure 6.7 illustrates the DNA cell cycle of the DU145 cell after 24 hours of being treated with MeOH-extracted *D. anomala* at 15 µg/mL and 30 µg/mL concentrations. Melphalan was used as the positive control.

The bar graph represents the average of one individual experiment in quadruplicate. SD is presented as error bars.

Figure 6.8 illustrates the DNA cell cycle analysis performed to ascertain the arrest of cells in certain phases of the cell cycle. Similarly, the DU145 prostate cancer cell line was exposed to methanolic extract at concentrations of 15 µg/mL and 30 µg/mL respectively for 48 hours.

Figure 6.8: DNA structure after 48 hours

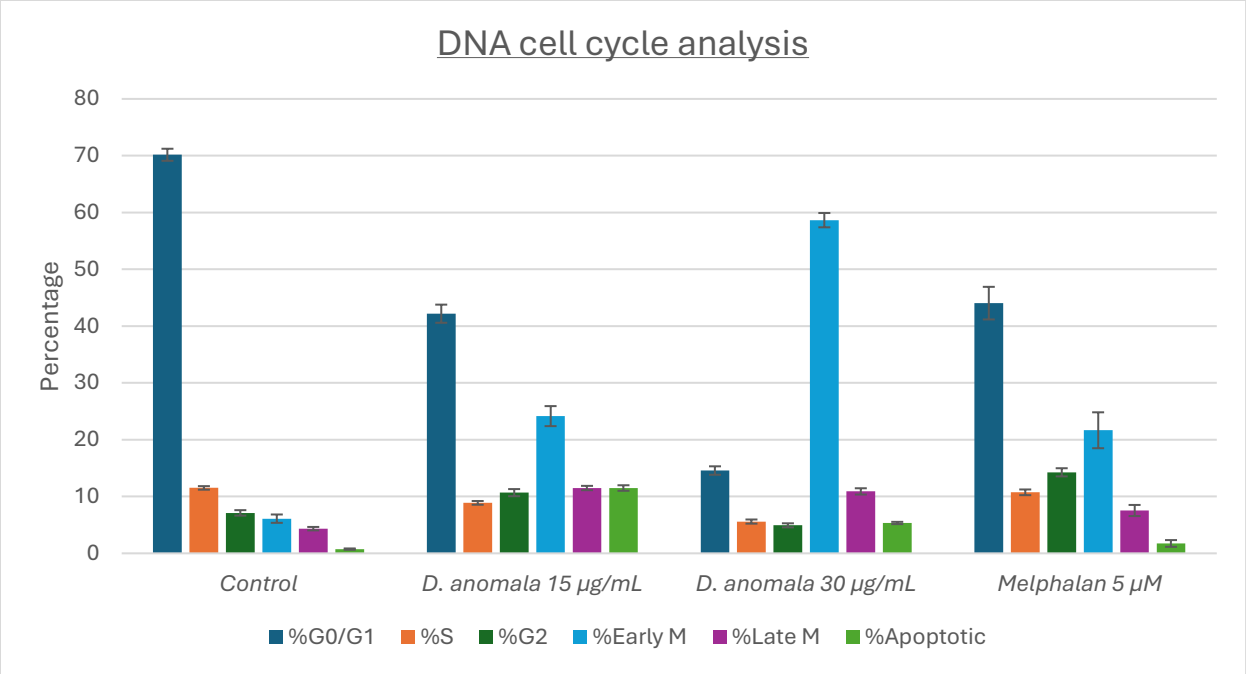

Figure 6.8 illustrates the DNA cell cycle of the DU145 cells after 24 and 48 hours of being treated with MeOH-extracted *D. anomala* at 15 µg/mL and 30 µg/mL concentrations. Melphalan was used as the positive control. The bar graph represents the average of one individual experiment in quadruplicate. SD is presented as error bars.

Correspondingly, each cell cycle phase suggests that *D. anomala* methanolic extracts arrested cells at S phase, almost identical to cells arrested by melphalan control, whereas the early M phase demonstrated more arrested cells at 15µg/mL concentration after 24 hours (see Figure 6.7). Cells arrested at the late M phase are similar at 15 µg/mL and 30µg/mL concentration levels of *D. anomala* methanolic extract after 24 hours. A similar depiction was observed after 48 hours of treatment. Early M phase at 15 µg/mL showed similar arrested cells, like the melphalan control, but in the late M phase more arrested cells were observed at 30 µg/mL concentration. An interesting observation made of apoptotic cells at 15 µg/mL concentration after 24 hours is comparable to apoptotic cells seen at 30 µg/mL concentration after 48 hours, as observed in Figure 6.8.

Figure 6.9 shows the DU145 prostate cancer cell line after 24 hours of exposure to methanolic *D. anomala* extract. These are cell cycle analysis morphologic images taken of treated cells and *D. anomala* at 15 µg/mL after 24 hours.

Figure 6.9: Morphological changes: (A) control untreated cells; (B) treated with *D. anomala* at 15 µg/mL for 24 hours, with different colours depicting different cell cycle phases

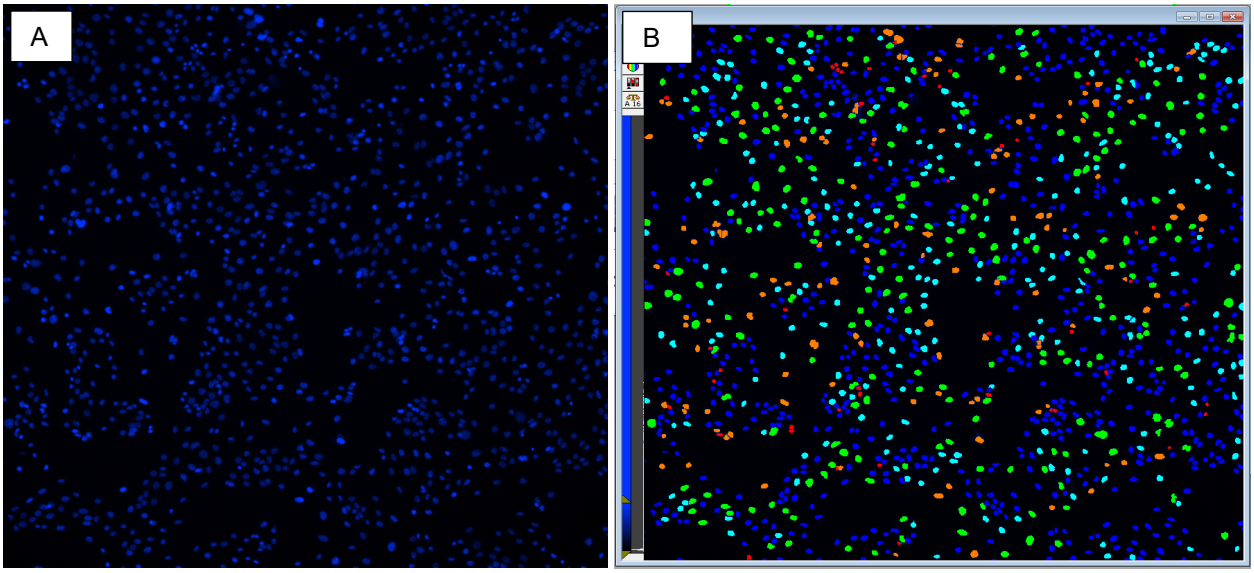

Figure 6.10: Morphological changes: (A) control melphalan; (B) treated cells with 15 µg/mL concentration of *D. anomala* after 24 hours

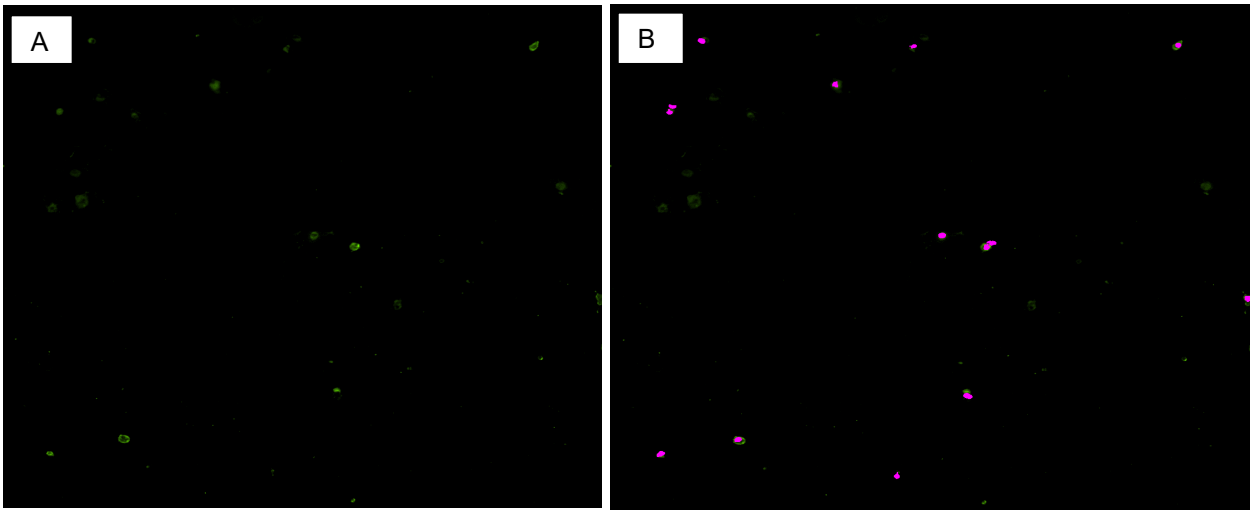

The mitotic classification summarised in Figure 6.11 is of the DU145 cells treated with *D. anomala* at 15 µg/mL after 24 hours.

Figure 6.11: DNA scatterplot

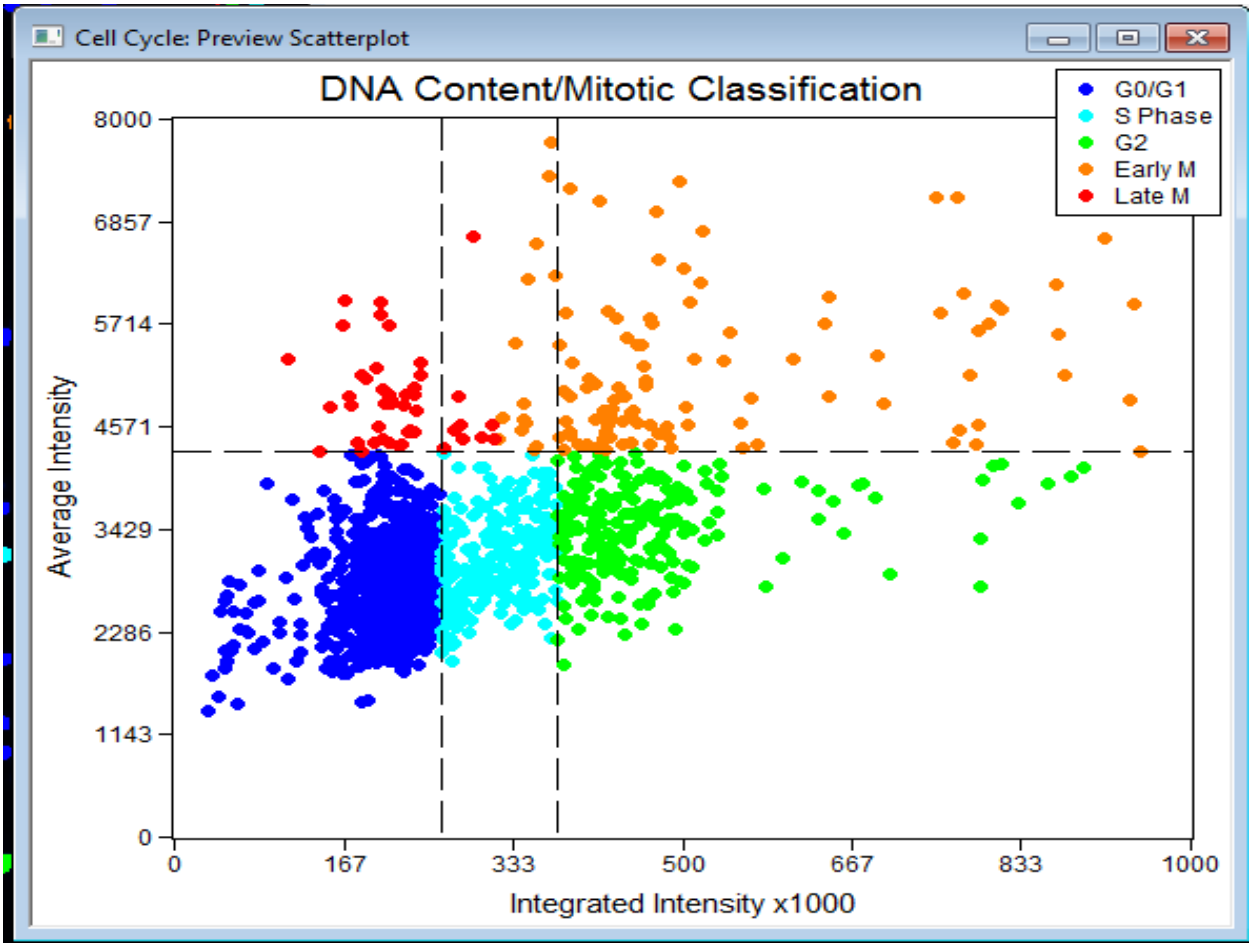

6.11.3 Mitochondrial membrane potential (MMP) analysis

Metabolically active cells generate MMP, as outlined in Figure 6.12. The loss of MMP and the subsequent release of pro-apoptotic proteins are an indicator of intrinsic apoptosis (see Section 6.2) (Swanepoel, 2019). To measure the MMP of the DU145 cells after exposure to *D. anomala* methanolic extracts, tetramethylrhodamine ethyl ester (TMRE), a lipophilic stain, was used.

For this study, the cells were seeded and treated as described for the cell cycle analysis method outlined in Section 6.10. The cells were stained by removing the treatment medium and adding 100-µL aliquots of a mixture of TMRE at a final concentration of 0.25 µM (50 µL of 0.05 mM stock) and Hoechst 3334 at a final concentration of 2 µg/mL (2µL

of 10 mg/mL stock) in 10 mL DPBS with Ca^{2+} and Mg^{2+}. The cells were incubated in the dark for 30 minutes at 37 °C prior to imaging.

6.11.3.1 MMP results

Figure 6.12 shows the MMP of the DU145 prostate cell line after exposure to *D. anomala* methanolic extracts at 15 µg/mL and 30 µg/mL for 48 hours.

Figure 6.12: Tetramethylrhodamine ethyl ester (TMRE) after 48 hours

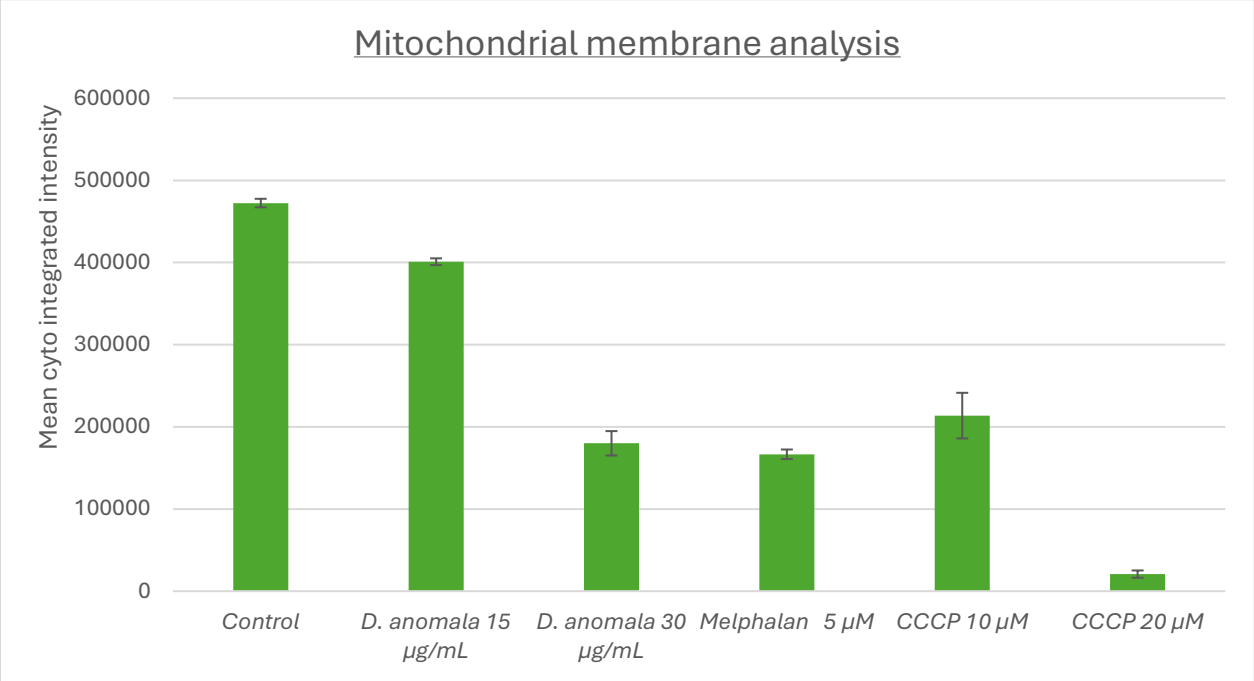

Figure 6.12 presents the MMP analysis of the DU145 cells after 48 hours of exposure to *D. anomala* at 15 µg/mL and 30 µg/mL concentrations. Melphalan was used as the positive control.

Ten µM and 20 µM concentrations of carbonyl cyanide m-chlorophenyl hydrazone (CCCP) were used as a mitochondrial depolarising control. The bar graph represents the average of one individual experiment performed in quadruplicate. SD is represented as error bars.

A decrease in fluorescence intensity is evident upon membrane depolarisation, where 30 µg/mL of *D. anomala* demonstrated a significant decrease after 48 hours. Although

the *D. anomala* methanolic extract at 15 µg/mL was able to display some degree of membrane depolarisation, it was not remarkable. The final analysis showed MeOH extracts from *D. anomala*'s abilities to indicate the onset of the intrinsic mode of apoptosis and the release of pro-apoptotic proteins from the mitochondria.

6.11.4 Caspase activation

Caspases are regarded as essential effector molecules that are responsible for many of the morphological and biochemical features of apoptosis. They are synthesised as pro-enzymes and exist as zymoges (Kroemer et al., 2009). This study focused on caspases that are the effectors of apoptosis and activators of apoptosis, namely caspase-3. The cleavage of several proteins results in morphological changes and caspase-3 is responsible for the cleavage of many proteins (Venables, 2013). The presence of active caspase-3 after treating the DU145 cells with *D. anomala* MeOH extract was examined.

Cleaved caspase-3 analysis cells were seeded and treated as described for the cell cycle analysis method as outlined in Section 6.10. The cells were treated for 24 and 48 hours, after which they were fixed and permeabilised. Cleaved caspase-3 (Asp 175) (D3E9) rabbit monoclonal antibodies (Cell Signalling Technology) were used to detect the presence of activated caspase-3. After permeabilisation, the cells were blocked using DPBS with Ca^{2+} and Mg^{2+} containing 0.5% BSA and thereafter incubated with the antibodies separately (1:200 for caspase-3) for one hour at 37 °C. The cells were washed and incubated with a conjugated secondary antibody (1:500), anti-rabbit IgG (H+L), and F(ab')2 Fragment (Alexa Fluor® 647 Conjugate) for 30 minutes at 37 °C in the dark. After staining with the secondary antibody, the cells were washed twice to eliminate unbound antibody and Hoechst33342 was used as a counterstain, at a final concentration of 2 µg/mL, prior to imaging.

6.11.4.1 Caspase activation results

The cleaved caspase-3 analysis of DU145 cell line is indicated in Figure 6.13 after 48 hours of exposure to *D. anomala* at 15 µg/mL and 30µg/mL.

Figure 6.13: Caspase-3 after 48 hours

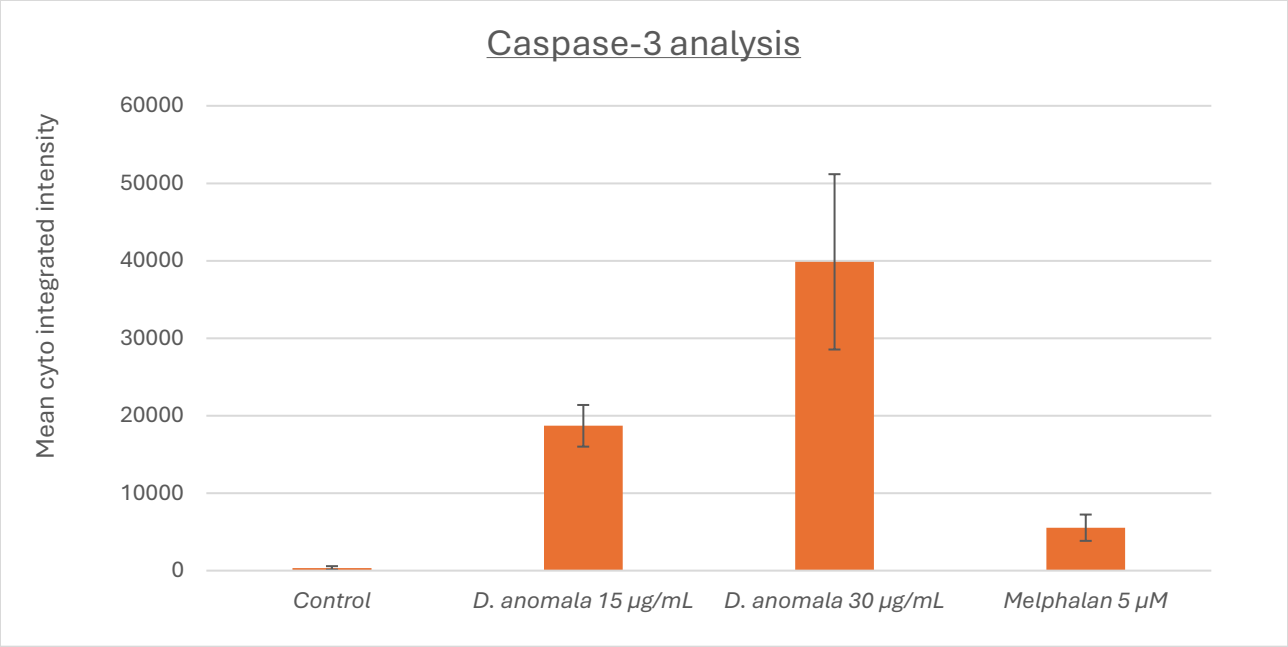

Figure 6.13 illustrates the cleaved caspase-3 analysis of the DU145 cells after 48 hours of exposure to *D. anomala* at 15 µg/mL and 30 µg/mL concentrations. Melphalan was used as the positive control.

The bar graph represents the average of one individual experiment in quadruplicate. SD is represented as error bars.

Antibodies against cleaved caspases were used to detect their presence. The activation process of caspase-3 was determined using immunochemistry techniques. An increase in mean fluorescence intensity indicated the presence of activated caspases. Following *D. anomala* at 15 µg/mL exposure, an increase in activated caspases was evident; however, an exponential increase was identified after 30 µg/mL of *D. anomala* extracts.

Figure 6.14 shows the DU145 prostate cancer cell line after 48 hours of exposure to methanolic *D. anomala* extract. Activated caspase-3 morphologic images were taken of treated cells and *D. anomala* at 15 µg/mL after 24 hours.

Figure 6.14: (A) Morphological changes control: melphalan; (B) treated 15 µg/mL concentration of *D. anomala*

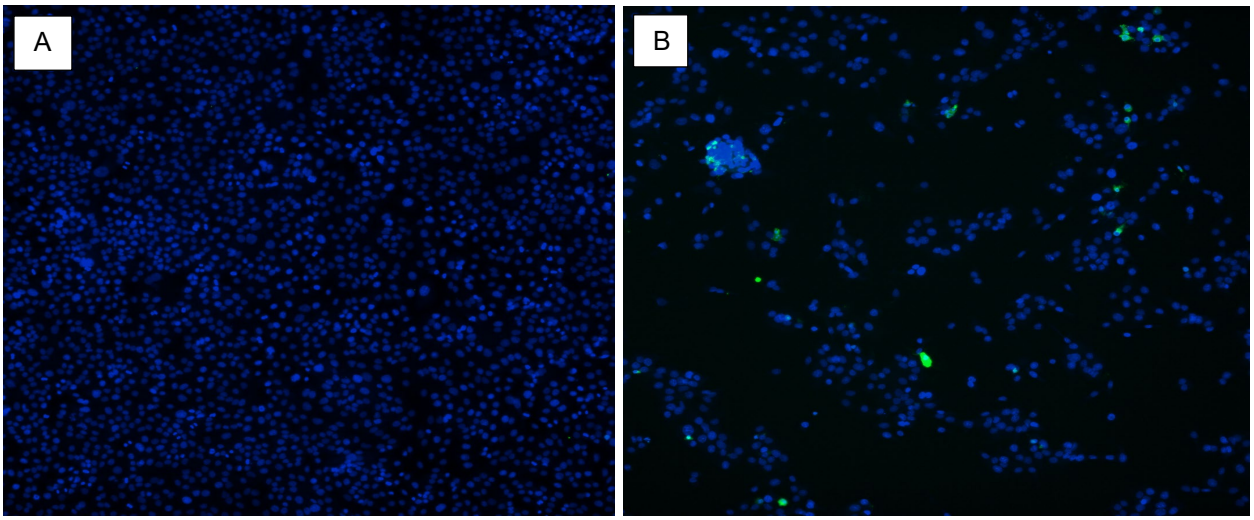

Figure 6.15: Treated 30 µg/mL concentration of *D. anomala*

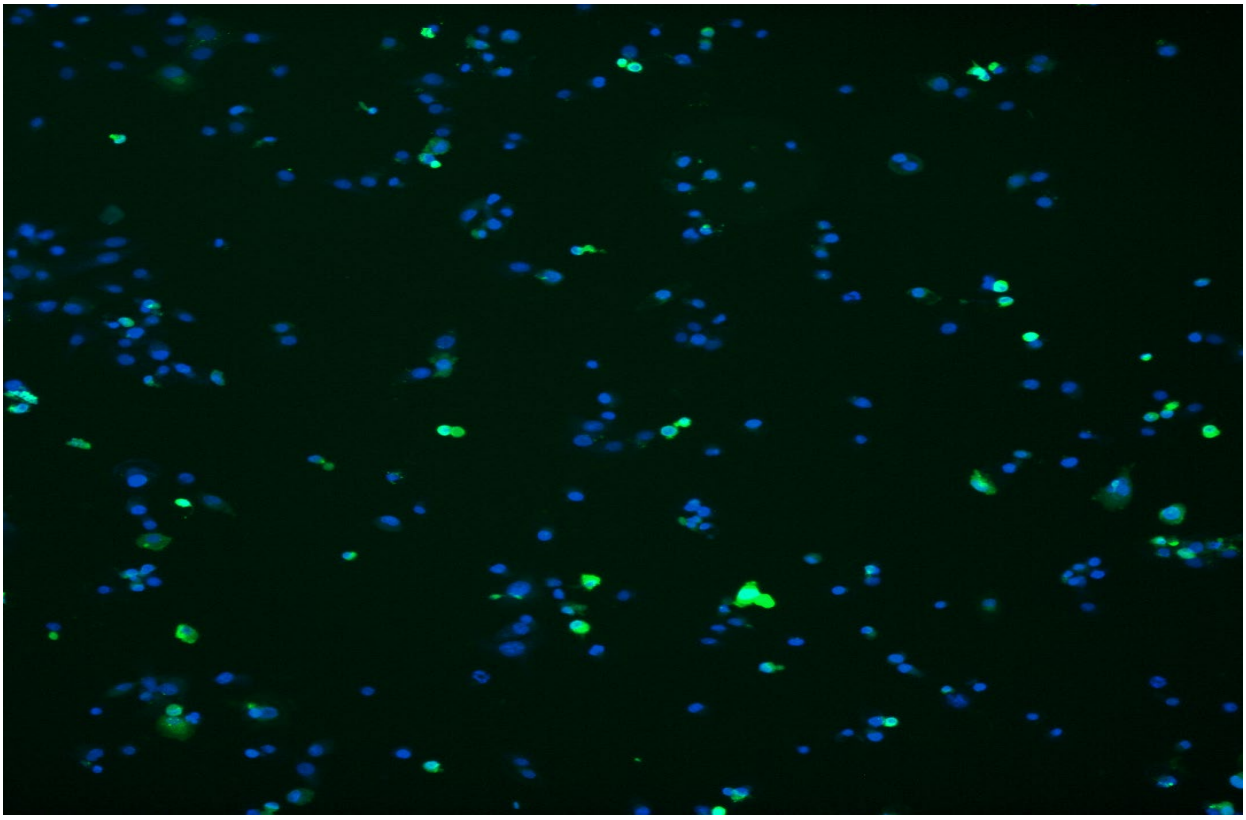

6.12 Data quantification

The quantification of live and dead cells for the screening assay was performed using the Image Xpress Micro XLS Widefield microscope and the acquired images were analysed using the Meta Xpress software and multi-wavelength cell scoring application module and the cell cycle module. The acquired data were transferred to Microsoft Excel spreadsheets and analysed.

6.13 Discussion

The findings highlight the anticancer activity of *D. anomala*, which appears to operate through several well-established mechanisms, including PS translocation, cell cycle arrest, mitochondrial membrane depolarisation, and caspase-3 activation. The bioactive compounds identified in *D. anomala*, particularly phenolic acids, flavonoids, and terpenoids, as outlined in Chapter 3, contribute to this multifaceted mechanism of action.

PS translocation, a hallmark of early apoptosis, was prominently observed, which suggests that *D. anomala* triggers apoptosis in cancer cells by externalising PS on the cell membrane. This process is an essential step in marking cells for phagocytic removal and underlines the ability of the plant's metabolites to initiate PCD pathways. In this study, there was an increase in cells that had lost phospholipid asymmetry and resulted in the appearance of PS on the outer surface of the cell membrane after 48 hours, as seen in the 15 µg/mL concentration of an extract when compared to 5 µM of melphalan positive control (see Figures 6.5 and 6.6). The implication is that the presence of PS in the outer surface of the cell membrane signal disrupted the cell membranes.

The cell cycle analysis revealed that *D. anomala* induces significant arrest at both the S phase and the early M phase, which suggests an antiproliferative effect on cancer cells. This dual-phase arrest implies that the bioactive compounds in the plant extract, particularly phenolic acids, flavonoids, and terpenoids, disrupt key regulatory checkpoints in the cell cycle (Chota et al., 2024). By arresting cells in the S phase, *D. anomala* inhibits DNA replication and prevents the proper synthesis of genetic material required for cell

division. The early M phase arrest's further disruption of mitotic progression halts the division of cancer cells before they can complete mitosis (Swanepoel, 2019).

These disruptions are likely mediated through the modulation of cyclins and CDKs, which control the transitions between these phases (Gallorini et al., 2012). Phenolic compounds are known to downregulate cyclin A and B, essential for S phase progression and mitotic entry, while flavonoids have been shown to inhibit CDKs and further preventing cell cycle progression (Woo & Poon, 2003). The ability of *D. anomala* to halt the cell cycle at these critical phases is a key mechanism in its antiproliferative action, which effectively limits cancer cell growth and proliferation.

The early M phase showed an increased number of cells when exposed to both 15 µg/mL and 30 µg/mL of *D. anomala* MeOH extract after 48 hours. Of particular interest to note is the 30 µg/mL extract, as there was an exponential increase in the number of cells arrested (see Figures 6.6 and 6.7). These were the highest proportions of cells found in the same cycle event at the specific time, especially when compared to the positive control, melphalan. Additionally, the numbers of cells arrested in the S phase were considerably high after 24 hours of exposure to the *D. anomala* MeOH extract, where the DNA responded to 30 µg/mL of the extract.

Additionally, during the late M phase, the margin between cells arrested appears to not be larger than the arrested cells after being exposed to the extract concentration of 15 µg/mL and 30 µg/mL after 24 hours, which demonstrates that extract concentration levels did not yield much influence on the cells.

Another key finding was the depolarisation of the mitochondrial membrane, which indicates the intrinsic apoptosis pathway activation. The mitochondrial dysfunction observed can be attributed to the terpenoids and flavonoids, which are known to induce oxidative stress that lead to the release of pro-apoptotic factors such as cytochrome c. This disruption of mitochondrial integrity is a crucial step in the activation of downstream apoptotic events (Wright et al., 2019). Depolarisation of the mitochondrial membrane was seen at 30 µg/mL of the extract after being exposed for 48 hours (see Figure 6.12). This suggests a cell membrane shift of electrical charge distribution that allows the release of

pro-apoptotic proteins that are responsible for the activation of caspases that results in the process of apoptosis (Swanepoel, 2019).

Caspase-3 activation further supports the pro-apoptotic effects of *D. anomala*. The activation of this executioner caspase confirms that the apoptosis observed is caspase-dependent, driven by both the intrinsic mitochondrial and extrinsic receptor-mediated pathways (Venables, 2013). The combined effects of these phytochemicals act in synergy to inhibit cancer cell survival and promote cell death. Caspases, a family of cysteine proteases, play an important role in apoptosis. Caspase-3 and caspase-7 are responsible for the cleavage of a large number of proteins, which results in morphological changes (Van Doorn, 2011). In this study, there was an increase in cleaved caspase-3 after the cells were exposed to 15 µg/mL extract (see Figure 6.13), but an even greater increase was seen after exposure to 30 µg/mL extract for 48 hours.

In the same way, Chota et al.'s (2024) investigation of green-synthesised silver nanoparticles (AgNPs) using *D. anomala* plant extract as the reducing agent reported that AgNPs at concentrations between 2 µg/mL and 8 µg/mL increased mitochondrial cytochrome c release. Although it was released at a high concentration of 30 µg/mL in this study, when compared with Chota et al.'s (2024) study on silver nanoparticles, it is noteworthy. In other words, the activities of caspase-3 were not significantly high in Chota et al.'s (2024) work on the green synthesis of AgNPs. Collectively, the findings point to cell death through caspases-8 and -9 cascade (Chota et al., 2020), where caspase-3 was greatly increased after exposure of the DU145 cells to 3.0 µg/m extract for 48 hours.

Caspase-3 is a crucial executioner caspase that is responsible for dismantling the cellular components necessary for apoptosis, which leads to controlled cell death (Van Doorn, 2011). The increase in cleaved caspase-3 following treatment therefore confirms that *D. anomala* methanolic extract promotes apoptosis in prostate cancer cells, specifically through the executioner phase of the apoptotic pathway. This finding aligns with the extract's observed ability to halt the cell cycle and supports the potential of *D. anomala* as a therapeutic candidate for inducing cancer cell death through apoptosis.

In the same way, the roots and leaves of *D. anomala* have been used extensively in treating various diseases, ranging from pneumonia to many renal anomalies. The use of *D. anomala* specifically for lung and breast carcinoma is attributed to the noted presence of flavonoids, sesquiterpenes, phytosterols, and triterpenes, which are known to possess anticancer properties (Chota et al., 2020).

Correspondingly, Sikhakhane's (2013) study recorded no morphological changes or cell death due to extracts of *H. hemerocallidea* on the SNO oesophageal cell line and attributed this to the lack of active enzymes in the SNO oesophageal cell line needed for conversion of hypoxoside to the cytotoxic anticancer active rooperol. The same may be assumed for the DU145 prostate cancer cell line, as the focus of this study. Although the absence of these enzymes from cell lines like DU145 and SNO is true, the proliferation seen after the aqueous extracts of *H. hemerocallidea* was alarming.

The use of *H. caespititium* for wound dressing during circumcision rites is well documented. However, minimal details have been provided about the plants other than the investigation done on *H. italicum* and *H. arenarium* and noting the remarks made on *Helichrysum* species as a group of poorly investigated medicinal plants (Akaberi et al., 2021). This study thus endeavoured to provide evidence from the corm of *H. caespititium* on the proliferation of the DU145 prostate cell line. It could be argued that the failure of *H. hemerocallidea* and *H. caespititium* to demonstrate cytotoxic effects on the DU145 prostate cancer cell line necessitates the practice of a combination of treatments, including the usage of other modalities such as hormone therapy, anti-angiogenic treatment, and stem cell therapies (Debela et al., 2021).

In conclusion, the phenolic acids, flavonoids, and terpenoids found in *D. anomala* orchestrate a robust anticancer response through multiple molecular pathways, including the induction of apoptosis via PS translocation, cell cycle inhibition, mitochondrial depolarisation, and caspase activation. These results highlight the potential of *D. anomala* as a natural source of anticancer agents and warrant further investigation into further therapeutic applications in cancer treatment.

REFERENCES

Akaberi, M., Najaran, Z. T., Azizi, N., & Emami, S. A. (2021). Metabolite profiling and antiprotozoal activity of three endemic Iranian helichrysum species. *Industrial Crops and Products*, *174*, 114196.

Barnum, K. J., & O'Connell, M. J. (2014). Cell cycle regulation by checkpoints. *Methods in Molecular Biology*, *1170*, 29-40.

Chota, A., Abrahamse, H., & George, B. P. (2024). Green synthesis and characterization of AgNPs, liposomal loaded AgNPs and $ZnPcS_4$ photosensitizer for enhanced photodynamic therapy effects in MCF-7 breast cancer cells. *Photodiagnosis and Photodynamic Therapy*, *48*, 104252.

Chota, A., George, B. P., & Abrahamse, H. (2020). Potential treatment of breast and lung cancer using *Dicoma anomala*, an African medicinal plant. *Molecules*, *25*(19), 4435.

Debela, D. T., Muzazu, S. G., Heraro, K. D., Ndalama, M. T., Mesele, B. W., Haile, D. C., Kitui, S. K., & Manyazewal, T. (2021). New approaches and procedures for cancer treatment: Current perspectives. *SAGE Open Medicine*, *9*, 20503121211034366.

Dickson, M., & Schwartz, G. K. (2009). Development of cell-cycle inhibitors for cancer therapy. *Current Oncology*, *16*(2), 36-43.

Fulda, S. (2010). Modulation of apoptosis by natural products for cancer therapy. *Planta Medica*, *76*(11), 1075-1079.

Fulda, S., & Debatin, D. M. (2006). Extrinsic versus intrinsic apoptosis pathways in anticancer chemotherapy. *Oncogene*, *25*(34), 4798-4811.

Gallorini, M., Cataldi, A., & Di Giacomo, V. (2012). Cyclin-dependent kinase modulators and cancer therapy. *BioDrugs*, *26*, 377-391.

Green, D. R., & Kroemer, G. (2004). The pathophysiology of mitochondrial cell death. *Science*, *305*(5684), 626-629.

Green, D. R., & Llambi, F. (2015). Cell death signaling. *Cold Spring Harbor Perspectives in Biology*, *7*(12), a006080.

Kroemer, G., Galluzzi, L., Vandenabeele, P., Abrams, J., Alnemri, E. S., Baehrecke, E., Blagosklonny, M., El-Deiry, W., Golstein, P., & Green, D. (2009). Classification of cell death: Recommendations of the Nomenclature Committee on Cell Death 2009. *Cell Death & Differentiation*, *16*(1), 3-11.

Nikoletopoulou, V., Markaki, M., Palikaras, K., & Tavernarakis, N. (2013). Crosstalk between apoptosis, necrosis and autophagy. *Biochimica et Biophysica Acta (BBA)-Molecular Cell Research*, *1833*(12), 3448-3459.

Obeng, E. (2020). Apoptosis (programmed cell death) and its signals: A review. *Brazilian Journal of Biology*, *81*, 1133-1143.

Oropesa Ávila, M., Fernández Vega, A., Garrido Maraver, J., Villanueva Paz, M., De Lavera, I., De la Mata, M., Cordero, M. D., Alcocer Gómez, E., Delgado Pavón, A. and Álvarez Córdoba, M. (2015). Emerging roles of apoptotic microtubules during the execution phase of apoptosis. *Cytoskeleton*, *72*(9), 435-446.

Rahman, M. A., Akhtar, J., & Arshad, M. (2016). Evaluation of cytotoxic potential and apoptotic effect of a methanolic extract of bauhinia racemosa lam. against a human cancer cell line, hela. *European Journal of Integrative Medicine*, *8*(4), 513-518.

Ravanan, P., Srikumar, I. F., & Talwar, P. (2017). Autophagy: The spotlight for cellular stress responses. *Life Sciences*, *188*, 53-67.

Rayfield, E. L. (2023). *Porifera: Biology and medicinal properties* (Honours thesis). Gardner-Webb University. https://digitalcommons.gardner-webb.edu/undergrad-honors/54/

Reape, T. J., & McCabe, P. F. (2010). Apoptotic-like regulation of programmed cell death in plants. *Apoptosis*, *15*, 249-256.

Riss, T. L., Moravec, R. A., Niles, A. L., Duellman, S., Benink, H. A., Worzella, T. J., & Minor, L. (2016). *Cell viability assays*. https://www.ncbi.nlm.nih.gov/books/NBK144065/

Science Facts. (2024). *What is the cell cycle?* https://www.sciencefacts.net/cell-cycle.html

Sikhakhane, X. (2013). Evaluating the anticancer and antimicrobial properties of extracts from *Hypoxis hemerocallidea* (African potato). University of Johannesburg.

Swanepoel, B. (2019). *New synergic biomaterials for anti-cancer therapy* (Master's thesis). Nelson Mandela University. https://core.ac.uk/reader/289223600

Uller, L., Andersson, M., Greiff, L., Persson, C. G., & Erjefält, J. S. (2004). Occurrence of apoptosis, secondary necrosis, and cytolysis in eosinophilic nasal polyps. *American Journal of Respiratory and Critical Care Medicine*, *170*(7), 742-747.

Van Doorn, W. G. (2011). Classes of programmed cell death in plants, compared to those in animals. *Journal of Experimental Botany*, *62*(14), 4749-4761.

Venables, L. (2013). *In vitro induction of cell death pathways by Artemisia afra extract and isolation of an active compound, isoalantolactone* (Master's thesis). Rhodes University.

Vermeulen, K., Van Bockstaele, D. R., & Berneman, Z. N. (2003). The cell cycle: A review of regulation, deregulation and therapeutic targets in cancer. *Cell Proliferation*, *36*(3), 131-149.

Woo, R. A., & Poon, R. Y. (2003). Cyclin-dependent kinases and S phase control in mammalian cells. *Cell Cycle*, *2*(4), 315-323.

Wright, G. S., Antonyuk, S. V., & Hasnain, S. S. (2019). The biophysics of superoxide dismutase-1 and amyotrophic lateral sclerosis. *Quarterly Reviews of Biophysics*, *52*, e12.

Yan, G., Elbadawi, M., & Efferth, T. (2020). Multiple cell death modalities and their key features. *World Academy of Sciences Journal*, *2*(2), 39-48.

CHAPTER 7:
CONCLUSIONS AND RECOMMENDATIONS

7.1 Conclusion

To conclude, it is significant to reflect on the stated aim of this study, which was to evaluate the effects of the corms of *H. hemerocallidea* (African potato), *H. caespititium*, and *D. anomala* on the proliferation of the DU145 prostate cancer cell line in vitro.

Direct maceration of corms, in dried powdered form by MeOH, followed by aqueous, resulted in higher yield of phytosterols, phenolic, flavonoids, and terpenoids compounds. The MeOH solvent yielded higher compounds compared to the aqueous solvent because of their different polarities. It should be noted that the intention was not to compare the weight of extracted fractions of the corms.

Compounds screened from the ion chromatogram of the negative ion mode set forth in Chapter 3 (see Figures 3.2 to 3.4) and those of the positive ion mode (see Figures 3.5 to 3.7) signalled the presence of phytosterols and glycosides from *H. hemerocallidea*, flavonoids and polyphenols existent in *H. caespititium* and phenolic acids, and flavonoids, tannins, and saponins in the *D. anomala* extracts.

A higher percentage inhibition observed from extracts of *H. hemerocallidea*, *H. caespititium*, and *D. anomala* (see Figures 4.1, 4.2, and 4.3) points to the presence of high anti-oxidant activity. The presence of anti-oxidants in the *H. hemerocallidea*, *H. caespititium*, and *D. anomala* corm extracts correlates to the active compound identified.

Cell viability data revealed that of the three extracts, namely *H. hemerocallidea*, *H. caespititium*, and *D. anomala*, it was the *D. anomala* methanolic extract that possessed significant antiproliferation activity against the DU145 prostate cancer cell line when compared to the standard anticancer drug, melphalan (see Figure 5.6). However, further characterisation of the cytotoxicity effects demonstrated being more cytocidal rather than cytostatic.

In summary, methanolic extracts of *D. anomala* corms are able to induce apoptosis on the proliferation of the DU145 prostate cancer cell line. This study further demonstrated the anti-oxidant and phytochemical properties of *H. hemerocallidea* (African potato), *H. caespititium*, and *D. anomala* corms using HRMS. Moreover, *D. anomala* demonstrated significant anticancer activity through a variety of mechanisms, including PS translocation, cell cycle arrest at the S and early M phases, mitochondrial membrane depolarisation, and caspase-3 activation. These effects are largely attributed to the presence of phenolic acids, flavonoids, and terpenoids in the methanolic extract, which not only exert direct anticancer effects but also possess strong anti-oxidant activities. The anti-oxidant properties of these compounds play a crucial role in reducing oxidative stress, protecting normal cells, and further enhancing the selective apoptosis of cancer cells. Collectively, the anti-oxidant and apoptotic activities of *D. anomala* highlight its potential as a natural therapeutic agent for treating cancers such as prostate cancer, which merits further research and clinical exploration.

7.2 Limitations of the study

The study was confined to in vitro evaluations of anticancer activity against prostate cancer cells, without examining the effects on normal cells, due to financial constraints. This limitation prevents understanding the plant extract's selectivity and potential cytotoxicity against healthy cells, which is crucial for determining therapeutic safety margins.

Moreover, the research could not extend to in vivo studies using animal models. This limitation means that important aspects such as bioavailability, metabolism, and systemic responses to the plant extracts remain unexplored.

While preliminary phytochemical screening successfully identified major classes of compounds present in *D. anomala* extracts, the study did not include isolation and structural elucidation of specific bioactive compounds. This restricts the understanding of which particular molecules are responsible for the observed anticancer activity.

The research focused solely on crude extracts (because traditional healers use plants as they are), without investigating potential synergistic or antagonistic interactions between different compounds present in the plant material.

7.3 Recommendations

Based on the findings and limitations of this study, the following recommendations are proposed for future research:

1. Future studies should evaluate the effects of *D. anomala* extracts on non-cancerous prostate cells to establish the selectivity index and safety profile of the plant extracts.

2. In vivo studies using appropriate animal models should be conducted to:
   - determine the bioavailability and pharmacokinetics of the extracts;
   - assess potential systemic toxicity; and
   - evaluate real-world efficacy in a complete biological system.

3. Bioassay-guided fractionation should be performed to isolate and identify the specific compounds responsible for the anticancer activity. This should include:
   - systematic fractionation of the crude extract;
   - isolation of pure compounds;
   - structural elucidation using advanced analytical techniques; and
   - activity profiling of isolated compounds.

4. Investigation of the specific mechanisms of action through which the plant extracts exert their anticancer effects should be undertaken, including studies on:
   - cell death pathways;
   - cell cycle regulation;
   - molecular targets; and
   - signalling cascades.

5. Research should be conducted to understand potential synergistic interactions between different compounds present in the extract, which could inform future drug development strategies.

6. The development of standardisation methods for extract preparation should be undertaken to ensure consistency in future research and potential therapeutic applications.

REFERENCES

Akaberi, M., Najaran, Z. T., Azizi, N., & Emami, S. A. (2021). Metabolite profiling and antiprotozoal activity of three endemic Iranian helichrysum species. *Industrial Crops and Products*, *174*, 114196.

Akuru, U., & Amadi, B. (2018). Phytochemicals and antioxidant properties of some selected medicinal plants. *Journal of Pharmacognosy and Phytochemistry*, *7*(5), 283-285.

Alimirah, F., Chen, J., Basrawala, Z., Xin, H., & Choubey, D. (2006). DU-145 and PC-3 human prostate cancer cell lines express androgen receptor: Implications for the androgen receptor functions and regulation. *FEBS Letters*, *580*(9), 2294-2300.

Aliya, S., Devi, Y., & Uma, A. U. (2016). Plants as potential resources of anticancer drugs. *Current Trends in Biotechnology and Pharmacy*, *10*(1), 92-107.

Arnold, J., & Isaacs, J. (2002). Mechanisms involved in the progression of androgen-independent prostate cancers: It is not only the cancer cell's fault. *Endocrine-Related Cancer*, *9*(1), 61-73.

Balogun, F., & Ashafa, A. (2017). Aqueous root extracts of *Dicoma anomala* (Sond.) extenuates postprandial hyperglycaemia in vitro and its modulation on the activities of carbohydrate metabolizing enzymes in streptozotocin-induced diabetic Wistar rats. *South African Journal of Botany*, *112*, 102-111.

Barnum, K. J., & O'Connell, M. J. (2014). Cell cycle regulation by checkpoints. *Methods in Molecular Biology*, *1170*, 29-40.

Bassey, K., Mamabolo, P., Mothibe, M., & Muganza, F. (2021). Phytochemical profiling and chemical marker compounds identification in *Helichrysum caespititium*: A chemometrics and 2D gas chromatography time of flight mass spectrometry (GCxGC-TOF-MS) perspective. *Pharmacognosy Journal*, *13*(2), 486-494.

Birben, E., Sahiner, U. M., Sackesen, C., Erzurum, S., & Kalayci, O. (2012). Oxidative stress and antioxidant defense. *World Allergy Organization Journal*, *5*, 9-19.

Boukes, G. J., & Van de Venter, M. (2011). Cytotoxicity and mechanism(s) of action of *Hypoxis* spp. (African potato) against HeLa, HT-29 and MCF-7 cancer cell lines. *Journal of Medicinal Plants Research*, *5*(13), 2766-2774.

Cao, W., Chen, H. D., Yu, Y. W., Li, N., & Chen, W. Q. (2021). Changing profiles of cancer burden worldwide and in China: A secondary analysis of the global cancer statistics 2020. *Chinese Medical Journal*, *134*(7), 783-791.

Charmsaz, S., Collins, D. M., Perry, A. S., & Prencipe, M. (2019). Novel strategies for cancer treatment: Highlights from the 55th IACR annual conference. *Cancers*, *11*(8), 1125.

Chota, A., Abrahamse, H., & George, B. P. (2024). Green synthesis and characterization of AgNPs, liposomal loaded AgNPs and $ZnPcS_4$ photosensitizer for enhanced photodynamic therapy effects in MCF-7 breast cancer cells. *Photodiagnosis and Photodynamic Therapy*, *48*, 104252.

Chota, A., George, B. P., & Abrahamse, H. (2020). Potential treatment of breast and lung cancer using *Dicoma anomala*, an African medicinal plant. *Molecules*, *25*(19), 4435.

Dal Pra, A., Cury, F. L., & Souhami, L. (2010). Combining radiation therapy and androgen deprivation for localized prostate cancer – A critical review. *Current Oncology*, *17*(5), 28-38.

Das, N., Islam, M. E., Jahan, N., Islam, M. S., Khan, A., Islam, M. R., & Parvin, M. S. (2014). Antioxidant activities of ethanol extracts and fractions of *Crescentia cujete* leaves and stem bark and the involvement of phenolic compounds. *BMC Complementary and Alternative Medicine*, *14*, 1-9.

Debela, D. T., Muzazu, S. G., Heraro, K. D., Ndalama, M. T., Mesele, B. W., Haile, D. C., Kitui, S. K., & Manyazewal, T. (2021). New approaches and procedures for cancer treatment: Current perspectives. *SAGE Open Medicine*, *9*, 20503121211034366.

Dickson, M., & Schwartz, G. K. (2009). Development of cell-cycle inhibitors for cancer therapy. *Current Oncology*, *16*(2), 36-43.

Ekwere, P. D., & Egbe, S. (2002). The changing pattern of prostate cancer in Nigerians: Current status in the southeastern states. *Journal of the National Medical Association*, *94*(7), 619.

Elbagory, A. M., Hussein, A. A., & Meyer, M. (2019). The in vitro immunomodulatory effects of gold nanoparticles synthesized from *Hypoxis hemerocallidea* aqueous extract and hypoxoside on macrophage and natural killer cells. *International Journal of Nanomedicine*, *14*, 9007-9018.

Ferlay, J., Soerjomataram, I., Dikshit, R., Eser, S., Mathers, C., Rebelo, M., Parkin, D. M., Forman, D., & Bray, F. (2015). Cancer incidence and mortality worldwide: Sources, methods and major patterns in GLOBOCAN 2012. *International Journal of Cancer*, *136*(5), E359-E386.

Fonmboh, D. J., Abah, E. R., Fokunang, T. E., Herve, B., Teke, G. N., Rose, N. M., Borgia, N. N., Fokunang, L. B., Andrew, B. N., & Kaba, N. (2020). An overview of methods of extraction, isolation and characterization of natural medicinal plant products in improved traditional medicine research. *Asian Journal of Research in Medical and Pharmaceutical Sciences, 9*(2), 31-57.

Fulda, S. (2010). Modulation of apoptosis by natural products for cancer therapy. *Planta Medica*, *76*(11), 1075-1079.

Fulda, S., & Debatin, D. M. (2006). Extrinsic versus intrinsic apoptosis pathways in anticancer chemotherapy. *Oncogene*, *25*(34), 4798-4811.

Gallorini, M., Cataldi, A., & Di Giacomo, V. (2012). Cyclin-dependent kinase modulators and cancer therapy. *BioDrugs*, *26*, 377-391.

Ghomari, O., Sounni, F., Massaoudi, Y., Ghanam, J., Kaitouni, L. B. D., Merzouki, M., & Benlemlih, M. (2019). Phenolic profile (hplc-uv) of olive leaves according to extraction procedure and assessment of antibacterial activity. *Biotechnology Reports, 23*, e00347.

Gohari, A., Hajimehdipoor, H., Saeidnia, S., Ajani, Y., & Hadjiakhoondi, A. (2011). Antioxidant activity of some medicinal species using FRAP assay. *Journal of Medicinal Plants*, *10*(37), 54-60.

Green, D. R., & Kroemer, G. (2004). The pathophysiology of mitochondrial cell death. *Science*, *305*(5684), 626-629.

Green, D. R., & Llambi, F. (2015). Cell death signaling. *Cold Spring Harbor Perspectives in Biology*, *7*(12), a006080.

Hage, D. S. (2018). Chromatography. In N. Rifai, A. R. Horvath, C. T. Wittwer, & A. Hoofnagle (Eds.), *Principles and applications of clinical mass spectrometry* (pp. 1-32). Elsevier.

Jomova, K., Jenisova, Z., Feszterova, M., Baros, S., Liska, J., Hudecova, D., Rhodes, C., & Valko, M. (2011). Arsenic: Toxicity, oxidative stress and human disease. *Journal of Applied Toxicology*, *31*(2), 95-107.

Kalita, P., Tapan, B. K., Pal, T. K., & Kalita, R. (2013). Estimation of total flavonoids content (TFC) and anti-oxidant activities of methanolic whole plant extract of *Biophytum sensitivum* linn. *Journal of Drug Delivery and Therapeutics*, *3*(4), 33-37.

Kewuyemi, Y. O., Kesa, H., & Adebo, O. A. (2022). Biochemical properties, nutritional quality, colour profile and techno-functional properties of whole grain sourdough and malted cowpea and quinoa flours. *International Journal of Food Science & Technology*, *57*(3), 1527-1543.

Knudsen, K. E., Arden, K. C., & Cavenee, W. K. (1998). Multiple G1 regulatory elements control the androgen-dependent proliferation of prostatic carcinoma cells. *Journal of Biological Chemistry*, *273*(32), 20213-20222.

Koinis, F., Chantzara, E., Samarinas, M., Xagara, A., Kratiras, Z., Leontopoulou, V., & Kotsakis, A. (2022). Emerging role of yap and the Hippo pathway in prostate cancer. *Biomedicines, 10*(11), 2834.

Koryakina, Y., Knudsen, K. E., & Gioeli, D. (2015). Cell-cycle-dependent regulation of androgen receptor function. *Endocrine-Related Cancer*, *22*(2), 249-264.

Koss, L. G., & Melamed, M. R. (2006). *Koss' diagnostic cytology and its histopathologic bases*. Lippincott Williams & Wilkins.

Kroemer, G., Galluzzi, L., Vandenabeele, P., Abrams, J., Alnemri, E. S., Baehrecke, E., Blagosklonny, M., El-Deiry, W., Golstein, P., & Green, D. (2009). Classification of cell death: Recommendations of the Nomenclature Committee on Cell Death 2009. *Cell Death & Differentiation*, *16*(1), 3-11.

Kumar, M., Sharma, A., & Kumar, P. (2020). *Pharmacotherapeutic botanicals for cancer chemoprevention*. Springer.

Kupe, M., Karatas, N., Unal, M. S., Ercisli, S., Baron, M., & Sochor, J. (2021). Phenolic composition and antioxidant activity of peel, pulp and seed extracts of different clones of the Turkish grape cultivar 'karaerik'. *Plants*, *10*(10), 2154.

Liao, R. S., Ma, S., Miao, L., Li, R., Yin, Y., & Raj, G. V. (2013). Androgen receptor-mediated non-genomic regulation of prostate cancer cell proliferation. *Translational Andrology and Urology*, *2*(3), 187-196.

Lin, H. H., Chan, K. C., Sheu, J. Y., Hsuan, S. W., Wang, C. J., & Chen, J. H. (2012). *Hibiscus sabdariffa* leaf induces apoptosis of human prostate cancer cells *in vitro* and *in vivo*. *Food Chemistry*, *132*(2), 880-891.

Liu, W., Xu, S., & Che, C. T. (2000). Anti-proliferative effect of ginseng saponins on human prostate cancer cell line. *Life Sciences*, *67*(11), 1297-1306.

Lourens, A., Viljoen, A. M., & Van Heerden, F. (2008). South African *Helichrysum* species: A review of the traditional uses, biological activity and phytochemistry. *Journal of Ethnopharmacology*, *119*(3), 630-652.

Made, F., Wilson, K., Jina, R., Tlotleng, N., Jack, S., Ntlebi, V., & Kootbodien, T. (2017). Distribution of cancer mortality rates by province in South Africa. *Cancer Epidemiology*, *51*, 56-61.

Mamabolo, M. P., Muganza, F. M., Olivier, M. T., Olaokun, O. O., & Nemutavhanani, L. D. (2018). Evaluation of antigonorrhea activity and cytotoxicity of *Helichrysum caespititium* (DC) Harv. whole plant extracts. *Biology and Medicine*, *10*(1), 1C.

Maroyi, A. (2019). *Helichrysum caespititium* (DC.) Harv.: Review of its medicinal uses, phytochemistry and biological activities. *Journal of Applied Pharmaceutical Science, 9*(6), 111-118.

Mathekga, A. D., Meyer, J. M., Horn, M. M., & Drewes, S. E. (2000). An acylated phloroglucinol with antimicrobial properties from *Helichrysum caespititium*. *Phytochemistry*, *53*(1), 93-96.

Matyanga, C. M., Morse, G. D., Gundidza, M., & Nhachi, C. F. (2020). African potato (*Hypoxis hemerocallidea*): A systematic review of its chemistry, pharmacology and ethno medicinal properties. *BMC Complementary Medicine and Therapies*, *20*, 1-12.

Merrimen, J. L., Evans, A. J., & Srigley, J. R. (2013). Preneoplasia in the prostate gland with emphasis on high grade prostatic intraepithelial neoplasia. *Pathology Journal of the RCPA*, *45*(3), 251-263.

Mfengwana, P. H. (2024). Phytochemical constituents, ferric reducing and radical scavenging activities of *Helichrysm caespititium*. *Natural Product Research*, *9*, 1-6.

Mfengwana, P. H., Mashele, S. S., & Manduna, I. T. (2019). Cytotoxicity and cell cycle analysis of *Asparagus laricinus Burch*. and *Senecio asperulus DC*. on breast and prostate cancer cell lines. *Heliyon*, *5*(5), e01666.

Mofokeng, M. M., Prinsloo, G., Araya, H. T., Amoo, S. O., Du Plooy, C. P., & Mashela, P.W. (2022). Nades compounds identified in *Hypoxis hemerocallidea* corms during dormancy. *Plants*, *11*(18), 2387.

Mothibe, M. E., & Sibanda, M. (2019). African traditional medicine: South African perspective. *Traditional and Complementary Medicine*, *2019*, 1-27.

Moyo, S. M. (2016). *Effects of cooking and drying on the phenolic compounds, antioxidant activity and antibacterial activity of Cleome gynandra (spider plant)* (Master's thesis). University of Johannesburg.

Munteanu, I. G., & Apetrei, C. (2021). Analytical methods used in determining antioxidant activity: A review. *International Journal of Molecular Sciences*, *22*(7), 3380.

Nikoletopoulou, V., Markaki, M., Palikaras, K., & Tavernarakis, N. (2013). Crosstalk between apoptosis, necrosis and autophagy. *Biochimica et Biophysica Acta (BBA)-Molecular Cell Research*, *1833*(12), 3448-3459.

Nwozo, O. S., Effiong, E. M., Aja, P. M., & Awuchi, C. G. (2023). Antioxidant, phytochemical, and therapeutic properties of medicinal plants: A review. *International Journal of Food Properties*, *26*(1), 359-388.

Obeng, E. (2020). Apoptosis (programmed cell death) and its signals: A review. *Brazilian Journal of Biology*, *81*, 1133-1143.

Oropesa Ávila, M., Fernández Vega, A., Garrido Maraver, J., Villanueva Paz, M., De Lavera, I., De la Mata, M., Cordero, M. D., Alcocer Gómez, E., Delgado Pavón, A. and Álvarez Córdoba, M. (2015). Emerging roles of apoptotic microtubules during the execution phase of apoptosis. *Cytoskeleton*, *72*(9), 435-446.

Pratima, N. A., & Gadikar, R. (2018). Liquid chromatography-mass spectrometry and its applications: A brief review. *Archives of Organic and Inorganic Chemical Sciences*, *1*, 26-34.

Pravettoni, A., Mornati, O., Martini, P., Marino, M., Colciago, A., Celotti, F., Motta, M., & Negri Cesi, P. (2007). Estrogen receptor beta (erbeta) and inhibition of prostate cancer cell proliferation: Studies on the possible mechanism of action in du145 cells. *Molecular and Cellular Endocrinology*, *263*(1-2), 46-54.

Pringle, N. A., Koekemoer, T. C., Holzer, A., Young, C., Venables, L., & Van de Venter, M. (2018). Potential therapeutic benefits of green and fermented rooibos (*Aspalathus linearis*) in dermal wound healing. *Planta Medica*, *84*(09/10), 645-652.

Rahman, M. A., Akhtar, J., & Arshad, M. (2016). Evaluation of cytotoxic potential and apoptotic effect of a methanolic extract of bauhinia racemosa lam. against a human cancer cell line, hela. *European Journal of Integrative Medicine*, *8*(4), 513-518.

Rao, L., Kang, N., & Rao, A. (2014). Lycopene and other antioxidants in the prevention and treatment of osteoporosis in postmenopausal women. In V. R. Preedy (Ed.), *Aging* (pp. 247-258). Elsevier.

Rasethe, M. T., Semenya, S. S., Potgieter, M. J., & Maroyi, A. (2013). The utilization and management of plant resources in rural areas of the Limpopo province, South Africa. *Journal of Ethnobiology and Ethnomedicine*, *9*, 1-8.

Ravanan, P., Srikumar, I. F., & Talwar, P. (2017). Autophagy: The spotlight for cellular stress responses. *Life Sciences*, *188*, 53-67.

Rayfield, E. L. (2023). *Porifera: Biology and medicinal properties* (Honours thesis). Gardner-Webb University. https://digitalcommons.gardner-webb.edu/undergrad-honors/54/

Reape, T. J., & McCabe, P. F. (2010). Apoptotic-like regulation of programmed cell death in plants. *Apoptosis*, *15*, 249-256.

Riaz, M., Khalid, R., Afzal, M., Anjum, F., Fatima, H., Zia, S., Rasool, G., Egbuna, C., Mtewa, A. G., & Uche, C. Z. (2023). Phytobioactive compounds as therapeutic agents for human diseases: A review. *Food Science & Nutrition*, *11*(6), 2500-2529.

Riss, T. L., Moravec, R. A., Niles, A. L., Duellman, S., Benink, H. A., Worzella, T. J., & Minor, L. (2016). *Cell viability assays*. https://www.ncbi.nlm.nih.gov/books/NBK144065/

Sikhakhane, X. (2013). Evaluating the anticancer and antimicrobial properties of extracts from *Hypoxis hemerocallidea* (African potato). University of Johannesburg.

Skowyra, M. (2014). *Antioxidant properties of extracts from selected plant materials (Caesalpinia spinosa, Perilla frutescens, Artemisia annua and Viola wittrockiana) in vitro and in model food systems* (Doctoral dissertation). Polytechnic University of Catalonia.

Smit, E., De Goede, S., & Rohwer, E. R. (2018). Class separation of the trace polar species present in diesel using hydrophilic interaction chromatography and high resolution mass spectrometry. Energy & Fuels, 32(9), 8944-8954.

Stauffer, S., Chen, X., Zhang, L., Chen, Y., & Dong, J. (2016). KIBRA promotes prostate cancer cell proliferation and motility. *The FEBS Journal*, *283*(10), 1800-1811.

Steenkamp, V., & Gouws, M. (2006). Cytotoxicity of six South African medicinal plant extracts used in the treatment of cancer. *South African Journal of Botany*, *72*(4), 630-633.

Stone, K. R., Mickey, D. D., Wunderli, H., Mickey, G. H. & Paulson, D. F. (1978). Isolation of a human prostate carcinoma cell line (du 145). *International journal of cancer,* 21(3): 274-281.

Sung, H., Ferlay, J., Siegel, R. L., Laversanne, M., Soerjomataram, I., Jemal, A., & Bray, F. (2021). Global cancer statistics 2020: Globocan estimates of incidence and mortality worldwide for 36 cancers in 185 countries. *CA: A Cancer Journal for Clinicians*, *71*(3), 209-249.

Swanepoel, B. (2019). *New synergic biomaterials for anti-cancer therapy* (Master's thesis). Nelson Mandela University. https://core.ac.uk/reader/289223600

Tan, J. B. L., & Lim, Y. Y. (2015). Critical analysis of current methods for assessing the in vitro antioxidant and antibacterial activity of plant extracts. *Food Chemistry*, *172*, 814-822.

Tan, M. E., Li, J., Xu, H. E., Melcher, K., & Yong, E. L. (2015). Androgen receptor: Structure, role in prostate cancer and drug discovery. *Acta Pharmacologica Sinica*, *36*(1), 3-23.

Uller, L., Andersson, M., Greiff, L., Persson, C. G., & Erjefält, J. S. (2004). Occurrence of apoptosis, secondary necrosis, and cytolysis in eosinophilic nasal polyps. *American Journal of Respiratory and Critical Care Medicine*, *170*(7), 742-747.

Uwineza, P. A., & Waśkiewicz, A. (2020). Recent advances in supercritical fluid extraction of natural bioactive compounds from natural plant materials. *Molecules, 25*(17), 3847.

Van Doorn, W. G. (2011). Classes of programmed cell death in plants, compared to those in animals. *Journal of Experimental Botany*, *62*(14), 4749-4761.

Vashchenko, N., & Abrahamsson, P. A. (2005). Neuroendocrine differentiation in prostate cancer: Implications for new treatment modalities. *European Urology*, *47*(2), 147-155.

Venables, L. (2013). *In vitro induction of cell death pathways by Artemisia afra extract and isolation of an active compound, isoalantolactone* (Master's thesis). Rhodes University.

Vermeulen, K., Van Bockstaele, D. R., & Berneman, Z. N. (2003). The cell cycle: A review of regulation, deregulation and therapeutic targets in cancer. *Cell Proliferation*, *36*(3), 131-149.

Woo, R. A., & Poon, R. Y. (2003). Cyclin-dependent kinases and S phase control in mammalian cells. *Cell Cycle*, *2*(4), 315-323.

Wright, G. S., Antonyuk, S. V., & Hasnain, S. S. (2019). The biophysics of superoxide dismutase-1 and amyotrophic lateral sclerosis. *Quarterly Reviews of Biophysics*, *52*, e12.

Yan, G., Elbadawi, M., & Efferth, T. (2020). Multiple cell death modalities and their key features. *World Academy of Sciences Journal*, *2*(2), 39-48.

Zhang, Q. (2018). Global situation and who strategy on traditional medicine. *Traditional Medicine and Modern Medicine*, *1*(1), 11-13.

Zhou, Z. H., Yang, J., & Kong, A. N. (2017). Phytochemicals in traditional Chinese herbal medicine: Cancer prevention and epigenetics mechanisms. *Current Pharmacology Reports, 3*, 77-91.

APPENDICES

Appendix A: Additional Results for Chapter 3

Results: HRMS Tables

Tables A1, A2, and A3 outline negative ion mode for compounds of methanolic extracts: *H. hemerocallidea, H. caespititium*, and *D. anomala* corms.

Elemental Composition Report

Multiple Mass Analysis: Tolerance = 10.0 PPM / DBE: min = -1.5, max = 50.0

Element prediction: Off

Monoisotopic Mass, Even Electron Ions

Elements Used:						
C: 0-500 H: 0-1000 O: 0-200 Si: 0-10						
Minimum:	10.00				-1.5	
Maximum:	100.00	5.0	10.0	50.0		

A- NEGATIVE

Table A1: Characteristics of major peaks from Methanolic A: *H. hemerocallidea* in negative mode

Mass	RA	Calc. Mass	mDa	PPM	DBE	Formula
68.9894	10.75	---				
68.9930	52.02	---				
68.9967	100.00	---				
69.0003	53.58	---				
102.9448	35.83	---				
102.9492	36.29	102.9492	0.0	0.0	2.5	H3 O Si3
102.9536	23.83	---				
112.9780	35.98	---				
112.9826	84.27	---				

112.9873	80.37		112.9875	-0.2	-1.8	4.5	C4 H O4
112.9879	-0.6	-5.3	3.5		C3 H5 O Si2		
112.9919	50.62		---				
112.9966	18.54		---				
114.9890	10.75		114.9879	1.1	9.6	-0.5	H3 O7
116.9233	14.49		---				
116.9280	24.14		116.9284	-0.4	-3.4	3.5	H O2 Si3
116.9328	22.12		---				
121.0277	16.98		---				
121.0325	11.84		121.0325	0.0	0.0	-0.5	C2 H13 Si3
121.0321	0.4	3.3	0.5		C3 H9 O3 Si		
130.9599	11.37		---				
130.9649	35.20		---				
130.9699	26.01		---				
130.9749	12.31		---				
134.9816	11.84		---				
134.9866	25.70		---				
136.9794	11.68		---				
136.9845	19.47		136.9848	-0.3	-2.2	10.5	C9 H Si
137.0049	11.06		137.0059	-1.0	-7.3	5.5	C6 H5 O2 Si
139.0073	14.33		139.0067	0.6	4.3	-0.5	C H11 O2 Si3
139.0063	1.0	7.2	0.5		C2 H7 O5 Si		
145.9240	14.17		---				
145.9293	14.02		---				
145.9346	12.15		---				
146.9341	23.21		---				
146.9394	19.94		146.9394	0.0	0.0	2.5	H7 Si5
146.9390	0.4	2.7	3.5		C H3 O3 Si3		
146.9553	22.74		146.9543	1.0	6.8	7.5	C5 H3 Si3
146.9606	23.99		---				
146.9659	10.59		---				
150.9129	10.59		---				
150.9182	11.99		---				
154.9447	10.75		154.9441	0.6	3.9	5.5	C3 H3 O2 Si3
154.9502	11.06		---				

158.9747	11.53		158.9750	-0.3	-1.9	4.5	C4 H3 O5 Si			
158.9754	-0.7	-4.4	3.5	C3 H7 O2 Si3						
162.9782	16.82		---							
162.9838	20.72		162.9851	-1.3	-8.0	7.5	C7 H3 O3 Si			
174.9463	28.50		---							
174.9521	44.24		174.9523	-0.2	-1.1	3.5	C2 H7 O2 Si4			
174.9519	0.2	1.1	4.5	C3 H3 O5 Si2						
174.9579	31.15		---							
174.9636	13.55		---							
178.9753	27.57		---							
178.9812	19.63		178.9805	0.7	3.9	6.5	C6 H7 O Si3			
178.9801	1.1	6.1	7.5	C7 H3 O4 Si						
178.9828	-1.6	-8.9	3.5	C4 H3 O8						
178.9870	11.84		178.9859	1.1	6.1	-1.5	H7 O9 Si			
180.9688	14.49		---							
180.9747	13.24		180.9746	0.1	0.6	11.5	C10 H O2 Si			
184.9413	18.22		---							
184.9473	30.37		---							
184.9532	14.64		184.9542	-1.0	-5.4	6.5	C5 H O6 Si			
184.9546	-1.4	-7.6	5.5	C4 H5 O3 Si3						
184.9515	1.7	9.2	10.5	C8 H O2 Si2						
194.8966	29.75		---							
194.9027	45.64		194.9030	-0.3	-1.5	7.5	C3 H3 O Si5			
194.9088	21.81		---							
195.9108	11.99		---							
206.9573	14.33		206.9574	-0.1	-0.5	7.5	C6 H7 O Si4			
206.9570	0.3	1.4	8.5	C7 H3 O4 Si2						
206.9636	35.20		206.9629	0.7	3.4	-0.5	H7 O9 Si2			
206.9625	1.1	5.3	0.5	C H3 O12						
206.9698	29.91		---							
206.9761	15.89		206.9754	0.7	3.4	7.5	C7 H7 O2 Si3			
206.9750	1.1	5.3	8.5	C8 H3 O5 Si	206.9777	-1.6	-7.7	4.5	C5 H3 O9	
206.9781	-2.0	-9.7	3.5	C4 H7 O6 Si2						
210.9373	17.13		210.9375	-0.2	-0.9	1.5	H11 O2 Si6			

	210.9371	0.2	0.9	2.5		C H7 O5 Si4		
	210.9366	0.7	3.3	3.5			C2 H3 O8 Si2	
210.9437	36.45		---					
210.9500	20.40		210.9492		0.8	3.8	11.5	C9 H3 O Si3
210.9519	-1.9	-9.0	7.5			C6 H3 O5 Si2		
239.8997	12.62		---					
240.9026	10.75		---					

B- NEGATIVE

Table A2: Characteristics of major peaks from Methanolic B: *H. caespititium* in negative mode

Mass	RA	Calc. Mass	mDa	PPM	DBE	Formula
68.9930	39.00	---				
68.9967	100.00	---				
69.0003	64.90	---				
69.0039	19.22	---				
102.9448	19.78	---				
102.9492	40.25	102.9492	0.0	0.0	2.5	H3 O Si3
102.9536	34.54	---				
112.9780	12.12	---				
112.9826	52.37	---				
112.9873	85.52	112.9875	-0.2	-1.8	4.5	C4 H O4
112.9879	-0.6	-5.3	3.5	C3 H5 O Si2		
112.9919	41.78	---				
112.9966	15.18	---				
114.9890	10.31	114.9879	1.1	9.6	-0.5	H3 O7
116.9280	18.25	116.9284	-0.4	-3.4	3.5	H O2 Si3
116.9328	25.07	---				
121.0325	13.37	121.0325	0.0	0.0	-0.5	C2 H13 Si3
121.0321	0.4	3.3	0.5		C3 H9 O3 Si	
130.9599	20.61	---				
130.9649	36.91	---				
130.9699	21.59	---				
134.9866	14.07	---				
134.9917	13.51	134.9930	-1.3	-9.6	2.5	C3 H3 O6

136.9845	10.72		136.9848	-0.3	-2.2	10.5	C9 H Si			
136.9896	11.98		136.9906	-1.0	-7.3	1.5	C2 H5 O5 Si			
145.9240	14.76		---							
145.9293	16.57		---							
145.9346	21.03		---							
146.9394	26.88		146.9394	0.0	0.0	2.5	H7	Si5	146.9390	
0.4	2.7	3.5		C H3 O3 Si3						
146.9447	10.31		---							
146.9553	15.60		146.9543	1.0	6.8	7.5	C5 H3 Si3			
146.9606	19.50		---							
146.9659	28.13		---							
150.9075	11.28		---							
150.9129	19.22		---							
150.9182	15.74		---							
151.9239	10.45		---							
158.9802	13.09		---							
162.9838	14.07		162.9851	-1.3	-8.0	7.5	C7 H3 O3 Si			
174.9463	13.93		---							
174.9521	43.04		174.9523	-0.2	-1.1	3.5	C2 H7 O2 Si4			
174.9519	0.2	1.1	4.5		C3 H3 O5 Si2					
174.9579	40.39		---							
174.9636	29.25		---							
178.9812	19.50		178.9805	0.7	3.9	6.5	C6 H7 O Si3			
178.9801	1.1	6.1	7.5		C7 H3 O4 Si					
178.9828	-1.6	-8.9	3.5		C4 H3 O8					
178.9870	10.45		178.9859	1.1	6.1	-1.5	H7 O9 Si			
180.9688	11.42		---							
180.9747	21.73		180.9746	0.1	0.6	11.5	C10 H O2 Si			
190.9206	12.26		---							
194.8966	12.40		---							
194.9027	21.03		194.9030	-0.3	-1.5	7.5	C3 H3 O Si5			
194.9088	17.27		---							
194.9149	12.67		---							
201.0397	11.84		201.0399	-0.2	-1.0	4.5	C8 H9 O6			
201.0403	-0.6	-3.0	3.5		C7 H13 O3 Si2					

201.0407	-1.0	-5.0	2.5		C6 H17 Si4		
206.9636	21.03		206.9629	0.7	3.4	-0.5	H7 O9 Si2
206.9625	1.1	5.3	0.5		C H3 O12		
206.9698	32.03		---				
206.9761	35.93		206.9754	0.7	3.4	7.5	C7 H7 O2 Si3
206.9750	1.1	5.3	8.5	C8 H3 O5 Si			
206.9777	-1.6	-7.7	4.5	C5 H3 O9			
206.9781	-2.0	-9.7	3.5		C4 H7 O6 Si2		
206.9824	14.62		206.9813	1.1	5.3	-1.5	H11 O7 Si3
206.9808	1.6	7.7	-0.5		C H7 O10 Si		
210.9437	33.84		---				
210.9500	14.35		210.9492	0.8	3.8	11.5	C9 H3 O Si3
210.9519	-1.9	-9.0	7.5		C6 H3 O5 Si2		
239.8929	11.70		---				
239.8997	30.64		---				
239.9065	12.53		---				
856.4031	11.70		---				

C- NEGATIVE

Table A3: Characteristics of major peaks from Methanolic C: *D. anomala* in negative mode

Mass	RA	Calc. Mass	mDa	PPM	DBE	Formula
61.9925	11.52	---				
68.9930	30.11	---				
68.9967	100.00	---				
69.0003	69.89	---				
69.0039	26.73	---				
91.0071	13.21	---				
102.9448	12.90	---				
102.9492	32.72	102.9492	0.0	0.0	2.5	H3 O Si3
102.9536	30.26	---				
112.9780	13.67	---				
112.9826	52.38	---				
112.9873	70.81	112.9875	-0.2	-1.8	4.5	C4 H O4
112.9879	-0.6	-5.3	3.5		C3 H5 O Si2	

112.9919	72.04		---				
112.9966	27.04		---				
114.9937	11.06		---				
115.9189	10.14		---				
116.9328	15.82		---				
130.9599	10.60		---				
130.9649	25.19		---				
130.9699	48.23		---				
130.9749	19.05		---				
134.9866	12.75		---				
134.9917	11.06		134.9930	-1.3	-9.6	2.5	C3 H3 O6
136.9794	23.81		---				
136.9845	13.52		136.9848	-0.3	-2.2	10.5	C9 H Si
136.9896	10.45		136.9906	-1.0	-7.3	1.5	C2 H5 O5 Si
145.9240	11.37		---				
145.9293	23.66		---				
145.9346	26.57		---				
145.9398	18.43		---				
146.9288	12.14		---				
146.9341	22.89		---				
146.9394	23.96		146.9394	0.0	0.0	2.5	H7 Si5
146.9390	0.4	2.7	3.5		CH3 O3 Si3		
146.9447	19.20		---				
146.9500	11.98		---				
146.9606	35.02		---				
146.9659	29.19		---				
146.9712	15.51		146.9722	-1.0	-6.8	7.5	C6 H3 O Si2
150.9129	11.06		---				
150.9182	17.67		---				
151.9239	11.98		---				
158.9802	24.12		---				
162.9782	13.36		---				
162.9838	20.89		162.9851	-1.3	-8.0	7.5	C7 H3 O3 Si
174.9521	38.25		174.9523	-0.2	-1.1	3.5	C2 H7 O2 Si4
174.9519	0.2	1.1	4.5		C3 H3 O5 Si2		
174.9579	45.93		---				

174.9636	36.71		---				
178.9753	17.20		---				
178.9812	20.58		178.9805	0.7	3.9	6.5	C6 H7 O Si3
178.9801	1.1	6.1	7.5		C7 H3 O4 Si		
178.9828	-1.6	-8.9	3.5		C4 H3 O8		
178.9870	14.13		178.9859	1.1	6.1	-1.5	H7 O9 Si
180.9747	17.20		180.9746	0.1	0.6	11.5	C10 H O2 Si
184.9532	10.29		184.9542	-1.0	-5.4	6.5	C5 H O6 Si
184.9546	-1.4	-7.6	5.5		C4 H5 O3 Si3		
184.9515	1.7	9.2	10.5		C8 H O2 Si2		
194.9027	27.80		194.9030	-0.3	-1.5	7.5	C3 H3 O Si5
194.9088	22.73		---				
195.9169	13.36		---				
196.9153	10.75		196.9155	-0.2	-1.0	11.5	C7 H Si4
201.0397	10.14		201.0399	-0.2	-1.0	4.5	C8 H9 O6
201.0403	-0.6	-3.0	3.5		C7 H13 O3 Si2		
201.0407	-1.0	-5.0	2.5		C6 H17 Si4		
201.0459	17.05		---				
206.9636	28.11		206.9629	0.7	3.4	-0.5	H7 O9 Si2
206.9625	1.1	5.3	0.5		C H3 O12		
206.9698	59.29		---				
206.9761	23.20		206.9754	0.7	3.4	7.5	C7 H7 O2 Si3
206.9750	1.1	5.3	8.5		C8 H3 O5 Si		
206.9777	-1.6	-7.7	4.5		C5 H3 O9		
206.9781	-2.0	-9.7	3.5		C4 H7 O6 Si2		
206.9824	17.67		206.9813	1.1	5.3	-1.5	H11 O7 Si3
206.9808	1.6	7.7	-0.5		CH7 O10 Si		
210.9437	24.42		---				
210.9500	22.89		210.9492	0.8	3.8	11.5	C9 H3 O Si3
210.9519	-1.9	-9.0	7.5		C6 H3 O5 Si2		
219.8398	15.36		---				
221.8468	10.91		---				
239.8997	18.13		---				
243.8761	10.29		---				

Tables A4, A5, and A6 outline the positive ion mode for compounds of methanolic extracts: *H. hemerocallidea, H. caespititium*, and *D. anomala* corms.

Multiple Mass Analysis: Tolerance = 10.0 PPM / DBE: min = -1.5, max = 50.0

Element prediction: Off

Monoisotopic Mass, Even Electron Ions

Elements Used:					
C: 0-500 H: 0-1000 O: 0-200 Si: 0-10					
Minimum:	10.00				-1.5
Maximum:	100.00		5.0	10.0	50.0

A- POSITIVE

Table A4: Characteristics of major peaks from Methanolic A: *H. hemerocallidea* in positive mode

Mass	RA	Calc. Mass	mDa	PPM	DBE	Formula
84.9405	15.75	---				
84.9446	10.75	---				
96.9413	10.52	---				
97.9458	16.44	---				
97.9501	18.28	---				
109.9821	11.48	---				
109.9867	13.09	---				
113.9377	10.29	---				
113.9424	10.26	---				
116.9503	10.82	---				
125.9591	21.93	---				
125.9641	13.98	---				
126.9463	13.38	---				
129.9807	11.31	---				
131.9249	11.44	---				
132.9301	11.31	---				
141.9195	15.92	---				

141.9247	65.83		---				
141.9299	100.00		---				
141.9351	30.98		---				
142.9307	14.44		---				
142.9359	12.50		---				
148.9665	11.41		---				
148.9718	18.65		148.9722	-0.4	-2.7	3.5	C3 H O7
148.9726	-0.8	-5.4	2.5		C2 H5 O4 Si2		
148.9730	-1.2	-8.1	1.5		C H9 O Si4		
148.9878	27.56		148.9879	-0.1	-0.7	6.5	C6 H5 O Si2
148.9875	0.3	2.0	7.5		C7 H O4		
148.9932	32.72		148.9934	-0.2	-1.3	-1.5	H5 O9
157.9633	14.47		---				
157.9687	37.32		---				
157.9742	23.64		---				
172.9308	11.28		---				
172.9366	40.22		172.9367	-0.1	-0.6	4.5	C2 H5 O2 Si4
172.9363	0.3	1.7	5.5		C3 H O5 Si2		
172.9423	44.43		---				
172.9480	13.81		---				
182.9388	15.72		182.9390	-0.2	-1.1	6.5	C4 H3 O3 Si3
182.9394	-0.6	-3.3	5.5		C3 H7 Si5		
182.9447	30.09		---				
182.9506	22.36		---				
195.0357	21.93		---				
195.0418	58.53		---				
195.0479	61.00		195.0477	0.2	1.0	5.5	C9 H11 O3 Si
195.0482	-0.3	-1.5	4.5		C8 H15 Si3		
195.0540	19.83		---				
217.0582	11.64		217.0564	1.8	8.3	-1.5	C4 H17 O6 Si2

B- POSITIVE

Table A5: Characteristics of major peaks from Methanolic B: *H. caespititium* in positive mode

Mass	RA	Calc. Mass	mDa	PPM	DBE	Formula
84.9446	16.48	---				
97.9501	14.58	---				
109.9867	17.65	---				
109.9912	13.47	---				
113.9424	14.58	---				
116.9550	10.30	---				
125.9591	14.91	---				
125.9641	16.08	---				
126.9512	10.66	---				
131.9801	14.29	---				
141.9247	37.56	---				
141.9299	100.00	---				
141.9351	66.10	---				
142.9359	10.53	---				
148.9718	13.73	148.9722	-0.4	-2.7	3.5	C3 H O7
148.9726	-0.8	-5.4	2.5	C2 H5 O4 Si2		
148.9730	-1.2	-8.1	1.5	C H9 O Si4		
148.9932	28.83	148.9934	-0.2	-1.3	-1.5	H5 O9
148.9985	16.15	---				
157.9687	29.39	---				
157.9742	28.90	---				
172.9366	18.18	172.9367	-0.1	-0.6	4.5	C2 H5 O2 Si4
172.9363	0.3	1.7	5.5	C3 H O5 Si2		
172.9423	38.31	---				
172.9480	22.13	---				
177.0211	11.51	177.0219	-0.8	-4.5	2.5	C5 H9 O5 Si
177.0223	-1.2	-6.8	1.5	C4 H13 O2 Si3		
182.9447	20.43	---				
182.9506	27.30	---				
182.9565	12.42	182.9570	-0.5	-2.7	6.5	C5 H3 O4 Si2
182.9574	-0.9	-4.9	5.5	C4 H7 O Si4		

195.0418	34.06		---				
195.0479	76.72		195.0477	0.2	1.0	5.5	C9 H11 O3 Si
195.0482	-0.3	-1.5	4.5		C8 H15 Si3		
195.0540	61.16		---				
195.0601	14.02		---				
301.0806	10.95		301.0783	2.3	7.6	-1.5	C6 H29 O2 Si6
301.0779	2.7	9.0	-0.5		C7 H25 O5 Si4		

C- POSITIVE

Table A6: Characteristics of major peaks from Methanolic C: *D. anomala* in positive mode

Mass	RA	Calc. Mass	mDa	PPM	DBE	Formula
84.9446	18.06	---				
84.9486	11.06	---				
97.9501	21.11	---				
97.9545	15.66	---				
109.9867	16.84	---				
109.9912	15.33	---				
113.9424	12.48	---				
113.9471	10.98	---				
116.9550	12.20	---				
120.9850	10.33	---				
125.9641	19.80	---				
126.9512	12.69	---				
131.9249	11.59	---				
131.9801	15.05	---				
141.9247	15.98	---				
141.9299	72.35	---				
141.9351	100.00	---				
141.9403	30.62	---				
142.9411	10.37	---				
143.9350	11.63	---				
148.9772	12.24	---				
148.9932	29.28	148.9934	-0.2	-1.3	-1.5	H5 O9
148.9985	30.83	---				

149.0038	11.83		149.0027	1.1	7.4	11.5	C11 H O
157.9687	22.61		---				
157.9742	45.22		---				
157.9797	29.77		---				
172.9366	10.65		172.9367	-0.1	-0.6	4.5	C2 H5 O2 Si4
172.9363	0.3	1.7	5.5		C3 H O5 Si2		
172.9423	40.91		---				
172.9480	47.42		---				
172.9538	18.67		172.9542	-0.4	-2.3	5.5	C4 H O6 Si
172.9546	-0.8	-4.6	4.5		C3 H5 O3 Si3		
172.9551	-1.3	-7.5	3.5		C2 H9 Si5		
177.0211	12.20		177.0219	-0.8	-4.5	2.5	C5 H9 O5 Si
177.0223	-1.2	-6.8	1.5		C4 H13 O2 Si3		
177.0269	10.04		---				
182.9506	32.66		---				
182.9565	31.07		182.9570	-0.5	-2.7	6.5	C5 H3 O4 Si2
182.9574	-0.9	-4.9	5.5		C4 H7 O Si4		
186.9241	11.35		---				
195.0418	20.74		---				
195.0479	69.17		195.0477	0.2	1.0	5.5	C9 H11 O3 Si
195.0482	-0.3	-1.5	4.5		C8 H15 Si3		
195.0540	88.78		---				
195.0601	31.07		---				
269.0670	10.04		269.0669	0.1	0.4	4.5	C10 H21 O Si4
269.0665	0.5	1.9	5.5		C11 H17 O4 Si2	269.0661	0.9
3.3	6.5		C12 H13 O7				
269.0693	-2.3	-8.5	1.5		C8 H17 O8 Si		
269.0697	-2.7	-10.0	0.5		C7 H21 O5 Si3		
299.1285	14.84		299.1283	0.2	0.7	9.5	C18 H19 O4
299.1287	-0.2	-0.7	8.5		C17 H23 O Si2		
299.1256	2.9	9.7	13.5		C21 H19 Si		
299.1315	-3.0	-10.0	4.5		C14 H23 O5 Si		
301.0806	10.00		301.0783	2.3	7.6	-1.5	C6 H29 O2 Si6
301.0779	2.7	9.0	-0.5		C7 H25 O5 Si4		
301.0882	14.23		301.0869	1.3	4.3	13.5	C19 H17 Si2

301.0896	-1.4	-4.6	9.5	C16 H17 O4 Si
301.0865	1.7	5.6	14.5	C20 H13 O3
301.0900	-1.8	-6.0	8.5	C15 H21 O Si3

Appendix B: Additional Results for Chapter 4

4.1 Anti-oxidant results using DPPH assay

Figure B1: Standard curve DPPH percentage scavenging activity

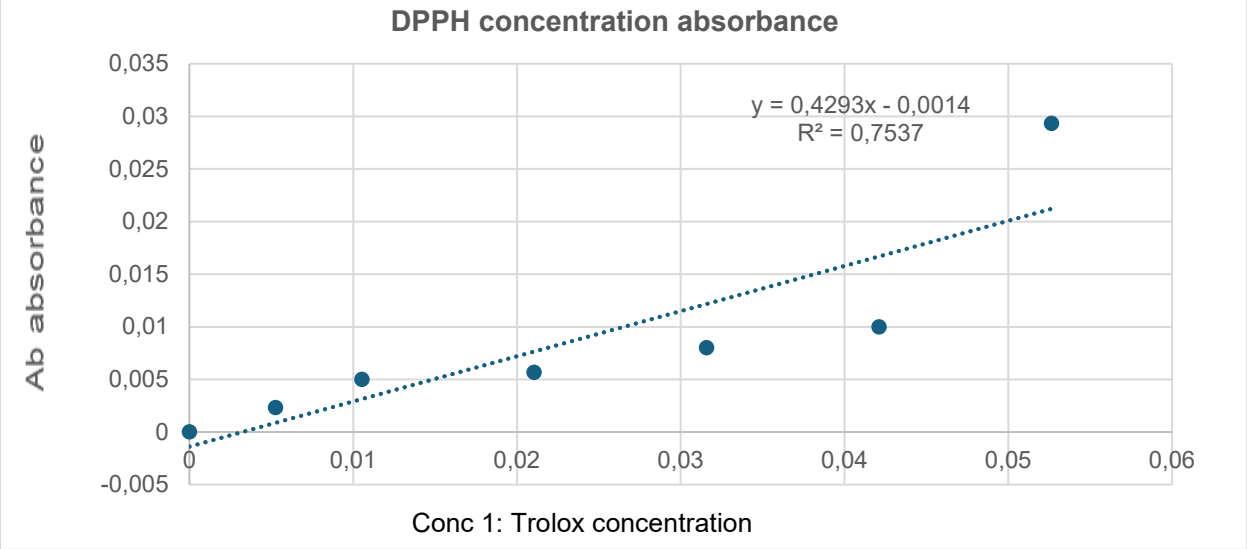

Figure B2: DPPH assay photograph: Determining anti-oxidant activities

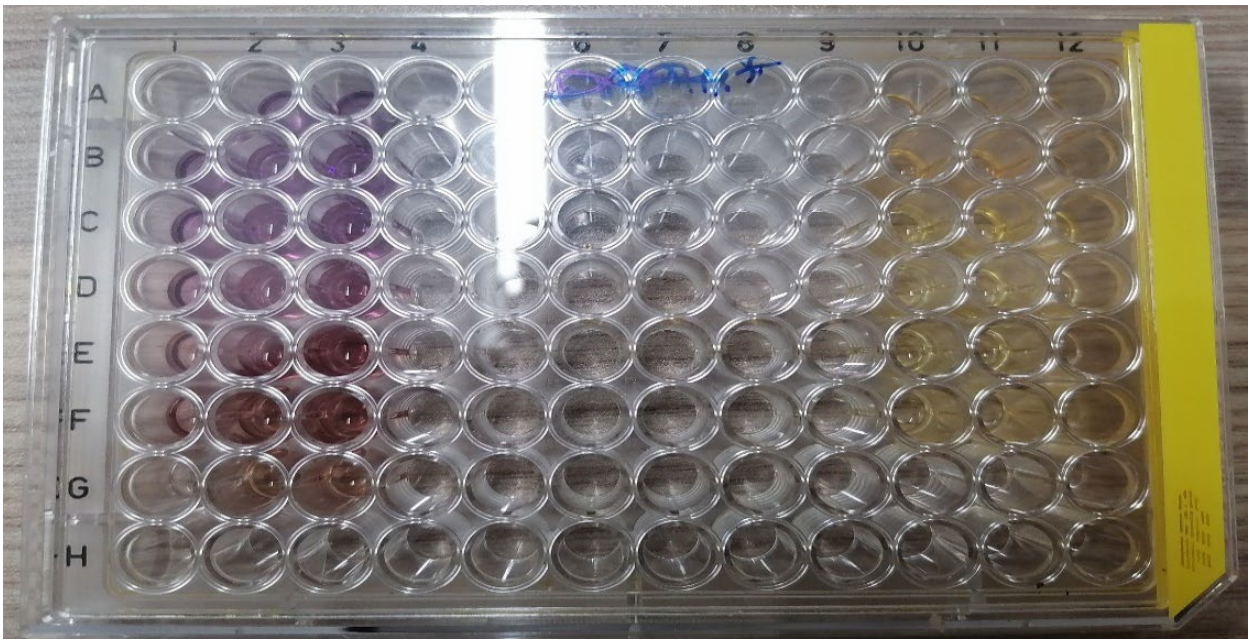

4.2 Anti-oxidant results using ABTS assay

Figure B3: Standard curve ABTS percentage scavenging activity

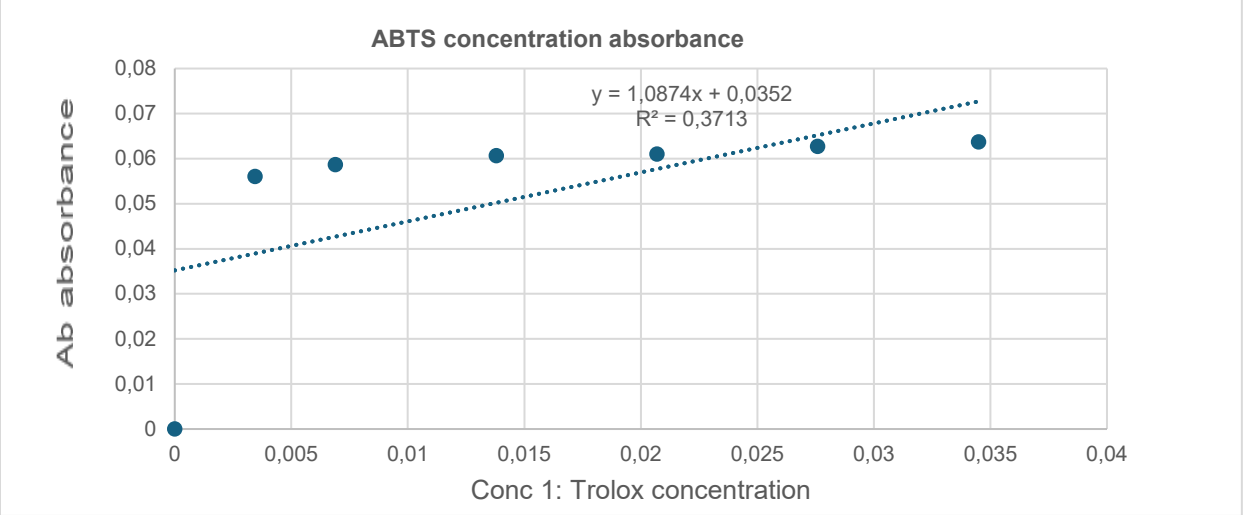

Figure B4: ABTS assay photograph: Determining anti-oxidant activity

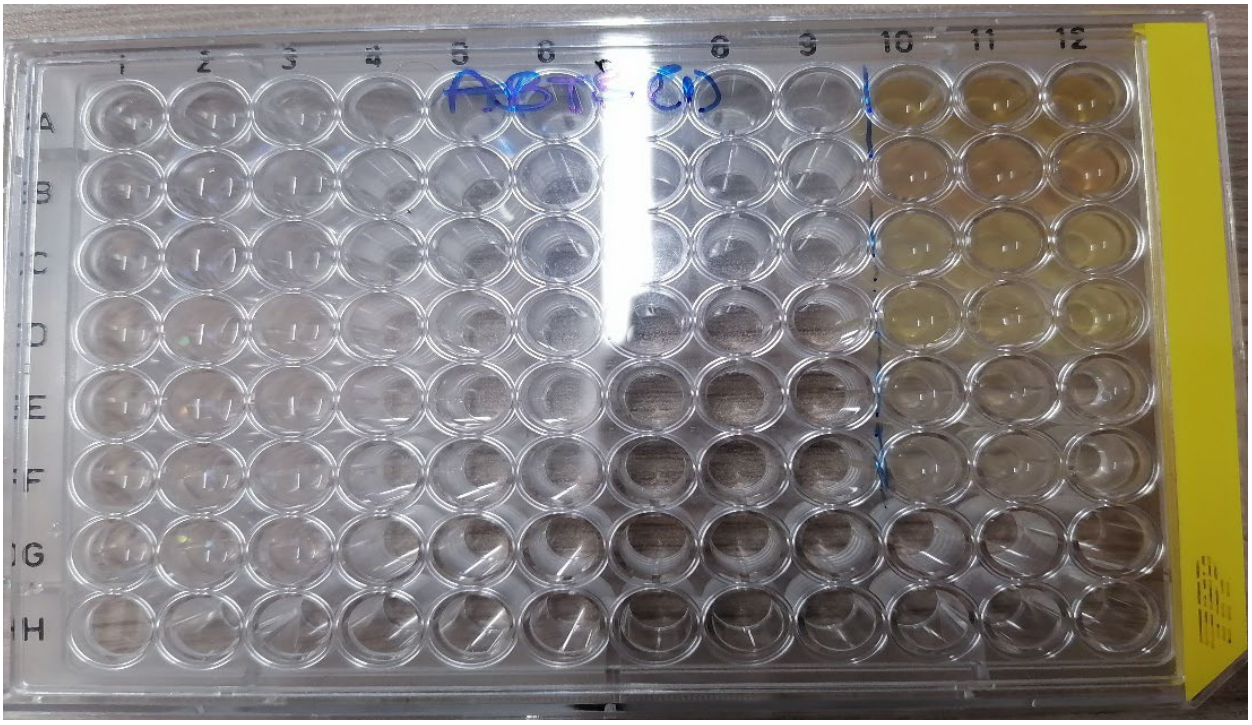

4.3 Anti-oxidant FRAP results

Figure B5: Standard curve FRAP percentage scavenging activity

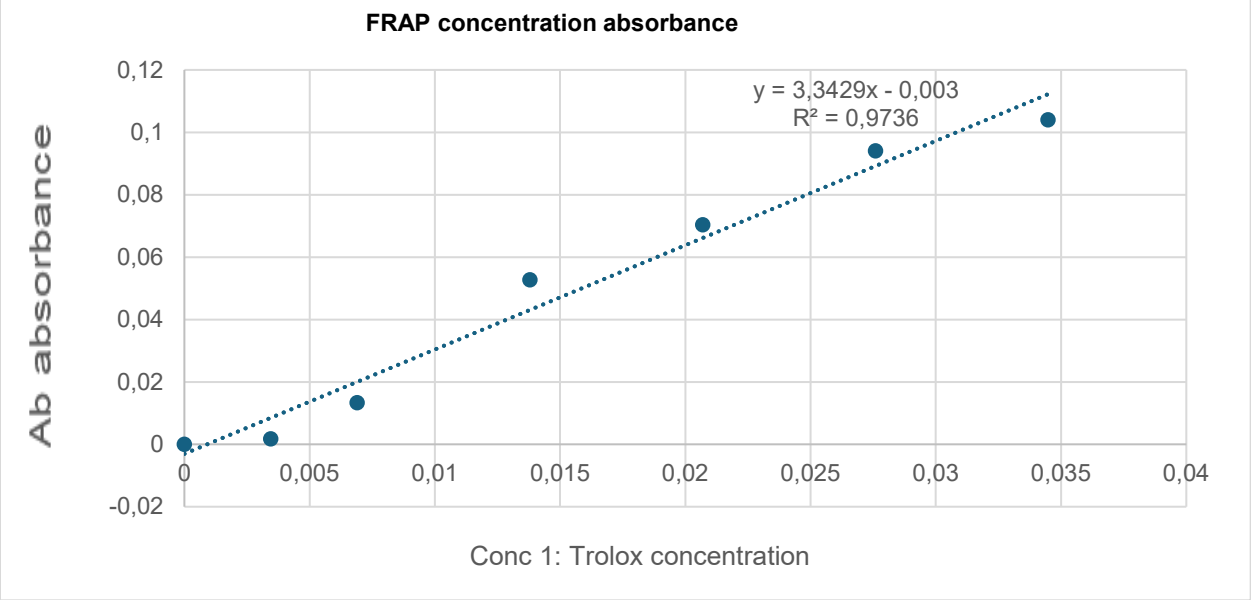

Figure B6: FRAP assay photograph: Determining anti-oxidant activity

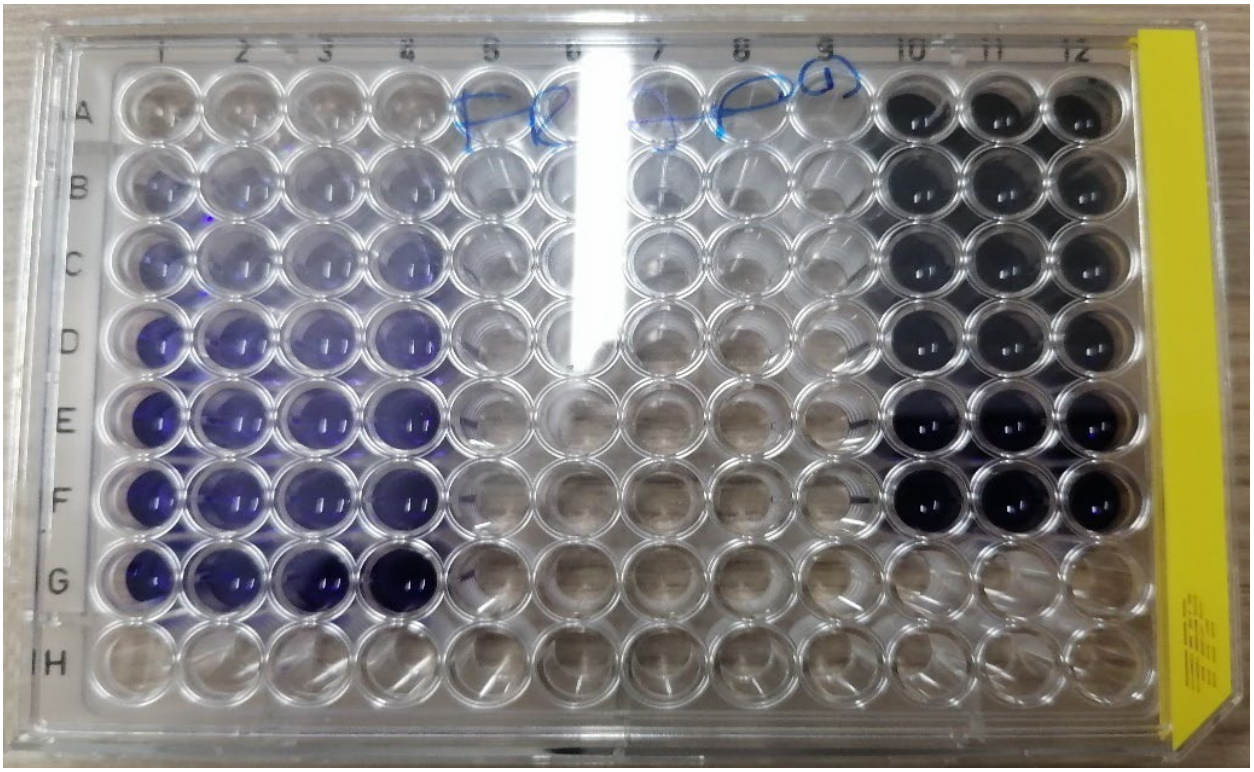

Appendix C: Additional Results for Chapter 5

5.1 Antiproliferation results

Table C1 shows the DU145 prostate cell line's viability after treatment with aqueous extracts from *H. hemerocallidea*, *H. caespititium*, and *D. anomala*.

5.1.1 Aqueous (ddH_2O) extracts

Table C1: Control: untreated cell line, A.: *H. hemerocallidea* B..: *H. caespititium* C.: *D. anomala* with solvent aqueous (ddH_2O), melphalan: cell line treated with melphalan

Average						
	15 µg/mL	**31 µg/mL**	**62.5 µg/mL**	**125 µg/mL**	**250 µg/mL**	**500 µg/mL**
Control	100%					
H. hemerocallidea	82%	89%	86%	81%	79%	79%
H. caespititium	94%	94%	94%	89%	82%	64%
D. anomala	92%	97%	93%	87%	67%	24%
Melphalan	19%	20%				
Standard deviation						
	15 µg/mL	**31 µg/mL**	**62.5 µg/mL**	**125 µg/mL**	**250 µg/mL**	**500 µg/mL**
Control	100%					
H. hemerocallidea	55%	66%	54%	28%	50%	49%
H. caespititium	49%	31%	47%	47%	33%	16%
D. anomala	32%	41%	23%	39%	38%	11%
Melphalan	41%	44%				

Table C2 shows the DU145 prostate cell line's viability after treatment with methanolic extracts of *H. hemerocallidea*, *H. caespititium*, and *D. anomala*.

5.1.2 MeOH extracts

Table C2: Control: untreated cell line, A..: *H. hemerocallidea* B..: *H. caespititium* C.M: *D. anomala* with solvent MeOH, melphalan: cell line treated with melphalan

Average						
	15 µg/mL	**31 µg/mL**	**62.5 µg/mL**	**125 µg/mL**	**250 µg/mL**	**500 µg/mL**
Control	100%					
H. hemerocallidea	81%	84%	81%	73%	70%	63%
H. caespititium	94%	88%	79%	70%	60%	54%
D. anomala	52%	31%	36%	40%	46%	70%
Melphalan	16%	20%				

Standard deviation						
	15 µg/mL	**31 µg/mL**	**62.5 µg/mL**	**125 µg/mL**	**250 µg/mL**	**500 µg/mL**
Control	100%					
H. hemerocallidea	73%	96%	58%	36%	85%	66%
H. caespititium	59%	100%	45%	81%	70%	66%
D. anomala	33%	26%	28%	72%	68%	26%
Melphalan	17%	21%				

IC_{50} determination

Table C3 indicates the determination of a viable DU145 cell line at different concentrations of methanolic *D. anomala* extracts.

Table C3: Control: untreated cell line, *D. anomala* with MeOH solvent, melphalan: cell line treated with melphalan

DU145 cell line viability								
Concentration	**3.9 µg/mL**	**7.8 µg/mL**	**15.625 µg/mL**	**31.25 µg/mL**	**62.5 µg/mL**	**125 µg/mL**	**250 µg/mL**	**500 µg/mL**
Control	100%							
D. anomala	97%	86%	55	24%	25%	26%	22%	28%
Melphalan	19%							

Appendix D: Project Output: Conference Output (Oral Presentation)

GENERAL ORAL PRESENTATIONS

Anticancer activity of *Hypoxis hemerocallidea (African potato)* corm, *Helichrysum caespititium* and *Dicoma anomala* on DU145 Prostate cancer cell line *in vitro*

Toona, L.M.[1], Mfengwana, H.[2] and Mthombeni, J.[1]

[1]Biomedical Sciences, University of Johannesburg, South Africa.
[2]Health Sciences, Central university of Technology, Bloemfontein, South Africa

ABSTRACT

Background: Prostate cancer accounts for 15% of cancers diagnosed in men annually. Almost 70% of the cancer is said to occurs in more developed regions of the world. Incidence rates vary more than 25-fold worldwide, with the highest in Australia, New Zealand, Northern America, Western and Northern Europe. Similarly, less develope regions such as the Caribbean, Southern Africa and South America, grapple with h rates of prostate cancer. Several chemotherapeutic agents are available and used in t management of cancer, and prostate cancer is no different. However, the challenge is in the indiscrimination of toxicity and adverse events that accompanies their usage. This has prompted interest in the discovery of novel anticancer agents from natural products. **Aim:** This study aimed to investigate the effectiveness of *Hypoxis hemerocallidea (African potato)*, *Helichrysum caespititium and Dicoma anomala* corm extracts against DU145 Prostate cancer cell line *in vitro*. **Methodology:** Propidium iodide (PI) a fluorescent molecule that intercalates with DNA at a specific ratio was used for cell cycle analysis. Treatment extract *Dicoma anomala* diluted was used to treat DU145 Prostate cancer cells, incubated at 37°C in humidified 5% CO2 incubator for 24hrs then other 96 well plate left for 48hours then treatment was removed. bisBenzamide H 33342trihydrochloride (Hoechst 33342) and Annexin stain were added and left for 10min at room temperature. Growth of cell was examined under the inverted microscope. Thereafter, cells were stained with PI to allow for listing of dead cells. Melphalan was used as a positive control in the examination. Cell image acquisition was done using ImageXpress Micro XLS fluorescent microscope and evaluated with Meta Xpress software. **Results:** Methanol extracts of *Dicoma anomala* induced cell death through apoptosis. *D. anomala* induced death through cell arrest at synthesis phase and G-phase. Observed from Annexin V-FITC, Hoechst-33342 and PI both 15µg/mL and 30µg/mL of *D. anomala* extracts demonstrated early M phase arrest after 48hrs. *Hypoxis hemerocallidea (African potato)*, and *Helichrysum caespititium* methanol extracts did not result in apoptosis. **Conclusion:** Extracts are usually taken combined and dissolved with aqueous; however, the methanol extract proved to induce apoptotic on DU145 prostate cell line. Recommendation is to further explore traditional herbal alternatives as they have numerous phytochemicals with pharmacological activities.

65

Key words: anticancer, apoptosis, cell line, propidium iodide, traditional h *Dicoma anomala*

Appendix E: Project Output: International Academy of Pathology Conference Output (Poster Presentation)

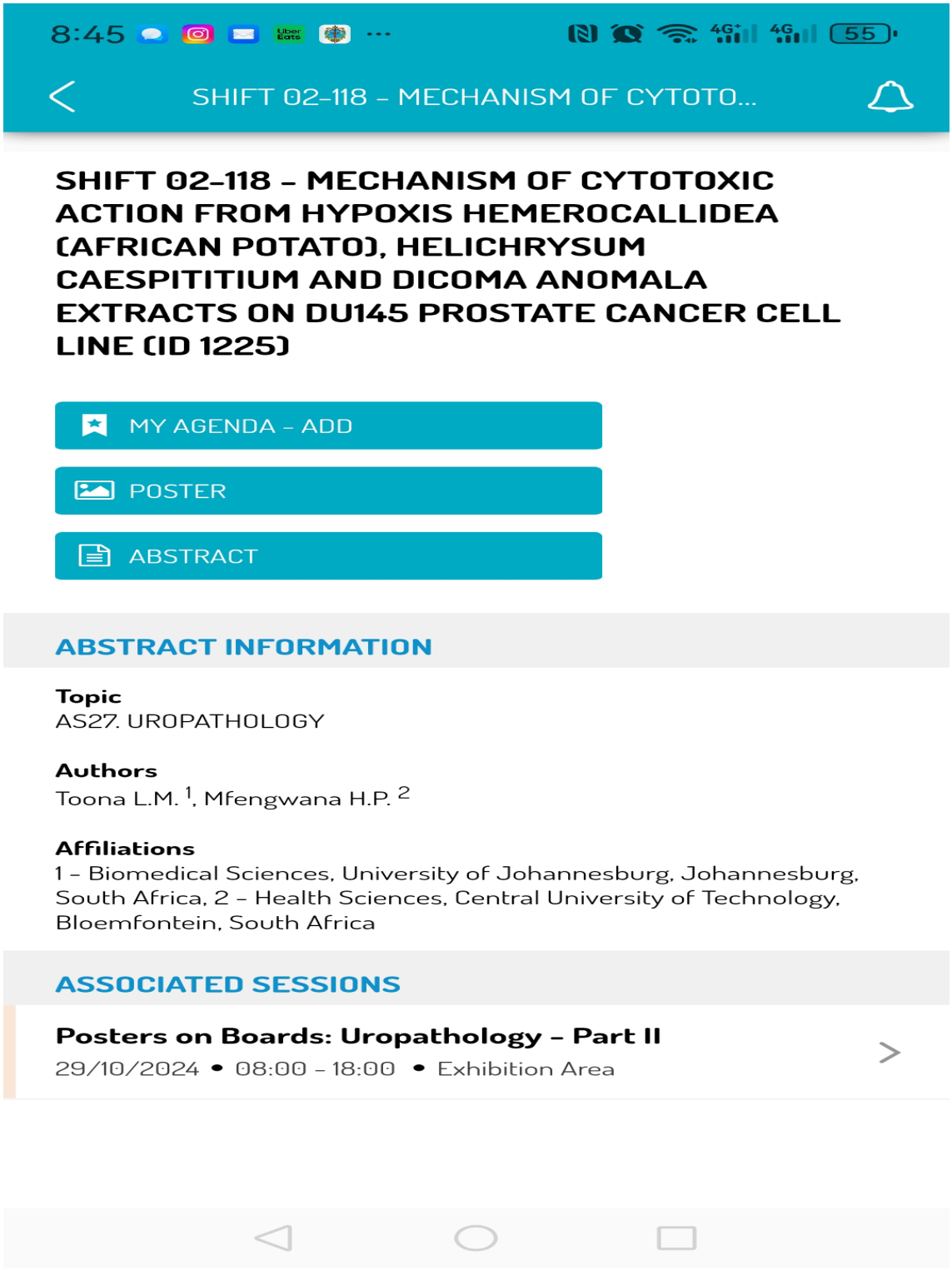

Appendix F: Turnitin Report

LMToonaThesis

by Lerato Toona

Submission date: 04-Nov-2024 06:29PM (UTC+0200)

Submission ID: 2508157186

File name: 6168_Lerato_Toona_LM_Toona_Thesis_783513_1634315563.docx (9.87M)

Word count: 27592

Character count: 159076

LM Toona Thesis

ORIGINALITY REPORT

18%	17%	15%	3%
SIMILARITY INDEX	INTERNET SOURCES	PUBLICATIONS	STUDENT PAPERS

PRIMARY SOURCES

1	**vital.seals.ac.za:8080** Internet Source	42%
2	**repository.up.ac.za** Internet Source	2%
3	**datapdf.com** Internet Source	1%
4	**tessera.spandidos-publications.com** Internet Source	1%
5	**www.ncbi.nlm.nih.gov** Internet Source	1%
6	**www.preprints.org** Internet Source	%
7	**Submitted to University of Johannesburg** Student Paper	1%

8 **Kewuyemi, Yusuf Olamide. "Development of a Healthy 3D Printed Cowpea-Quinoa Snack for the Hospitality Industry", University of Johannesburg (South Africa), 2023**

Publication 1%

---

9 **www.ufrsdv.u-bordeaux2.fr** 1%

Internet Source

---

10 **Oropesa Ávila, Manuel, Alejandro Fernández Vega, Juan Garrido Maraver, Marina Villanueva Paz, Isabel De Lavera, Mario De La Mata, Mario D. Cordero, Elizabet Alcocer Gómez, Ana Delgado Pavón, Mónica Álvarez Córdoba, David Cotán, and José Antonio Sánchez-Alcázar. "Emerging roles of apoptotic microtubules during the execution phase of apoptosis: Apoptotic Microtubules", Cytoskeleton, 2015.** 1%

Publication

---

11 www.japsonline.com 1%

Internet Source

---

12 Kokoette Bassey, Sandra Combrinck, Weiyang Chen. "Hypoxis hemerocallidea", Elsevier BV, 2023 1

Publication

1%

13 ir.cut.ac.za

Internet Source

14 bookcafe.yuntsg.com 1%

Internet Source

15 ink.springer.com 1%

Internet Source

16 www.nature.com 1%

Internet Source

LMToonaThesis

by Lerato Toona

Submission date: 04-Nov-2024 06:29PM (UTC+0200)

Submission ID: 2508157186

File name: 6168_Lerato_Toona_LM_Toona_Thesis_783513_1634315563.docx (9.87M)

Word count: 27592

Character count: 159076

LM Toona Thesis

ORIGINALITY REPORT

18%	17%	15%	3%
SIMILARITY INDEX	INTERNET SOURCES	PUBLICATIONS	STUDENT PAPERS

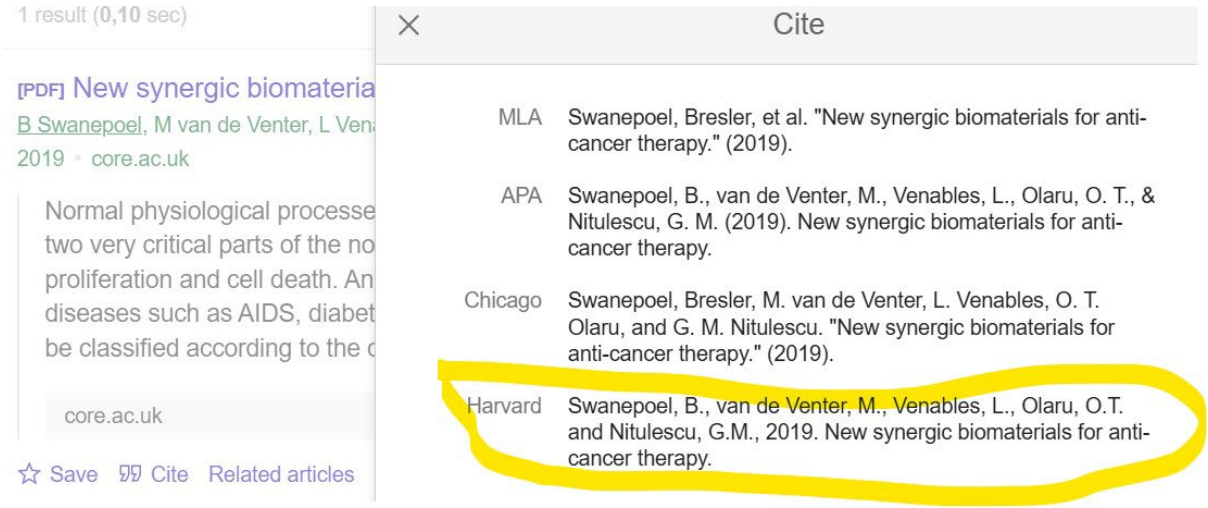

Molecular Biology : Open Access

Knox, Mol Bio 2018, 7:3
DOI: 10.4172/2168-9547.1000215

Review Article Open Access

Wave/Particle Duality and Biomedical Research Designs

Sarah S. Knox*

Department of Epidemiology, School of Public Health, Member WVU Cancer Institute, West Virginia University, USA

***Corresponding author:** S Knox, Professor of Epidemiology, School of Public Health, Member WVU Cancer Institute, West Virginia University, USA, Tel: 304-293-1058; E-mail: sknox@hsc.wvu.edu

Received date: July 03, 2018; **Accepted date:** July 10, 2018; **Published date:** July 14, 2018